UNIVERSITÀ DEGLI STUDI DI PADOVA

SEDE AMMINISTRATIVA: UNIVERSITÀ DEGLI STUDI DI PADOVA

Dipartimento di Farmacia

Dipartimento di Biologia-Istituto di Tecnologie Biomediche-CNR

SCUOLA DI DOTTORATO DI RICERCA IN:

BIOLOGIA E MEDICINA DELLA RIGENERAZIONE

INDIRIZZO: INGEGNERIA DEI TESSUTI E DEI TRAPIANTI

CICLO: XXII

Experimental approaches *in vitro* and *in vivo* for the pathogenic understanding of Alzheimer's Disease: potential role of metal ions

DIRETTORE DELLA SCUOLA: CH.MO PROF. Pierpaolo Parnigotto

SUPERVISORE: CH.MO PROF. Paolo Zatta

DOTTORANDA: SILVIA BOLOGNIN

31 GENNAIO 2009

"Il mondo è un libro e chi
non viaggia ne legge solo una pagina"
Sant' Agostino

"The fact is, I think we almost always underestimate the
complexity of life and of nature"
Craig C. Mello, Nobel lecture 2006

Ai miei genitori, a Marco e Nicola

Index

Sommario

Il mio lavoro di tesi ha riguardato lo studio dell'implicazione di alcuni metalloioni come promotori del *misfolding* del peptide amiloidogenico β-amiloide (Aβ), che sembra essere coinvolto nella patogenesi del morbo di Alzheimer (AD).

I risultati ottenuti dimostrano come la conformazione del peptide Aβ cambi in funzione del metallo ad esso legato (alluminio, rame, zinco e ferro). In particolare, lo studio ha chiaramente messo in luce come tra i vari ioni metallici testati, l'alluminio sia il catione più efficiente nel promuovere l'aumento sia dell'idrofobicità superficiale che dell'aggregazione del peptide *in vitro.* Queste modificazioni si riflettono in un notevole aumento della neurotossicità di tale complesso sia rispetto al solo peptide che agli altri complessi metallici. La conformazione ed i diversi effetti biologici sono quindi da attribuirsi unicamente al diverso tipo di aggregato formato in seguito al legame del peptide con i singoli metalli. Si è inoltre confrontata la propensione a formare aggregati dei complessi di Aβ-metalli in presenza ed in assenza del frammento $A\beta_{17\text{-}28}$. I dati ottenuti indicano una maggiore idrofobicità e capacità di aggregazione del complesso Aβ-alluminio in presenza del frammento $A\beta_{17\text{-}28}$, caratteristiche che determinano una maggiore tossicità rispetto a tutti gli altri complessi testati.

Si è approfondito inoltre il ruolo geno-tossico dei complessi Aβ-ioni metallici su colture cellulari di neuroblastoma umano, come modelli per la comprensione dell'eziopatogenesi molecolare di AD. Le alterazioni genetiche prodotte da tali complessi sono state correlate con il pattern di espressione genica di campioni di sangue periferico di pazienti AD selezionati dall'ospedale "G. Rossi" di Verona al fine di identificare test potenzialmente prognostici da sperimentare sulla definizione clinica della patologia. Il dato ottenuto più interessante è relativo alla glutaminil ciclasi, enzima che potrebbe essere coinvolto nella patologia ed il cui gene è stato visto essere sovraespresso nel sangue periferico di soggetti malati di AD.

Complessivamente, i dati sperimentali finora ottenuti fanno quindi supporre un possibile coinvolgimento dell'alluminio, complessato con Aβ, nel processo eziopatogenico dell'AD. È stato infine condotto uno studio sull'effetto della carenza di rame su topi adulti che ha messo in evidenza come la rimozione di un metallo essenzia-

le dalla dieta per un periodo di tre mesi determini, a livello cerebrale, una variazione significativa nella concentrazione non solo del rame ma anche di altri metalli essenziali quali ferro, zinco e non-fisiologici come l'alluminio. Questo a sottolineare come esista una stretta correlazione tra i diversi sistemi di regolazione nell'omeostasi degli ioni metallici. Tale aspetto è di fondamentale importanza per la progettazione di terapie chelanti che mirino a rimuovere depositi anomali di ioni metallici che potrebbero stimolare la patologica aggregazione del peptide Aβ.

Summary

The etiopathogenesis of Alzheimer's disease (AD) is far from being clearly understood. However, the involvement of metal ions as a potential key factor towards conformational modifications and aggregation of β-amyloid peptide (Aβ) is widely recognized. The aim of this thesis was to investigate the potential and differential role of metal ions (aluminum, copper, iron and zinc) in affecting the fibrillogenesis of Aβ. Data herein reported demonstrated that the aggregational profile of the Aβ peptide was greatly different according to the metal bound. Particularly, aluminum was the most effective, among the tested metals, in promoting a conformational modification of Aβ which resulted in an increased aggregation rate and expousure of hydrophobic clusters. This modification stabilized the peptide in an oligomeric state which is higly toxic to neurons. Furthemore, the peculiar hydrophobic conformation of Aβ-aluminum complex was markedly enhanced in the presence of the $A\beta_{17\text{-}28}$ fragment with a consequent increase of deleterious effects on cell culture.

Moreover, the geno-toxic role of Aβ and Aβ-metal complexes was investigated on neuroblastoma cell culture as a model for the understanding of AD ethiopathogenesis. In collaboration with the "G. Rossi" hospital (VR), several genetic alterations determined by the Aβ-metal complexes have been correlated with the genetic expression pattern of pheripheral blood samples from AD patients, with the aim of identifying potential diagnostic biomarkers. The most promising data was obtained for the gene which encodes for glutaminyl cyclase. According to the recent literature, this enzyme could be involved in the pathology, even if the mechanism is still elusive, and a significant overexpression of this gene was indeed found in AD patients compared to age-match controls.

Additionally, the effect of a 3 month copper-deficient diet on the distribution of several metal ions (aluminum, calcium, copper, iron and zinc) in organs and tissues of adult mice was uncovered. The study highlighted that the copper-deficient diet, besides being effectively in determining copper decrease especially in the frontal area and liver, was also able to determine a decrease in the concentration of the other tested metals, creating a sort of domino effect which detrimentally altered the general

metal homeostasis. This aspect has to be taken into account especially when the use of chelating compounds, aiming at restoring the correct metal homeostasis in the brain, is proposed as therapeutic approach for AD.

Abbreviations

Aβ	β-amyloid
AD	Alzheimer's disease
ANS	Anilinonaphtalene-sulfonic acid
APP	Amyloid precursor protein
BBB	Blood Brain Barrier
CD	Circular Dichroism
CQ	Clioquinol
DLS	Dynamic Light Scattering
ETAAS	Electrothermal atomic absorption spectrometry
FAAS	Flame atomic absorption spectrometry
HFIP	Hexafluorisopropanol
MAPT	Microtubule-associated protein tau
MTT	3-(4,5-dimethylthiazol-2-yl)-2,5-diphenyltetrazolium bromide
NFTs	Neurofibrillary tangles
PHFs	Paired-helical filaments
QPCT	Glutaminyl cyclase gene
qRT-PCR	Taqman real-time quantitative polymerase chain reaction
SEM	Scanning Electron microscopy
SPs	senile plaques
TEM	Trasmission electron microscopy
ThT	Thioflavin T

1 Introduction

1.1. Amyloidoses

The term amyloidoses defines a group of diseases in which a physiological soluble protein starts to aggregate and to form insoluble fibrils. This protein structure derives from a progressive nucleation-dependent assembly process in which the thermodynamically unfavourable seed formation is followed by elongation (Bhak et al., 2009). The term **amyloid** describes the proteinaceous deposits found in several pathological conditions. Particularly, amyloid formation has been observed as a peculiar feature in various neurodegenerative diseases (NDs) including Alzheimer's Disease (AD), Parkinson's Disease (PD) and Prion Disease. This event typically occurs because of the failure of several proteins to fold correctly, or to remain correctly folded, giving rise to many different types of biological malfunctions such as misfolding and aggregation and, therefore, to many forms of diseases (Soto and Estrada, 2008). The amyloid fibril formation has been identified as a potential pathological aspect of the neurodegenerative process although the mechanism of protein deposition remains partly elusive. Recently, it has been highlighted that the oligomeric structures of the various amyloidogenic proteins could be more relevant for the activation of neurotoxic pathways. Moreover, it has been demonstrated in AD that the initial clinical symptoms often precede the formation of fibrillar deposits in the brain.

Although being formed by different proteins, amyloid fibrils are all characterized by a high β-sheet content, which explains the higly propensity to aggregate.

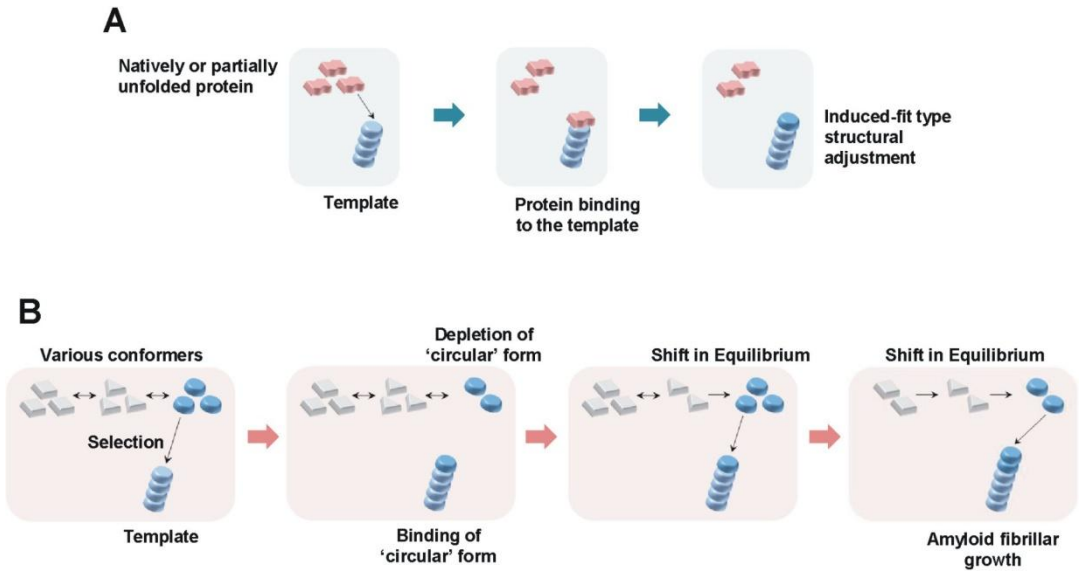

Figure 1.1. ***Template-dependent fibrillation.*** *(A) Fibril formation is characterized by the progressive binding of monomers. (B) Several conformations exist at equilibrium for a single amyloidogenic protein (from Bhak et al., 2009).*

1.2. Alzheimer's Disease

AD is the most common cause of dementia in the elderly and with the increasing life expectancy in the developing countries it is becoming a problem with a relevant health and social impact. Neurologically, it is initially characterized by a series of mild cognitive impairments, deficits in short-term memory, loss of spatial memory, and emotional imbalances. As the disease progresses, these symptoms become more severe, and ultimately result in the total loss of executive functions. Histologically, the disease is characterized by the loss of neurons in the cerebral cortex, by intracellular neurofibrillary tangles containing hyperphosphorylated τ protein and by the presence of extraneuronal senile plaques (SP), whose core is mainly constituted by a peptide mixture of 39-43 residues called β-amyloid (Aβ) (Haass and Selkoe, 2007; Iqbal et al., 2009).

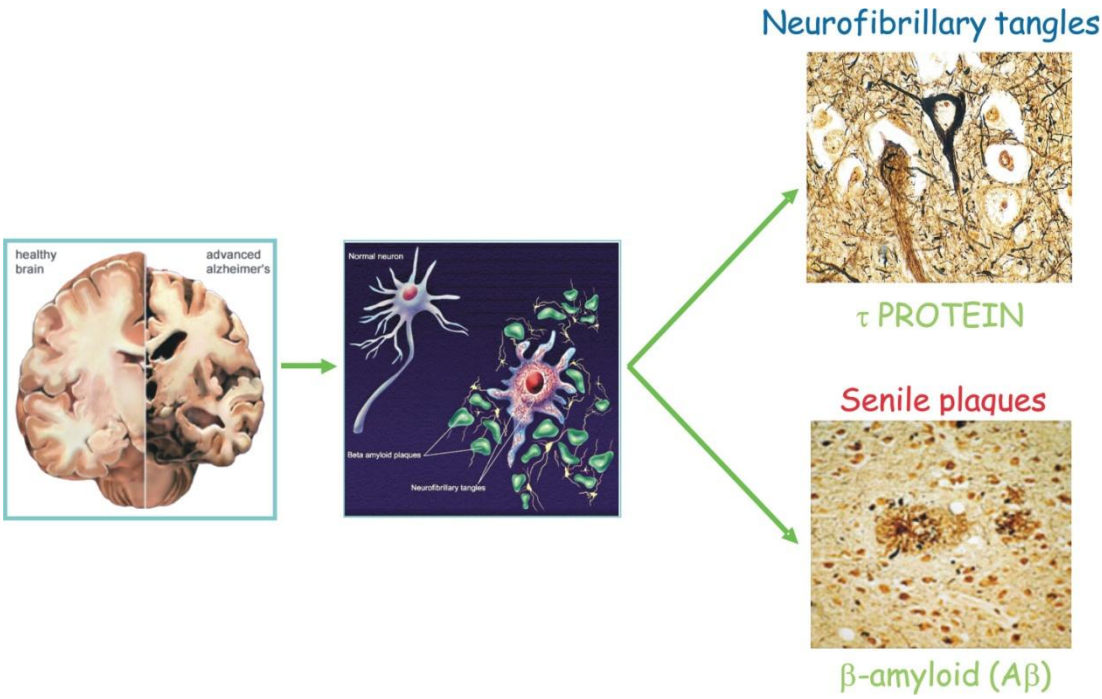

Figure 1.2.1. ***AD histological features.*** *The AD brain is characterized by a huge neuronal loss and atrophy. Histologically, aggregates of τ protein and Aβ are relevant features of the AD brain.*

1.2.1 Proteolytic processing of APP and formation of Aβ

Aβ derives from a large transmembrane precursor protein called APP. The proteolytic processing of APP can be divided into two different pathways (Figure 1.2.2.).

- The **amyloidogenic pathway** is characterized by the cleavage of β-secretase which results with the secretion of the large ectodomain sAPPβ. The remaining C-terminal fragment of 99 amino acids (C99) is further processed by γ-secretase, generating Aβ peptide and a free APP intracellular domain (AICD).
- The **non-amyloidogenic** pathway starts with APP cleavage by α-secretase, generating the N-terminal ectodomain sAPPα and the C83 fragment. This latter is further processes by γ-secretase in a similar way as in the previous pathway with the final release of AICD and of another small peptide, p3.

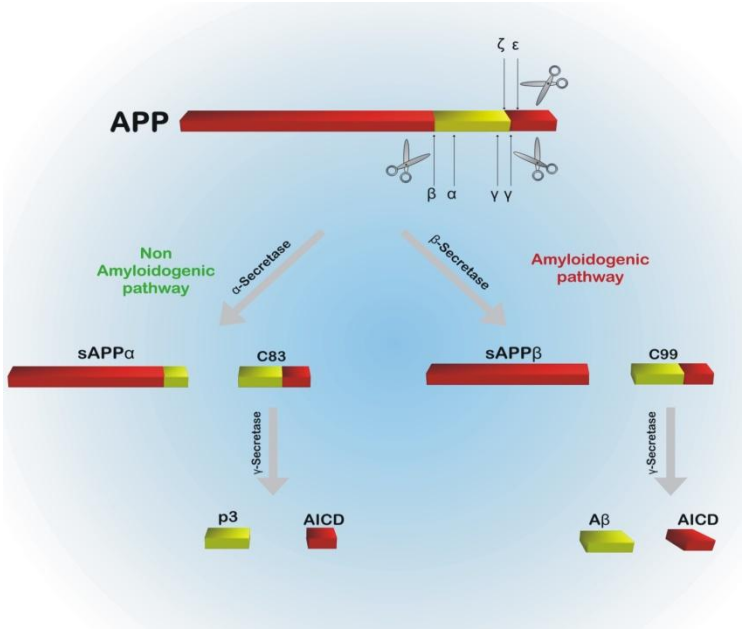

Figure 1.2.2. ***APP processing.*** *The amyloidogenic pathway involves the sequential cleavage by β-secretase and γ-secretase with the production of Aβ and AICD. The non-amyloidogenic pathway involves the cleavage by α-secretase with the release of sAPPα from the cell surface.*

Although APP processing has been extensively studied, its exact biological functions have not been completed uncovered. Recent evidence suggests a potential role of APP in the developing of adult nervous system, neuronal survivol and modulation of synaptic plasticity. sAPPα has indeed been shown to enhanced long-term neuronal survivor in rat cortical neurons (see Jacobsen & Iverfeldt, 2009). On the contrary, AICD has been proposed to be involved in apoptosis activation in differentiated neuronal cells (Nakayama et al., 2008). Nevertheless, as stated by Hardy (2009) it is surpirsing that, despite being discovered 20 years ago, we have very little idea about APP functions and no conclusive idea as to weather Aβ has a function or not. Some hypotheses have been drown: Aβ has been implicated in neuronal survival in cultured neurons (Plant et al., 2003). Moreover, Kamenetz et al. (2003) suggested that Aβ may serve as a normal negative feedback mechanism in the regulation of synaptic activity.

1.2.2. The amyloid cascade and oligomer hypotheses

In the early '90s several scientists proposed that the key event in AD etiopathogenesis was the increased production and decreased clearance of Aβ peptides, which resulted in the extracellular deposition of insoluble proteinaceus deposits into SP (Hardy & Higgins, 1992). This detrimental deposition was suggested to trigger a cascade of events, finally promoting neuronal death (**amyloid cascade hypothesis**). Over time, the initial idea that SP are the only pathogenic responsible initiating neuronal loss has fallen out of favour in the light of more recent evidence. First, the pathological relevance of SP has been questioned by many investigators as fibrillar deposits have been detected also in non-demented individuals and thus the plaque load does not correlate well with the degree of dementia in humans. Moreover, many AD patients with severely impaired memory show no plaques at *post-mortem* analysis (Nordberg, 2008) and mouse models of AD display memory deficits before the observation of SP in the brain (Lesne et al., 2006).

These observations have given rise to new speculations supporting the need of an amyloid cascade revision. Current studies, investigating the importance of the various soluble Aβ assembly, indicate that early-stage Aβ aggregates, **oligomers**, could be more relevant to AD etiology and correlate better than insoluble deposits with the severity of dementia (Naslund et al., 2000). Significantly, elevated levels of soluble oligomers were indeed found in AD brain compared to controls (Tomic et al., 2009). The focus of the research moved then toward Aβ oligomerization pathway which finally ends with fibril formation. Thus, soluble oligomers seem to act a paramount role in triggering the early events causing the disease while SP, despite contributing to neuronal injury (Tsai et al., 2004), are more likely a reservoir of toxicity or even a protection (Caughey & Lansbury, 2003).

It is emerging that Aβ accumulates also intracellularly in mouse models of AD and in human AD brains and this could represent a previously unknown detrimental contribution to the disease progression (LaFerla et al., 2007).

The pathway of Aβ generation and consequent oligomer formation are, at least in part, still elusive (Figure 1.2.3).

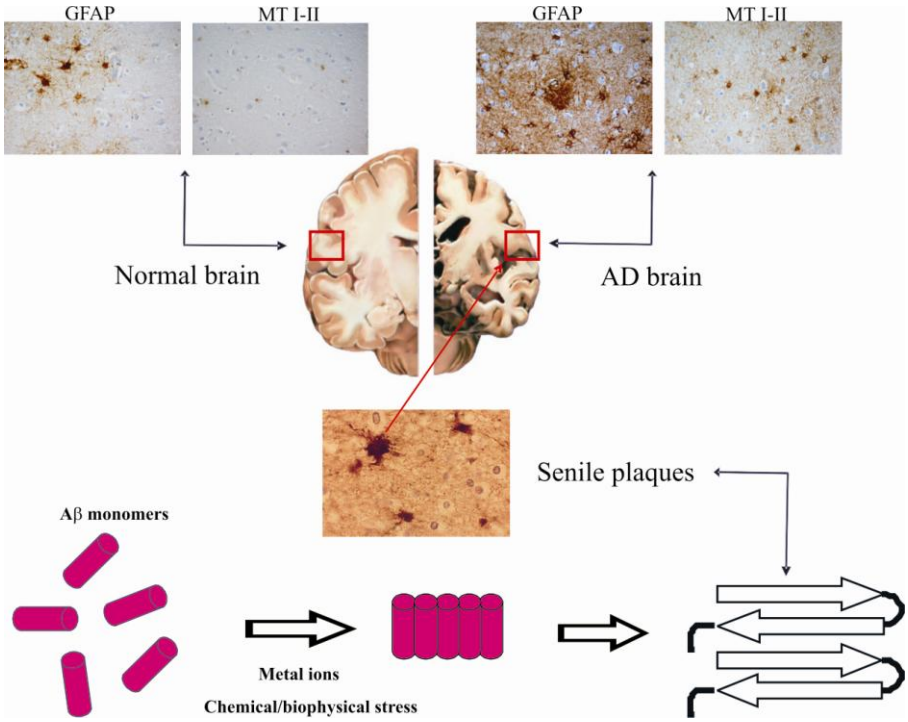

Figure 1.2.3. ***Pathological hallmarks of AD.*** *Extracellular deposition of the Aβ fibrils in the* ***SP*** *and intraneuronal aggregates of paired helical filaments (PHFs) of the hyperphosphorylated τ protein in* ***neurofibrillary tangles (NFTs)*** *represent the hallmark pathogenic features of the disease, and their observation in a post-mortem examination is still required for a diagnosis of AD. In accordance with the amyloid cascade hypothesis, it has been proposed that Aβ aggregation follows a sequence by which the accumulation of soluble Aβ, is followed by the appearance of low molecular weight oligomers that rapidly associate in higher-order aggregates and finally precipitate to form senile plaques. Aβ aggregation is greatly influenced by all the metal ions (e.g., Al, Cu, Fe, and Zn) that are found in both the core and rim of the AD senile plaques (Zatta et al., 2009).*

The *in vitro* investigations using synthetic peptides have shown a complex pattern of Aβ aggregation, with differences between $A\beta_{1\text{-}40}$ and $A\beta_{1\text{-}42}$ oligomerization (Ricchelli et al., 2005). Nevertheless, it is almost unanimously recognized that Aβ exists in a 'natively unfolded' conformation which undergoes nucleation-dependent polymerization (Roychaudhuri et al., 2009). On the contrary, there is not a general consensus in discriminating which is the most toxic specie of Aβ. According to few studies the highest neurotoxicity was associated only with the Aβ dimers and not with the higher oligomers (Shankar et al., 2008). Other groups showed that much larger oligomers, termed Aβ*56, rather than the smaller dimeric/trimeric aggregates could be more detrimental (Lesne et al., 2006; Cheng et al., 2007). These oligomers possibly composed of 12 monomers, despite being observed in a transgenic mouse model, have not already been isolated in AD brains.

1.2.3. Aβ and cell membranes

Results from several studies suggested that Aβ neurotoxicity might be mediated through direct interaction between the peptide and cellular membranes (Kayed et al., 2004; Demuro et al., 2005) with the resulting activation of apoptotic pathway (Demeester et al., 2000). From this prospective, the amphipathic character of Aβ renders it an ideal target which might pathologically associate with the membrane. In addition, several papers have highlighted the promoting effects of neuronal lipid membranes on Aβ-conversion into toxic oligomers (Curtain et al., 2003; Kakio et al., 2002). It has also been proposed that part of the critical balance between toxic and inert Aβ pools is determined by the relative amounts of lipids in the direct environment of the plaques (Martins et al., 2008).

Overall, these studies indicate that the relationship between Aβ and cellular membrane could be crucial in the process leading to the pathology. In accordance, perturbation in the lipid distribution is evident in many AD patients (Ji et al., 2002; Pettegrew et al., 2001) and hypercholesterolemia is an early risk factor for the development of AD (Kivipelto et al., 2001). *In vitro* studies indicated that increased cellular cholesterol levels result in the increased production of Aβ peptides (Fassbender et al., 2001). Moreover, it has been reported that proteins relevant to Aβ generation localize in the membrane rafts (Reid et al., 2007). Nevertheless, the possible mechanism underlying this interaction is an unsolved issue. Many hypotheses have been made ranging from the alteration of the physiological characteristics of the membrane (Ji et al., 2002), lipid peroxidation (Koppaka et al., 2000) to the formation of calcium-permeable ion channels which allow excessive Ca^{2+} influx which disrupts physiological homeostasis (Li et al., 2001). This latter event could occur either through the modulation of an existing Ca^{2+} channel or through the formation of a new cation-selective channel. The type of membrane modifications determined by the interaction with Aβ are unknown, although Durrel et al. (1994) developed theoretical models to describe the structures of ion channels formed by the membrane bound to $Aβ_{1-40}$. Nevertheless, $Aβ_{1-42}$ seems to be more prone in inducing cellular morphological changes, even at nanomolar concentrations (Li et al., 2002).

1.2.4. τ protein

Neurofibrillary tangles (NFTs) are composed of hyperphosphorylated forms of the microtubule associated τ protein. τ interacts with tubulin and promotes its assembly into microtubules and helps stabilize their structures. Thus, hyperphosphorylation of τ impaires microtubule structures and compromises axonal transport (Iqbal et al., 2009). In addition, conformational changes and cleavage of τ have also been implicated in the pathogenesis of AD (Luna-Munoz et al., 2005).

The importance of this protein for the development of AD has been enhanced by findings demonstrating that the number of NFT, and not SP, better correlates with the degree of dementia (Iqbal et al., 2009). Thus, neurofibrillary lesions seem to be required for the AD clinical manifestation.

1.3. Brain and metal ion dysmetabolism

Along with many other etiological factors, metal ions such as copper (Cu), zinc (Zn), iron (Fe) and aluminum (Al) have been all advocated as cofactor for AD development in that they have been reported to act as modulators of the aggregation of some specific proteins that are directly linked to the disease, especially Aβ. In addition, AD but also other common ND show, among other features, a common impairment of metal ion brain homeostasis. The above metals, apart from Al, are fundamental for the correct brain functioning, however at the same time they need to be strictly regulated to avoid the triggering of detrimental cell processes; indeed, depletion and accumulation of these metals can lead both to abnormal interactions with proteins or nucleic acids and to consequent cell damage. The brain therefore strictly regulates the metal ion fluxes as there is no passive transport of metal ions across the blood brain barrier (BBB). Thus, for the major ND, the described metal imbalance is not simply and solely due to an increased exposure to metals but, rather, to a more complicated impairment in relevant homeostatic mechanisms.

Intriguingly, ageing is considered as one of the most relevant risk factors for AD and accumulating evidence has revealed a general age-related increase for the above metals in the brain (see next paragraph). Brain metal accumulation, especially for redox metals such as Cu and Fe, leads to increased oxidative stress (with the pro-

duction of excess superoxide and hydroxyl radicals), and is associated with severe neuronal damage in physiological ageing as well as in AD (Butterfield et al., 2007).

In a way, metals may provide the link between protein misfolding and aggregation, oxidative stress and the cascade of biochemical alterations, eventually leading to neuronal cell death. Consequently, the transport and the distribution/accumulation processes of metals are of particular interest especially because NDs with a distinct etiology could share some common pathogenetic pathways. The essential role of metals for a variety of general cellular functions is unanimously recognized, as well as the fact that they are required by at least one quarter of all proteins as cofactors (Ferrer et al., 2007).

Several excellent reviews dealing with metal ions physiology have been published recently (*e.g.* Garrick and Garrick, 2009 for Fe; Nakashima and Dyck, 2009 for Zn). The issue is so complicated that it is very difficult to effectively summarize the countless aspects of the Cu, Fe, and Zn metabolic pathways and for this reason we refer to those specific reviews. In turn, the occurrence of metal dysregulation or dyshomeostasis in the brain has been described by a vast literature under a variety of conditions ranging from normal ageing to genetic diseases, from reduced metal supplementation to excessive metal exposure and in relation to a variety of NDs (Zatta, 2003; Zatta et al., 2009). However, the detailed significance of brain metal dyshomeostasis (BMD) is still a matter of intense debate. It is generally accepted that BMD can be defined in terms of the occurrence of relevant modifications of metal concentrations either in the total mass of the brain or in specific brain areas as a consequence of physio-pathological events. According to this definition, the assessment of metal dyshomeostasis would primarily depend on the obtainment of reliable and unambiguous analytical data on brain tissues, mainly by sophisticated techniques such as atomic absorption spectroscopy or inductively coupled plasma-mass spectrometry measurements. Indeed, metal dyshomeostasis may arise from an abnormal metabolic activity of a specific metal ion due either to misallocation or to the lack or insufficiency of specific metal binding proteins. This latter kind of dyshomeostasis is far more difficult to establish given that either a detailed metal speciation or metal distribution studies are required. Unfortunately, so far, the availability of adequate sets of analytical and/or speciation data for brain metals is disappointingly scarce, in

that most studies report only fragmentary and sporadic data which are sometimes contradictory.

The collection of reliable analytical data for brain metals is complicated further by the extreme structural, functional, topographical and architectural complexity of the brain itself**.** Thus, the assessment of BMD is currently founded on several independent, often unrelated, qualitative indications rather than on conclusive quantitative data. It follows that new and systematic analytical data on brain metal concentration distribution and speciation are strongly required.

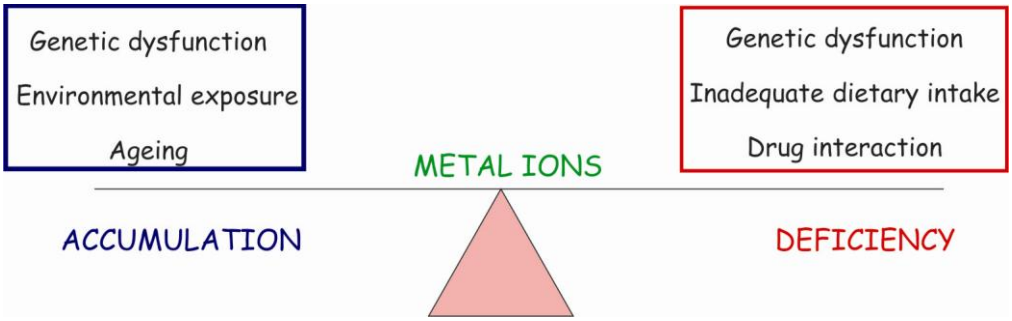

Figure 1.3.1. ***Schematic representation of the factors affecting the delicate balance between metal ion accumulation and deficiency.***

1.3.1. Metal dysmetabolism in ageing

The ageing process, though physiological in nature, has been considered as a critical condition characterized by a progressive deterioration of the overall homeostatic mechanisms. In the human brain, ageing implies a variety of morphological alterations which include enlargement of ventricles and progressive decrease of brain weight (Bertoni-Freddari et al., 2008). Moreover, a significant reduction in the number of synapses has been reported for different regions of the central nervous system (CNS) both in animals and in humans, confirming that this is a characteristic feature of the ageing brain (Bertoni-Freddari et al., 1996). Thus, a distinction between the neurological alterations occurring in normal aged brains and in NDs is not always easy to identify.

Interestingly, it has been demonstrated in different animal species, including humans, that ageing itself is characterized by an alteration in brain metal content and specific topographical distribution. The mechanisms responsible for this imbalance

are not clearly understood: one possible explanation might lie in age-induced progressive failure of metal controlling systems and ineffective functionality of physiological barriers (e.g. BBB, gastrointestinal tract) due to cumulative errors occurring throughout the course of life. Tarohda et al., (2004) observed in rats a variation with age of manganese (Mn), Fe, Cu, and Zn. The concentrations of each of these metals were was quite specific. Cross et al., (2006) showed, in aged rats, reduced bulk transport of Mn from the olfactory bulb to the anterior tract, highlighting a significantly decreased rate of Mn transport when compared to young rats.

Metal distribution in relation to age has also been widely analyzed in humans. Zn concentration in the brain is typically 150 μmol/l (Takeda et al., 2003). However, its distribution is not homogeneous since it is significantly higher in gray than in white matter. Brain regions particularly rich in this metal are the hippocampus, the amygdala and the cortex (Weiss et al., 2000). Even if during ageing Zn distribution in the brain changes in relation to the region considered, many studies have reported little or no decrease in its levels in mice and humans (Del Corso et al., 2000).

Investigation of the Cu content in the aged human brain has not yet allowed a definite conclusion to be reached. However, normal ageing seems to increase Cu levels in several tissues, including the brain (Morita et al., 1994). The highest concentrations of Cu were found in *substantia nigra* (SN) and in other cerebellar regions (Rajan et al., 1997).

The total brain Fe, after the very early stage of life, increases rapidly and remains stable for the rest of the lifespan. According to recent reports, it increases in the aged brain (Stankiewicz and Brass, 2009) particularly in SN and *globus pallidus* (GP) (Gotz et al., 2004).

Al concentration during the lifespan appears to be biphasic: there is an increase with age up to 40 years, followed by a plateau up to 70 years. A second increase is observed in the course of the eighth and ninth decade of life (Roider and Drasch, 1999). Of the different brain areas analysed, GP, SN, and *nucleus ruber* (NR) were found to be the richest in Al in the aged population (Speziali and Orvini, 2003). It therefore seems that a breakdown of metal regulation could be an inevitable consequence of ageing.

1.3.3. Metal dysmetabolism in AD

Many are the studies which have implicated biometals in the development and/or progression of AD (Crichton et al., 2008). In analytical studies, the hippocampus and amygdala were sites where the concentrations of various elements were most frequently found to be different between control and AD groups (Speziali & Orvini, 2003). Convincing results have shown increased metal concentrations within the SP compared with surrounding tissues both in transgenic mice (Rajendran et al., 2009), as well as in humans (Lovell et al., 1998).

Zinc

The potential role of Zn as a cofactor in the pathogenesis of AD was strengthened when Lovell et al. (1998) found a Zn enrichment in SP and a Zn elevation in the neuropil of AD patients as compared to controls. These results were later confirmed by several other research groups (Stoltenberg et al., 2005; Miller et al., 2006). However, controversial results have been published in an attempt to quantify Zn in AD serum (Rulon et al., 2000; Dong et al., 2008) or cerebrospinal fluid (CSF) (Molina et al., 1998; Gerhardsson et al., 2008).

Despite these controversial reports, studies on the role of Zn in AD have shown that variation of brain Zn levels may contribute to precipitate Aβ giving rise to protease-resistant unstructured aggregates which synergistically increase Aβ neurotoxicity (Bush, 2003). In addition, Zn binding to Aβ could also reduce Zn availability at the synaptic cleft leading to deleterious effects in terms of the role of Zn in neuronal signaling and synaptic plasticity (see Frederickson et al., 2005). As a second observation, several studies have supported the hypothesis that vesicular Zn released in the synaptic cleft during neurotransmission may be one contributing factor for the recruitment of Aβ oligomers to synaptic terminals (Deshpande et al., 2009).

Furthermore, when transgenic mice lacking Zn transporter 3 (ZnT3) were crossed with Aβ-producing mice, a marked decrease of the plaque load was observed (Lee et al., 2002), suggesting that synaptic Zn may play a role in enhancing Aβ aggregation and plaque deposition. Moreover, it is worth noting that MT I and II were

histochemically found to be dramatically increased in astrocytes of AD brains compared with those of controls (Zambenedetti et al., 1998). Considering that Zn is an inducer of this family of proteins, a correlation between Zn levels and the pathology should be further investigated.

Behavioral studies on transgenic mice examining the effect of Zn supplementation reported an increased impairment of spatial memory, but with a concomitant unexpected reduction of Aβ deposits (Linkous et al., 2009). In contrast, compounds affecting Zn homeostasis have been shown to decrease Aβ brain deposition (Lee et al., 2004; Adlard et al., 2008).

Cuajungco and Faget (2003) conducted a good review of several controversial findings and conclude in favour of a paradoxical role for Zn in AD. It could indeed be that Zn is released following oxidative/nitrosative stress factors implicated in AD etiology. In turn, this Zn increase can trigger neuronal death giving rise to a vicious cycle.

In any case, several aspects of the potential involvement of Zn in AD pathogenesis remain unclear. Better understanding the correlation between Zn and AD is of key interest given that Zn supplementation has been found to be protective in the treatment of age-related macular degeneration (AREDS, 2001) and it has been proposed as haveing beneficial properties for the elderly (see Moccheggiani et al., 2005). In any case, studies reporting the effect of Zn supplementation in AD patients are still very scarce. Although it is difficult to evaluate the real effect of Zn supplementation, given that several other micronutrients were contextually administered, much caution in designing Zn protocols is required. It is well known that increased dietary Zn causes Cu deficiency and that in turn, given that Cu is involved in Fe transport, it can induce anaemia (Salzman et al., 2002). Thus, if any Zn supplementation therapy is proposed then a strict regulation of other nutrients must be implemented.

Copper

The potential involvement of Cu in physiology (Kramer et al., 2003) and pathology (Bush, 2003) is even more complicated. There is a general agreement with the hypothesis that the AD brain could be characterized by an excess of Cu in the extracellular space (Crouch et al., 2006), given that the metal ion accumulates in large

quantities in the SP (Lovell et al., 1998), and at the same time by an intracellular decrease of Cu as compared to healthy control brain. Nevertheless, the analytical data are often controversial: Deibel et al., (1996) reported a general decrease in total Cu brain level of approximately 20% in AD brain compared to controls, even if other groups have failed to confirm this data (Loeffler et al., 1996).

The link between AD and Cu metabolism could be explained by the potential control exerted by Cu on Aβ levels. It has been demonstrated that exposing cells over-expressing APP to high Cu levels results in a decrease of secreted Aβ (Borchardt et al., 1999). The same effect was obtained by elevating Cu levels in the brain both by genetic (Phinney et al., 2003) as well as with dietary supplementation (Bayer et al., 2003) in AD animal models. It has been proposed that an overproduction of APP, and consequently of Aβ can lead to a Cu efflux from the cell which then causes a concomitant reduction of the protective superoxide dismutase (SOD-1) enzyme (Figure 1.3.2).

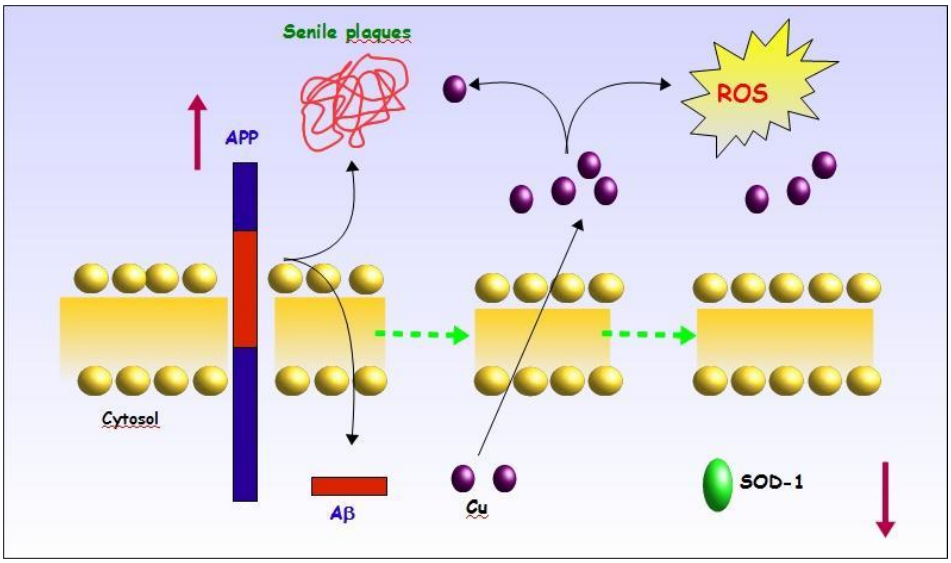

Figure 1.3.2. ***Potential interaction between APP and Cu.*** *It has been proposed that Aβ overproduction could stimulate Cu efflux from cell cytoplasm, which consequentially causes the reduction of superoxide dismutase 1 activity (SOD-1) (Bolognin et al., 2009).*

Thus, Cu supplementation, or better proper delivery into the brain, could be beneficial (Bayer et al, 2006). In this regard, Crouch et al. 2009 demonstrated that increased intracellular Cu availability inhibited the accumulation of Aβ oligomers

and τ phosphorylation. Kessler et al. (2008) recently evaluated the effect of oral Cu supplementation on AD CSF biomarkers in a pilot phase 2 clinical trial. They reported a stabilizing effect of the supplementation in terms of contrasting the decrease of $A\beta_{1-42}$ in the CSF, which is generally reported in AD patients compared to controls (Lewczuk et al., 2004). However, this effect does not correspond to any improvement in cognitive performance and, more generally, as highlighted by Quinn et al. (2009), none of the above studies have demonstrated a Cu deficiency in AD patients.

Iron

Much of the literature reports increased Fe levels and Fe-binding proteins in the AD brain (Lovell et al., 1998; Cahill et al., 2009) and several hypotheses have been proposed which attempt to clarify this involvement (see Altamura & Muckenthaler, 2009). Smith et al. (2007) stated this could be a secondary effect caused by, for example, increased heme oxygenase activity in response to oxidative stress (Schipper, 2004). This could be further strengthened by the fact that, despite being found to interact with Aβ *in vitro* (Hu et al., 2006), Fe does not co-purify with Aβ extracted from plaques (Opazo et al., 2002). Most recently, other pathways have been explored; in particular, it has been assumed that Fe could directly influence Aβ production through the modulation of furin, a ubiquitous enzyme, whose proteolytic activity is required for many cellular processes, including α- and γ-secretase processing. According to Silvestri & Camaschella (2008) high cellular Fe levels lower furin activity, which in turn reduces α-secretase activity favouring β- and γ-secretase activity with the consequent enhancement of Aβ production. In accordance, the furin mRNA level was reduced in AD brain patients (Hwang et al., 2006).

A further correlation between Fe and AD is based on the observation that oxidative stress markers are highly expressed in AD-affected brain regions (*e.g.* Zambenedetti et al., 1998) and this matches with the redox-active nature of Fe. Fe-dependent ROS production is indeed able to increase Fe cellular uptake (Pantopoulos & Hentze, 1998) which, in turn, could increase oxidative damage giving rise to a vicious cycle.

Another aspect highlighted by Rogers et al. (2002) was the presence of a functional Fe-regulatory element in the 5'-URT mRNA encoding the APP. Intracellular Fe levels were shown to modulate APP synthesis in neuroblastoma cells, while the addition of an Fe-chelator reduced APP levels.

In summary, although the mechanism for Fe accumulation in AD is still unknown, it is necessary to consider Fe as an important cofactor. It is also undeniable that diseases directly related to increased levels of this metal (*e.g.* haemochromatosis) are not characterized by enhanced deposition of SP, proving that it could be one of many other contributing factors.

Aluminum

Since the 1970's it has been hypothesized that exposure to Al may enhance the pathogenesis of AD, mainly in genetically predisposed subjects (Campbell, 2006). Significantly raised levels of Al were indeed reported in the parietal cortex of the AD brain as compared with controls (Srivastava & Jain, 2002; Yumoto et al., 2009). Moreover, early studies using Laser Microprobe Mass Analysis (LAMMA) showed high Al concentrations within the AD neurofibrillary tangles (Good & Perl, 1993). Up until now, no physiological role has been established for this element (Bala Gupta et al., 2005). Some studies have summarized the effects of occupational exposure to Al suggesting that it induces relevant neurotoxic effects following acute or subacute exposure (see Krewski et al., 2007).

Alfrey et al. (1976) described for the first time a neurological condition resembling AD dementia which was called dialysis encephalopathy (DE). DE consists of an abnormal accumulation of Al in the brain of uremic patients with renal failure undergoing chronic dialysis, which occurs when tap water, without any further purification, was used in the dialysis process (Zatta et al., 2004; Zatta, 2006). The effects of Al on cognitive functions were reversible since DE patients greatly improved following treatment with desferrioxamine (DFO) (Yokel, 1994). Once Al was removed from the "dialysis bath" the DE practically disappeared. These findings have given rise to widespread speculation as to whether AD and Al could be linked, but no conclusive results were established (Reusche, 2003). Indeed, the epidemiological results which addressed the problem of Al in drinking water in connection with the inci-

dence of AD were controversial (Reusche, 2003). In addition, many nephrologists currently use Al salts to decrease the hyperphosphatemia in uremic subjects with no major incidence of AD among these patients with respect to general population. Thus, Al itself cannot be a sufficient trigger of AD and there must be another reason for the potential AD-Al connection.

In this complex scenario, we have recently proposed that the binding of Al to Aβ can promote a conformational change which stabilizes the peptide in its oligomeric form (Drago et al., 2008b; Zatta et al., 2009), considered by the recent literature as the most toxic species (Glabe, 2005). Such Aβ-Al metal complex showed a dramatic reduction in the sequestration in the brain microcapillaries and an increased high permeability across BBB, a phenomenon that is leading to intra-cerebral accumulation of Aβ-Al (Banks et al., 2006). Al favors the exposure of peptide hydrophobic clusters which result in a peculiar aggregation pattern compared to the other metals tested (Cu, Fe, Zn). Furthermore, we have demonstrated that in neuronal cell cultures exposed to different Aβ-metal complexes (Aβ-Cu, Aβ-Zn, Aβ-Fe, and Aβ-Al), only the Aβ-Al complex is able to alter glutamate-driven intracellular calcium (Ca) rises and to inhibit the oxidative respiration in isolated rat brain mitochondria (Drago et al., 2008b). Finally, Al dyshomeostasis was also recently found in a triple transgenic AD mouse, the 3xTg-AD: experiments employing mass spectrometry indicate that, when compared with the distribution of other AD-relevant metals (Zn, Cu, and Fe), Al is the only metal ion that is increases significantly in the cortex of 14 month old 3xTg-AD mice (Drago et al., 2008b).

In summary, the potential involvement of Al in AD still remains of great interest yet controversial along with many other hypotheses on AD etiology (*www.alzforum.com*) (Figure 1.3.3).

Finally, several other arguments *pro and con* the possible role of Al in AD are represented in the literature; however, we pinpoint two aspects that necessarily have to be considered before approaching this issue. Firstly, Al has a complex hydrolysis pH-dependent chemistry in biological systems which can account for many inconsistencies reported in the literature on the effects of Al on animal or cellular models. As an example, when Al inorganic salts such as chloride, sulphate, hydroxide or perchlorate are dissolved in water at a calculated concentration of 10 mM, the ana-

lytical Al concentration in solution is about 50 μM. The use of Al-lactate or Al-aspartate, however, increases the soluble Al concentration to 50-330 μM (Zatta, 2002). Hence, the examination of the metal bioavailability under physiological conditions has to be taken into account while designing Al studies. Secondly, a distinction has to be made between the concepts of neurotoxicity and neurodegeneration. Al has been aptly described as a neurotoxic element (Zatta, 2002) if it can not be physiologically excreted or it is in direct contact with the brain. Besides the neurotoxicity of Al at high concentration, the role of this metal ion in affecting pathways related to neurodegenerative mechanisms should be further investigated.

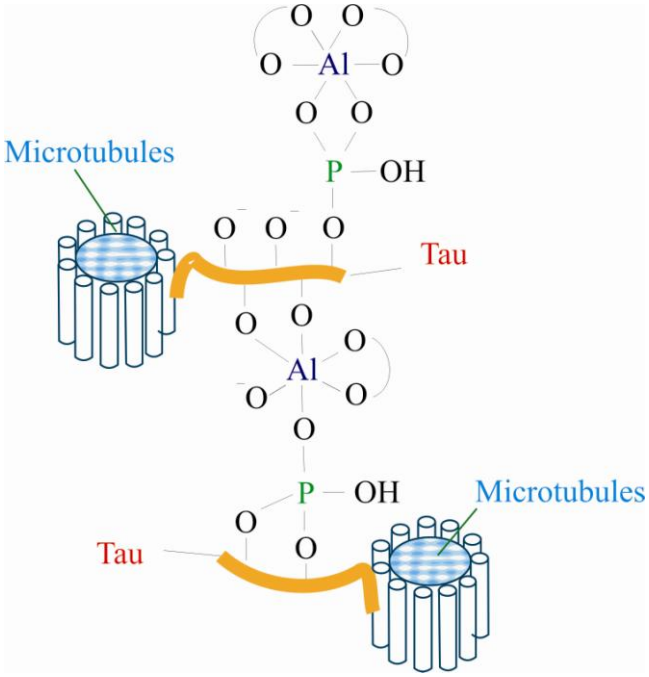

Figure 1.3.3. ***The tau and tangle hypothesis.*** *Tau binding to microtubules is disrupted by phosphorylation. Decreased tau binding to microtubules might result in increased free tau which, under the appropriate conditions, will self-aggregate to form insoluble paired helical filaments. Loss of tau binding is predicted to result in loss of microtubule function.*

1.4. Chelation therapy

Since the demand of new and effective strategies for the treatment of ND continues to grow, the use of chelating agents to scavenge free metals, that are present in excess in the brain or are experiencing severe dishomeostasis, may represent a very promising and well grounded therapeutic option. In principle, treatment with chelat-

ing agents should aim at abstracting and removing metal ions such as Cu, Fe, Zn and Al which may be responsible for inducing direct neurotoxic effects. Indeed, this type of approach turned out to be successful for a few rare diseases where a dramatic brain metal accumulation takes place, in most cases as a results of gene defects. In contrast, for most other cases, the design of novel and effective non-toxic chelating molecules represents today a very challenging task and a number of specific requirements must be met to obtain candidate drugs, as detailed below; an excellent review on these aspects recently appeared (Gaeta & Hider, 2005).

An important requirement for an effective metal targeting agent in ND is its ability to cross the BBB. This excludes a large number of common metal ligands because of a marked hydrophilic nature. Moreover, specific and moderate, rather than indiscriminate and massive chelation of excess metals is highly preferred when dealing with the most frequent ND. Thus, ligands with intermediate affinity and appreciable metal selectivity should be designed, capable of disrupting a few relevant metal-peptide interactions (Storr et al., 2007) rather than inducing generalised, and thus highly toxic, metal depletion. Indeed, strong metal chelators are expected to compete successfully with metal-binding proteins, thereby altering physiological metal distribution and inhibiting essential metal-containing enzymes.

These observations feature, for the major ND, a type of chelation therapy that is radically different from the classical protocols, originally developed in the frame of clinical toxicology to contrast heavy metal poisoning. In fact, the main goal here is not really that of removing huge amounts of deleterious and non-physiological metals from the brain (indeed, the observed increase of total brain metal concentrations in the major ND are never that spectacular) but to endeavour to redistribute more conveniently brain biometals (either intracellularly or intraregionally). This goal may be achieved by abolishing abnormal metal/protein interactions, by contrasting localised metal excesses, by normalising intra/extra cellular metal ratios or by restoring the correct balance among the main biometals (Cu, Fe and Zn). In some cases, this latter objective may be better reached by supplying a defective metal capable of counteracting the effects of the excess metal (for example, consider the well known Cu/Zn antagonism) rather than by directly removing the excess metal itself. In all cases, as mentioned above, specific attention must be paid to the nature of the ligand

(hydrophobic/hydrophilic), to its toxicological profile, to the strength and selectivity of its metal binding, to its targeting to specific brain areas, and to the nature of the resulting metal complexes. Overall, these considerations warrant novel and smart therapeutic approaches for the major ND, that are highly peculiar and might be better defined as metal targeted strategies rather than metal chelation.

1.4.1. The "domino effect"

When approaching AD it seems reasonable not to consider the metal dyshomeostasis as the only causative factor for disease etiology. However, in the context of the impairment of the homeostatic mechanisms, largely reported in the aged brain, this imbalance may play a relevant role in the progression of these pathologies. It also follows that the imbalance of only one metal can not be the exclusive triggering factor as, for example, Cu excess as well as deficiency have been well characterized in Wilson's disease and Menke's disease, respectively. These genetic disorders are described by a specific neurological scenario which is different from the kind of impairment seen in, for example, AD. Nevertheless, the above mentioned biometals can all interact with a key protein enhancing their neurotoxicity (*e.g.* Aβ) or activating detrimental processing pathways.

The understanding of the real role played by metal dyshomeostasis is greatly hindered by the scarce knowledge of the mechanisms underlying these diseases. In any case, there is no clear consensus about the real metabolic state of the different metals in the disease (*e.g.* Cu). Thus, for the main biometals supplementation, lowering as well as redistribution strategies have all been proposed. It must be highlighted that focusing only on a single metal as the culprit of the disease could be misleading or reductive. The change of a single metal can indeed upset the whole metal pool or part of it (*e.g.* the Cu deficiency following Zn deficiency). This effect produced by modifying the uptake or the metabolism of one single element as the cause for the alteration in the physiological distribution, concentration, and excretion of several other elements is called "domino effect" and it must be taken into account when proposing metal-modulating strategies as a therapeutic approach. Thus, if a single-metal modulating strategy must be undertaken, it will also be important to monitor the distribution of the other metals.

1.4.2. Clioquinol (CQ)

Clioquinol (5-chloro-7-iodo-8-hydroxyquinolone, CQ) is an old anti-amoeboic compound used until 1970 when it was withdrawn because it was epidemiologically linked to some cases of subacute myelo-optic neuropathy (SMON) (Bush & Masters, 2001). Acute CQ treatment in mice caused alteration in vitamin B_{12} distribution in the kidneys and skin, while chronic treatment decreased B_{12} blood concentrations and also its uptake in the brain (Yassin et al., 2000). CQ is a hydrophobic molecule which is able to cross the BBB; moreover it has a great affinity for Zn and Cu (Di Varia et al., 2004). Therefore, CQ has been proposed as a modulator of metal homeostasis, helpful in reducing Aβ levels and slowing the rate of cognitive decline in AD patients (Ritchie et al., 2003).

Preliminary studies showed that treating Tg2576 mice orally for 9 weeks with CQ resulted in a 49% reduction of Aβ levels (Cherny et al., 2001). Furthermore, CQ was used in a small clinical trial showing that it mildly slowed, compared with the placebo control, the cognitive decline in a subset of AD patients (Ritchie et al., 2003). Conversely, according to others, the number of recruited patients was too small and it did not permit the detection of long-term adverse effects of CQ (Jenagaratnam et al., 2006). Recent findings showed an increased lethality of APP (amyloid precursor protein) transgenic mice upon CQ treatment (Schafer et al., 2007). On the other hand, controversial reports have appeared concerning the actual molecular mechanism of CQ. The observed decrease of Aβ levels is thought to be the consequence of copper-driven metalloprotease activation.

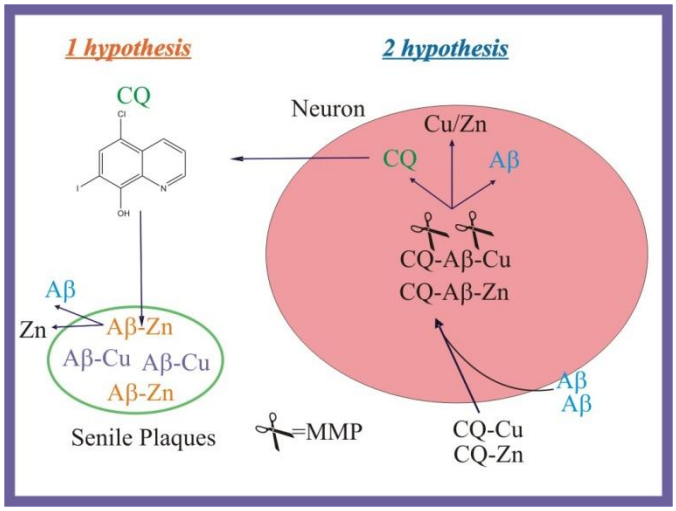

Figure 1.4.1. ***Clioquinol (CQ): proposed action mechanisms.*** *CQ seems to have ionophore activity that favors the entrance into cells of Zn and Cu. Cu entry in particular determines the activation of metalloproteases (MMP) resulting in the degradation of Aβ. In addition CQ could also remove Cu and Zn that is sequestered in SP, thereby reducing the oligomerization of the peptide.*

However, it is conceivable that CQ may exert its pharmacological effects through other different mechanisms. Recent findings indicate that CQ may act also as an inhibitor of carbonic anhydrase (CA) (Innocenti et al., 2008) probably thanks to its biciclyc ring system and to the presence of heteroatoms which allow better hydrophobic interactions with the metalloenzyme. Nevertheless, the consequence of the CA inhibition in neuronal cells has yet not been investigated in details. Thus, further studies are now warranted to better evaluate the safety and the effectiveness of CQ as a possible medical treatment for AD.

2 Materials and Methods

2.1. Chemicals

Synthetic $A\beta_{1-42}$ was purchased from Biosource (Camarillo, CA USA). $Al(C_3H_5O_3)_3$, $CuCl_2$, $ZnCl_2$, $FeCl_3$, hexafluoroisopropanol (HFIP), 3-(4,5-dimethylthiazol-2-yl)-2,5-diphenyltetrazolium bromide (MTT), thioflavin T (ThT), and 8-anilinonaphtalene-sulfonic acid (ANS), $A\beta_{17-28}$ were obtained from Sigma Aldrich (St. Louis, MO). Synthetic dimyristoylphosphatidylcholine and dimyristoylphosphatidylethanolamine were purchased from Avanti Polar Lipids (ALA, USA).

2.2. Aβ and Aβ-metal complexes preparation.

Aβ was dissolved in hexafluorisopropanol (HFIP) for 40 min at room temperature and then separated into aliquots. HFIP was removed under vacuum in a Speed Vac (Sc110 Savant Instruments). This treatment was repeated three times (modified protocol from Dahlgren et al., 2002). The Aβ-metal complexes were prepared by 24h dialysis against metal solutions ($Al(C_3H_5O_3)_3$, $CuCl_2$, $ZnCl_2$, $FeCl_3$) at T= 4°C using Spectra/Por^R Float-A-Lyser^R tubes (Spectrum Labs) with 1000 Molecular Weight Cut Offs (MWCO). Then, Aβ-metal complexes were dialysed against distilled water (three water changes) for 24h in order to remove the excess of metals. The same treatment was also performed with Aβ alone (Drago et al., 2008a). Aliquots of Aβ, and Aβ-metal complexes were stored at -20 ºC until used.

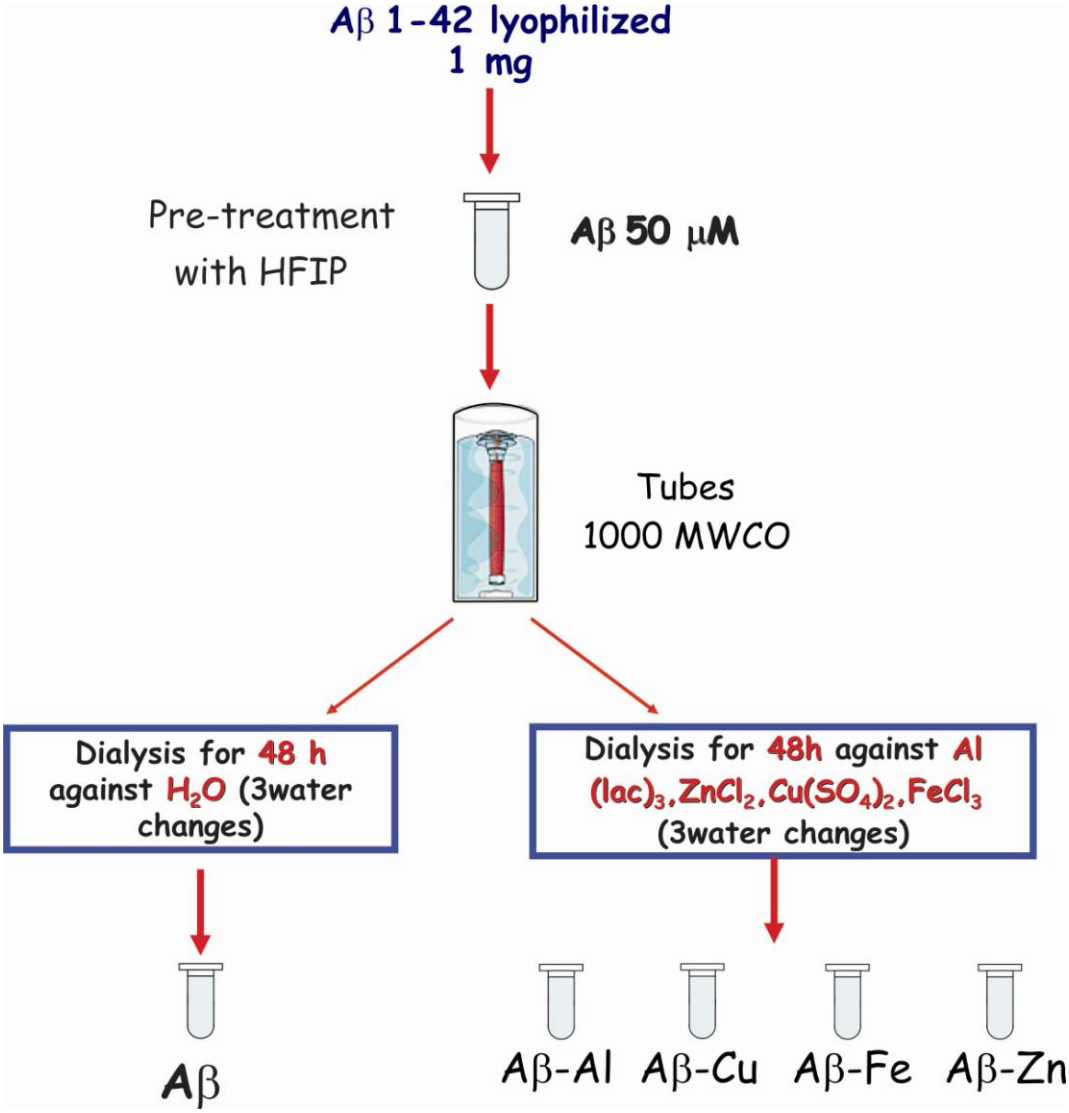

Figure 2.1. ***Schematic representation of Aβ and Aβ-metal complexes protocol preparation.***

2.3. X-ray diffraction studies of phospholipid multilayers

The ability of Aβ-metal complexes to perturb the structures of DMPC and DMPE multilayers was determined by X-ray diffraction. About 2 mg of each phospholipid was mixed in eppendorf tubes with 200 μl of distilled water, and aqueous solutions of Aβ-Al, Aβ-Cu, Aβ-Zn, Aβ-Fe complexes in a range of concentrations (1 to 20 μM). The specimens were incubated for 30 min at 30ºC and 60ºC with DMPC and DMPE respectively, and centrifuged for 20 min at 2000 rpm. The samples were then transferred to 1.8 mm dia special glass capillaries (Glas Technik and Konstruktion, Berlin, Germany) and X-ray diffracted with Ni-filtered CuKα from a Bruker

Kristalloflex 760 (Karlsruhe, Germany). Specimen-to-film distances were 8 and 14 cm, standardized by sprinkling calcite powder on the capillary surface. The relative reflection intensities were obtained in an MBraun PSD-50M linear position-sensitive detector system (Garching, Germany); no correction factors were applied. The experiments were performed at 17 ± 2°C, which is below the main phase transition temperature of both DMPC and DMPE. Each experiment was repeated three times, and additional experiments were carried out when there were doubts. Blanks consisted in mixtures of DMPC and DMPE with metal-free Aβ, and with Al-lactate, $CuCl_2$, $ZnCl_2$ and $FeCl_3$.

2.4. Electrospray ionization mass spectrometry (ESI-MS)

ESI-MS spectra of the Aβ and of Aβ -metal complexes (10 μM after dilution with HCOOH 0.5%) were recorded by direct introduction at 5 μl/min flow rate on an LTQ-Orbitrap high-resolution mass spectrometer (Thermo, San Jose, CA, USA), equipped with a conventional ESI source. The working conditions were the following: the spray voltage was 3.1 kV, the capillary voltage was 12 V and the capillary temperature was kept at 220 °C. The sheath and the auxiliary gases were set, respectively, at 17 (arbitrary units) and 1 (arbitrary units) while the sweep gas was kept to 0 (arbitrary units). For acquisition, Xcalibur 2.0. software (Thermo) was used and monoisotopic and average deconvoluted masses were obtained by using the integrated Xtract tool. For spectra acquisition a nominal resolution (at m/z 400) of 100,000 was used.

2.5. Dynamic Light Scattering (DLS)

The instrument used for the dynamic light scattering measurements analysis was a Zetasizer Nano (Malvern Instruments Ldt). All the measurements were performed in a low-volume black quartz cuvette (T=20°C) and the samples were left equilibrating 2 minutes before data collection. Attenuation and sampling were defined automatically by the instrument. Samples were prepared at a final $A\beta_{1-42}$ and

$A\beta_{1-42}$ -metal complex concentration of 10 μM in water. Each protein sample was centrifuged 30 minutes at 14000 rpm at 4°C before acquiring its size distribution to remove dust particles. The use of 0.2 μm filter units was avoid to exclude the possibility to alter the composition of the samples in terms of size and percentage of aggregates.

2.6. Fluorescence measurements

Fluorescence measurements were performed with a Perkin Elmer LS 50B spectrophotofluorimeter equipped with a thermostatic cell holder and magnetic stirring. The experiments were carried out in the standard medium pH 7.4, at 25 °C. ThT (20 μM) binding to 5 μM Aβ/Aβ-metal complexes was followed for 24 hours by monitoring the increase in the dye fluorescence intensity at 482 nm with excitation at 450 nm.

ANS (25 μM) binding to 5 μM Aβ/Aβ-metal complexes was followed by the increase of fluorescence emission in the range 430-650 nm (λ_{exc} = 360).

The effect of $A\beta_{17-28}$ on the $A\beta_{1-42}$/$A\beta_{1-42}$-metal complex aggregation pathway and expousure of hydrophobic clusters were studied at $A\beta_{1-42}$/$A\beta_{17-28}$ ratio equal to 1. For the two dyes, each spectrum was the average of two scans and was smoothed using an average function.

2.7. Turbidity measurements

Turbidity assays were performed in 96-well plates. $A\beta_{17-28}$ (5 μM) with or without Al, Cu, Fe, Zn (5 μM) and $A\beta_{1-42}$/$A\beta_{1-42}$-metal complexes (5 μM) was followed for 24 hours by monitoring the absorbance at 405 nm using a Microplate SPECTRAmax^{R}. The background absorbance was subtracted.

2.8. Transmission electron microscopy (TEM)

Aliquots of $A\beta_{17-28}$ and $A\beta_{1-42}$ and $A\beta_{1-42}$-metal complexes were absorbed onto glow-discharged carbon-coated butwar films on 400-mesh copper grids. The grids were negatively stained with 1% uranyl acetate and observed at 40,000 x by TEM (Fei Tecnai 12). All experiments were carried out at 10 μM peptide concentration.

2.9. DOT-BLOT

For dot blots, the 0.2-μg samples (Aβ, Aβ-Al, Aβ-Zn, Aβ-Cu, Aβ-Fe prepared as described above) were applied as 1-μl spots to a nitrocellulose membrane, allowed to dry at room temperature, then blocked with 10% nonfat milk in low-Tween TBS-T, (20 mM Tris, 137 mM NaCl, 0.01% Tween 20 pH 7.6) for one hour at room temperature with shaking. Following three 5-minute washes, the blots were incubated for one hour at room temperature with the fibril specific conformation-dependent antibody, OC or the annular protofibril specific antiserum, αAPF (1:10,000 and 1:2,000 in 5% milk in low-Tween TBS-T, respectively). After washing, the blots were incubated with goat-α-rabbit HRP conjugated secondary antibody (Promega, 1:10,000 in 5% nonfat milk in TBS-T) for one hour at room temperature, washed again and detected with ECL chemiluminescence kit (Amersham Biosciences)

2.10. Neuroblastoma cells

SH-SY5Y human neuroblastoma cells were purchased from ECACC (European Collection of Cell Culture, Salisbury, UK). SH-SY5Y, all passage 27, were cultured in DMEM/F12 (Gibco, Carlsbad, CA USA) medium containing 15% (v/v) fetal bovine serum (FBS, Sigma Aldrich, St. Louis, MO), 100 units/ml penicillin and 100 μg/ml streptomycin (Gibco, Carlsbad, CA USA), at 37 °C with 5% CO_2 in a humidified atmosphere (90 % humidity). The culture medium was replaced every 2 days.

2.11. Cell viability assay

Cell viability was assessed using the MTT reduction assay. Briefly, SH-SY5Y cells were seeded into 96-well plates (at a density of 8 x 10^4 cells per well). 2 % FBS-culture medium containing human Aβ, Aβ-metal complexes (at 0.5 μM peptide concentration) and metals alone (5 μM) were added to the cells for 24h. MTT (5 mg/ml) was added to each well and incubated in the dark at 37 ºC for 3h, then cells were lysed with acidic isopropanol (0.04 M HCl in absolute isopropanol) in each well [40]. Colour was measured with a 96-well ELISA plate reader at 550 nm (Microplate SPECTRAmax^R). All MTT assays were performed three times, in triplicate. The readings of the various cell-Aβ/Aβ-metal complexes/metals combinations were compared with the control (untreated cells), which represented 100% viability. Experiments with $A\beta_{17-28}$ (0.5 μM) fragment were done in the same conditions.

2.12. Scanning electron microscopy (SEM) of SH-SY5Y

SH-SY5Y cells were seeded onto glass cover slips and treated with human Aβ, Aβ-metal complexes (0.5 μM peptide), metals alone (5 μM concentration) and $A\beta_{17-28}$ (0.5 μM). After 24h of incubation, the cells on glass cover slips were fixed with formaldehyde pH 7.4 and dehydrated in a graded ethanol series. Then, the samples were critical point dried with CO_2 in a HCP-2 Hitachi 2 Critical Point Dryer and gold-coated for examination under a JEDL JSM-6490 scanning electron microscope. The working pressure was 4.2-4.3 bar and the temperature was 5°C. For comparison, also untreated cells (control) were examined by SEM under the same experimental conditions.

2.13. Enzyme-linked immunosorbent assay (ELISA) for detection of APP and Tau181 in SH-SY5Y

SH-SY5Y were treated with Aβ, Aβ-metal-complexes (0.5 μM) and metals alone (5 μM) for 48 and 72h. The pellets were lysed in a cell extraction buffer (Invitrogen, Camarillo, USA) supplemented with protease inhibitors (Sigma Aldrich, St.

Louis, MO). Lysates were collected, centrifuged at 13,000 rpm for 10 minutes and quantified for total protein content using a BCA protein assay standard solution (Sigma Aldrich, St. Louis, MO). APP was quantified after 48h treatment using a commercial ELISA kit following manufacturer's instruction (Invitrogen, Camarillo, USA). The capture antibody for this assay binds to the N-terminal part of human APP and the detection antibody recognizes the N-terminal part of Aβ peptide. Therefore, this ELISA kit will detect soluble APPα which is cleaved by α-secretase, but not soluble APPβ which is cleaved by β-secretase.

Tau181 was quantified after 72h treatment using a commercial ELISA kit following manufacturer's instruction (Invitrogen, Camarillo, USA).

2.14. Bovine brains

Two series of bovine brains (series A, age 8-12 months; series B, age 9-12 years) were supplied from a local slaughter house (Cittadella and Campo San Martino, Padova, Italy), removed immediately after slaughtering, immersed in ice and rapidly transferred to the laboratory. Animals older than two years were previously tested for possible Bovine Spongiform Encephalopathy (BSE) infection according to the Italian Public Health Regulations. Only disease-free animals were utilized for our purpose. All animals were treated according to the European Communities Council directive (86/609/EEC) concerning animal welfare during the commercial slaughtering process, and were constantly monitored under mandatory official veterinary medical care.

2.15. Mice care and Cu-deficient diet

Twenty-three male CD-1 mice (15 months old) were purchased from Harlan (Udine, Italy). They were housed one mouse per cage under the standard laboratory conditions (23 ± 1 ºC, 55 ± 5% humidity, 12h light/dark cycle) and had access to bi-distilled water and food ad libitum. They were allowed to acclimatize for 1 months before starting the treatment. Mice were randomly divided in two groups for the Cu-deficient (CuD) diet (n=12) and Cu-adequate (CuA) diet (n=11) and treated for 12

weeks. The diet with (6 mg of cupric carbonate per kilo) and without copper was purchased from Mucedola (Settimo Milanese, Italy). Controls were run to check the Cu concentration of diet upon arrival. All experimental procedures were approved by the University Veterinary Service and conducted in accordance with the D.L.vo 116-92, art 5.

2.15.1 Tissue Sampling

Mice were killed by decapitation/cervical dislocation. Blood samples were collected from the carotid arteries after decapitation, kept on ice and centrifuged for 15 minutes at 1500 rpm. Spot of different tissues were removed, weighted and homogenated for MTs content or mineralized for metal analyses.

2.16. Metal analyses

Fresh tissues were mineralized in HNO_3 Suprapur (Merk, Milan, Italy) at 70ºC for 24 h. After digestion the solution was brought to the final volume using milliQ water and filtered with pore size 0.2 μM (Sigma, Milan, Italy).

The concentration of Cu, Zn, Ca and Mn in the different brain regions as well as oragns was determined by a Perkin-Elmer A100 flame atomic absorption spectrophotometer, using metal ion standard solutions for instrument calibration (Sigma, Milan, Italy).

Al concentration was determined in helium mode by inductively coupled plasma mass spectrometry (ICP-MS) on an Agilent 7500ce, Tokyo, Japan, using The Babington nebuliser and a Scott-type spry chamber. A nickel sampler and skimmer with 1.0 and 0.4 mm come orifices, respectively, were used. Treatment of data was performed with the Agilent ChemStation software. ICP-MS operating conditions for determination of Al are described elsewhere (Murko et al., 2007). Before analysis samples were diluted with MilliQ water, so that to measured Al concentrations ranged between 1 and 100 μgL^{-1}.

2.17. Immunohistochemistry

Tissues used for immunohistochemical analyses were fixed by immersion in buffered formalin, washed in phosphate saline buffer 0.01M pH 7.4, processed for paraffin embedding, sectioned at a thickness of 5 μm and mounted on poly-L-lysine coated slides. Mouse monoclonal antibody directed against MT I/II and polyclonal against glial fibrillary acidic proteins (GFAP) (Dako, Milan, Italy) were utilized according to the manufacturer's instructions. Immunohistochemistry was carried out as follows. Microsections were incubated in 3% H_2O_2 in PBS for 10 minutes. Non-specific binding sites were blocked by a 30 minute incubation with normal goat serum. Sections for MTs staining were pre-treated with citrate buffer pH 6, then incubated overnight at 4 ºC with anti-MT I/II at a 1:50 dilution. Sections for GFAP staining were pre-treated with 0.1% trypsin in Tris/HCl pH 7.2 at 37 ºC for 10 minutes, then incubated 30 minutes at round temperature with anti-GFAP at a 1:200 dilution. After washing, sections were reacted for 30 minutes with EnVision®, developed with 3,3'-diaminobenzidine (Dako, Milan, Italy) and, finally, counterstained with hematoxylin. The sections were then dehydrated, cover-slipped with balsam, observed and photographed with an Olympic Vanox AH-3 and a Olympus BX51 photomicroscopes. Specificity of the antibody for MT I/II has been verified by replacing the primary antibody with normal swine serum. Under these conditions there was no immunostaining.

To identify possible co-localizations of GFAP protein and MT I/II in the same cell type, sample tissue from the bovine brain were fixed as described above, washed with PBS, pre-treated with citrate buffer pH 6 and then incubated overnight at 4 °C with primary antibodies against a) MT I/II and b) GFAP. Excess primary antibody was eliminated by rinsing twice in PBS. The sections were then incubated (1 h at 37 °C) with secondary fluorescent antibodies against rabbit immunoglobulins-TRITC, (DakoCytomation, Glostrup, DK, dilution 1:100) and goat anti-mouse IgG-FITC, (Santa Cruz Biotechnology, Santa Cruz, CA, USA, dilution 1:100). Afterwards, sections were washed twice in PBS and finally mounted with FlourSave™ Reagent (Calbiochem, San Diego, CA, USA). Immunostained slides were observed, and images obtained, using a Leika TCS confocal microscope. Negative controls

were performed by substituting primary antibodies with bovine serum albumin in PBS as described above.

2.18.1 Tyrosine hydroxylase (TH) immunohistochemistry

All chemicals were from Sigma (Milano, Italy) unless otherwise stated. For tyrosine hydroxylase (TH) counterstaining slides were deparaffined, permeabilized with Triton X-100 2% in PBS (phosphate buffered saline, 10 mM phosphate, 148 mM NaCl, pH 7.2) for 15 minutes, blocked in 2% bovine serum albumin and Triton X-100 1% for one hour, incubated overnight in anti-Tyrosine hydroxylase (TH, Santa Cruz Biotechnology N-19, Heidelberg, Germany, made in rabbit, 1:100 in blocking solution), followed by anti-rabbit Alexa 594 (Molecular Probes, Eugene, Oregon, USA) secondary antibody, 1:350, for 40 minutes at 37°C. Intensity of staining was evaluated by grading - (faint labelling of cell bodies), +/- (detectable cell bodies and fibers), + (moderate labelling), ++ (intense labelling) and +++ (very intense). Images were acquired with the same parameters at 782x582 pixels in TIFF format, using the resident software of a Leica epifluorescence microscope.

2.18. Metallothioneins (MTs) chemical determination

Total MTs concentration was determined following a silver-saturation assay as described in detail elsewhere (Scheuhammer & Cherian, 1986; 1991).

2.19. Behavioural tests

The behavioural tests were run in an isolated room during five days, with a four-days pause between days 2 and 3. Mice were weighted every day and tested for the following neurologic deficits: general condition, deambulation, posture, righting from the side, placing reaction of hindlimbs, geotaxic reaction, avoiding of borders and equilibrium: no neurologic sign was found.

Tests were chosen to explore different cognitive, sensory, motor and emotional domains; data were analyzed with mixed design ANOVA using Statistica software version 5 '97 edition (www.statsoft.com). The significant level was set at $p<0.05$.

2.19.1 Open field test

This test, performed on day 1, evaluates locomotor and exploratory activity, and emotional reactivity to a novel environment (Mucignat-Caretta et al., 2004). The mouse was put on a plastic cage (55x33x20 cm), with opaque walls and black floor, and videorecorded for 3 minutes. The software SMART 2.5 (2 Biological Instrument, Varese, Italy) was used to quantify: the overall distance travelled (in cm), as an index of motor activity; the number of rearings with both forepaws on the lateral walls, as an index of exploratory activity; the time spent without moving, as an index of freezing; the number of fecal boli and urine drops, as an index of autonomic activation.

2.19.2 Pole test

This test evaluates bradykinesia and motor performance (Sedelis et al., 2001; Kurosaki et al., 2004). The mouse was put head upward on a vertical pole (1,5 cm diameter x 50 cm height), the latency (in seconds) to climb down until the four paws were on the ground was recorded. The maximum time was 120 seconds.

This test was repeated on days 1, 2 and 3, thus providing a measure for long-term contextual and procedural memory.

2.19.3 Predatory aggression test

The emotional reactivity to a different animal species was tested on day 1, by putting an earthworm *(Lombricus terrestris)* on the homecage floor. The latency (in seconds) to the first attack was recorded, then the test was stopped. The maximum time was 10 minutes. This test requires the sensory detection of the prey, choosing the appropriate behavioural pattern of attack and correctly executing it, therefore it refers to a compex sensory-motor and cognitive-emotional domain mainly mediated by basal forebrain structures and olfactory projection areas (Mucignat-Caretta et al., 2004).

2.19.4 Habituation/Dishabituation smell test

From the second day onward, mice were tested for their ability to discriminate novel olfactory stimuli and their short-term memory (Pankevich et al., 2004). The mouse was put in the open-field arena and videorecorded as above, it was left undisturbed for 5 minutes to habituate. A plastic well (20x7 mm) containing 10 microliters of water was then fixed to the floor (10 cm from the short and 16 cm from the long wall) for 2 minutes, then it was removed for 1 minute. This procedure was repeated for 3 times to provide habituation, seen as a lack of interest for the introduction of already known stimuli. Then a well containing 10 microliters thymol (1:1000 in liquid paraffin) was introduced for three times, followed by three presentations of a well containing camphor (1:1000 in liquid paraffin). When a new odour is presented, the mouse should be aware of it and explore it for a longer time. The area around the well (17x18 cm) was considered the target zone, in which the following measures were taken: latency to the first entry into the target zone (in seconds), distance travelled in cm, time spent in it (in seconds), resting time (in seconds), number of entries. Data were analyzed with a three-way mixed design ANOVA, for the factors Group (control vs. Cu-depleted), odor (no odor, thymol, camphor), repetition (the first, second, third).

2.20. Real time quantitative polymerase chain reaction (RT-PCR)

2.20.1 Sample preparation and extraction of total RNA

12 AD patients were recruited at "G. Rossi" Hospital (Verona) and underwent a standard battery examinations, including medical history, physical and neurological examination, neurocognitive evaluation (to asses memory and language), brain magnetic resonance imaging (MRI). The severity of the dementia was assessed by the Clinical Dementia Rating (CDR) and the Mini Mental State Examination (MMSE). The control group consisted of 13 age-matched controls, without memory impairment.

Centrifugation of collected blood and harvesting serum samples were done by using three steps of centrifugation to decrease lymphocytes.

Total RNA was extracted from 1ml of serum and from SHSY5Y pellets terated as described fro the MTT assay, using the RNeasy Mini kit (Qiagen, Chatsworth, CA) with DNase treatment. Isolated RNA was quantified by reading absorbance at 260 and 280 nm (A260/A280 ratio).

2.20.2 Reverse transcription

cDNA was obtained using a high capacity cDNA Reverse Transcription Kit (Applied Biosystems), following manufacturer's instructions. cDNA aliquots were kept at -80ºC until used.

2.20.3 TaqMan real-time quantitative PCR

A RT-PCR analysis was performed on SH-SY5Y neuroblastoma treated with Aβ, Aβ-metal complexes and metals to verify the gene expression profile of glutaminyl cyclase (QPCT). RT-PCR was carried out in a total volume of 50 μl for QPCT containing 1X Taqman Universal PCR Master mix, no AmpErase UNG and cDNA using the TaqMan assay (TAB) on ABI 7300 Sequence Detection System (ABI, Foster City, CA). Gene-specific primers and probe sets for the gene QPCT (Hs00202680-m1) and for GAPDH (Hs99999905-m1) were obtained from Applied Biosystems. Duplicate samples were run for each gene alone. The housekeeping gene GAPDH was used as an internal control to normalize the expression of the target gene. The real time amplifications included 10 minutes at 95°C (AmpliTaq Gold activation), followed by 40 temperature cycles for 15 seconds at 95°C and for 1 minute at 60°C. Relative expression levels were calculated for each sample after normalization against the housekeeping gene GAPDH, using the ΔΔCt method for comparing relative fold expression differences (Livak & Schmittgen, 2001).

2.21. Statistical analysis

Statistical data regarding MTT assay, RT-PCR experiments and metal concentrations were performed by ANOVA followed by Student-Newman-Keuls *t*-test as post-hoc test. Statistical data regarding ELISA assay were performed by student *t*-

test. Results were reported as statistically significant if $P < 0.05$ and highly statistically significant if $P < 0.01$.

3 Results

3.1. Interaction between Aβ and Aβ-metal complexes with cell membranes: X-ray diffraction studies of phospholipid multilayers

Fig. 3.1.1 A exhibits the results obtained by incubating DMPC with water and metal-free Aβ.

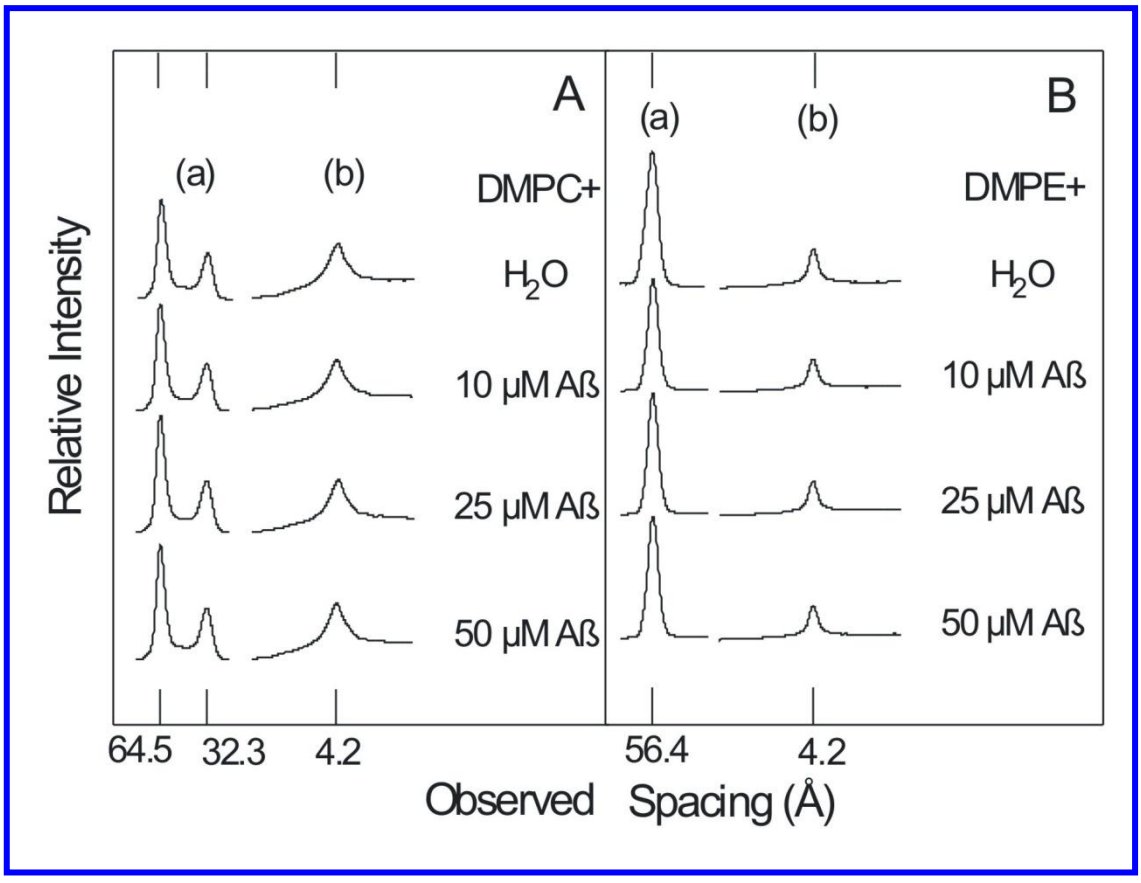

Figure 3.1.1 ***Microdensitograms from X-ray diffraction diagrams of DMPC (A) and DMPE (B)*** *in water and aqueous solutions of Aβ; (a) low-angle and (b) wide-angle reflections (N=3) .*

As expected, water altered the DMPC structure: its bilayer repeat (bilayer width plus the width of the water layer between bilayers) increased from about 55 Å in its dry crystalline form (Suwalsky, 1996) to 64.5 Å when immersed in water, and

its low-angle reflections (indicated as (a) in the figure), which correspond to DMPC polar terminal groups, were reduced to only the first two orders of the bilayer repeat.

On the other hand, only one strong reflection of 4.2 Å (indicated as (b) in the figure) showed up in the wide-angle region, which corresponds to the average distance between fully extended acyl chains organized with rotational disorder in hexagonal packing. These results were indicative of the fluid state reached by DMPC bilayers, which showed the typical characteristics of a Pβ' phase (Katsaras, 1998). Fig. 1A shows that after exposure to metal-free Aβ in the 10-50 μM concentration range the DMPC diffraction pattern remained practically unchanged. Similar experiments were performed on DMPE bilayers. Fig. 3.1.1 B shows that the DMPE bilayer repeat expanded from about 51 Å when dry (Suwalsky, 1996) to 56.4 Å when subjected to maximum hydration. On the other hand, only two reflections were observed, one more pronounced of 56.4 Å, corresponding to the first order of the bilayer repeat, and the other of 4.2 Å, indicating the fluid state reached by DMPE. Fig. 3.1.1 B also shows that metal-free Aβ in the 10-50 μM concentration range did not induced changes to DMPE bilayers. From these results it can be concluded that the metal-free Aβ did not produced any significant structural perturbation to DMPC nor to DMPE bilayers.

Fig. 3.1.2 presents the results obtained after incubating DMPC with Aβ-metal complexes. Fig. 3.1.2 A shows that after exposure to 2 μM Aβ-Al complex there was a considerable weakening of the low- and wide-angle lipid reflection intensities. The fact that all reflections practically disappeared at a 4 μM Aβ-Al complex concentration indicated that the periodic structure of the multilamellar stacking was lost. Results from similar experiments with the Cu(II), Zn(II) and Fe(III) β-amyloid complexes are shown in Fig. 3.1.2 B, C and D, respectively. As it can be appreciated, none of these complexes induced any significant structural change to DMPC in the range of concentrations in which the Aβ-Al complex induced the loss of the lipid bilayer structure. Fig. 3.1.2 also shows that the Cu and Fe complexes did not caused any effect to DMPC even at a concentration as high as 20 μM; only the Aβ-Zn complex showed at this maximum assayed concentration a moderate reduction in DMPC reflection intensities.

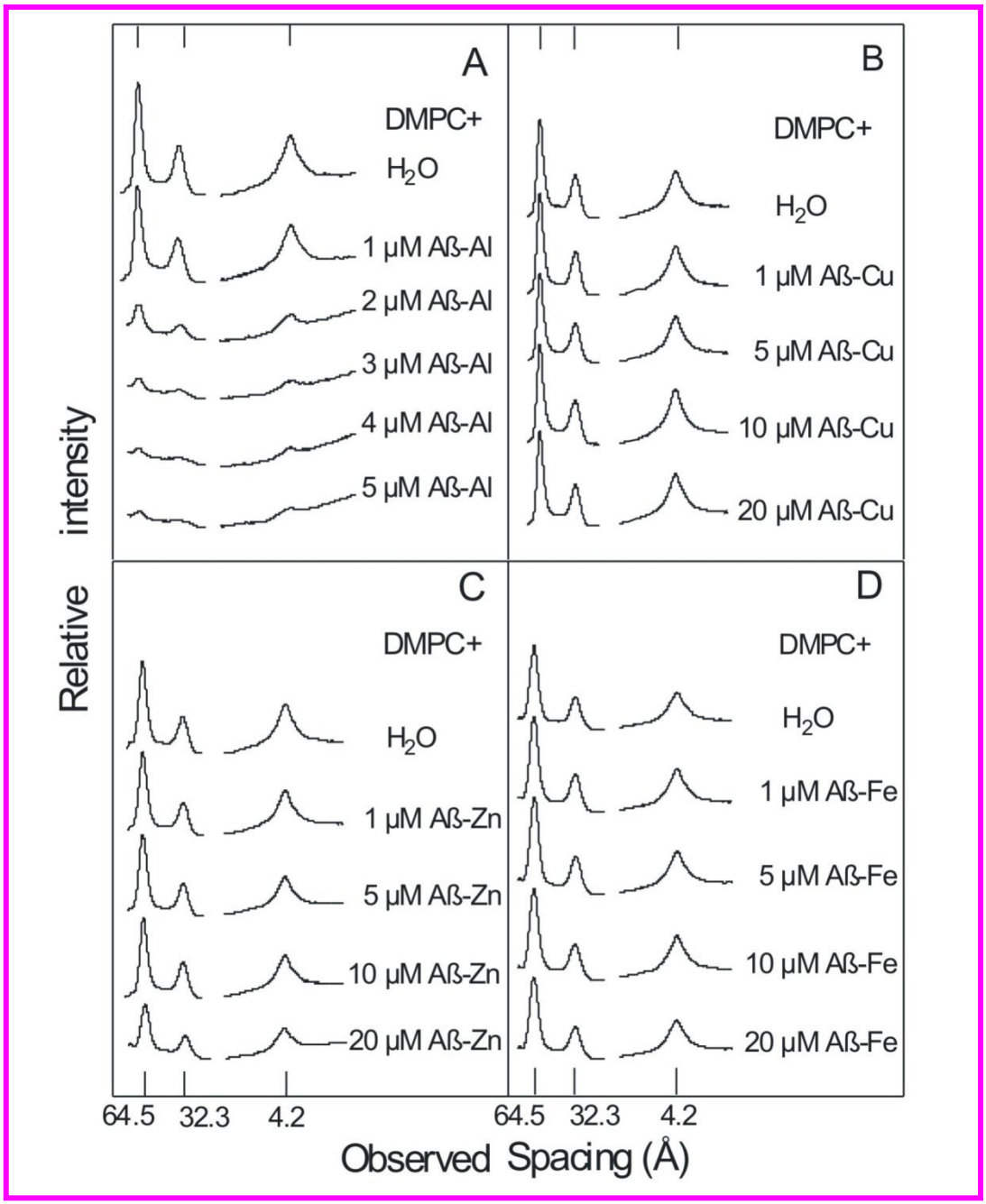

Figure 3.1.2 ***Microdensitograms from X-ray diffraction diagrams of DMPC (A) and DMPE (B)*** *in water acqueous solution of Aβ-Al (A); Aβ-Cu (B); Aβ-Zn (C) and Aβ-Fe (D); (a) low-angle and (b) wide-angle reflections (N=3) .*

Fig. 3.1.3 shows that increasing concentrations of the four Aβ-metal complexes up to 20 µM had only negligible effects on DMPE bilayer structure.

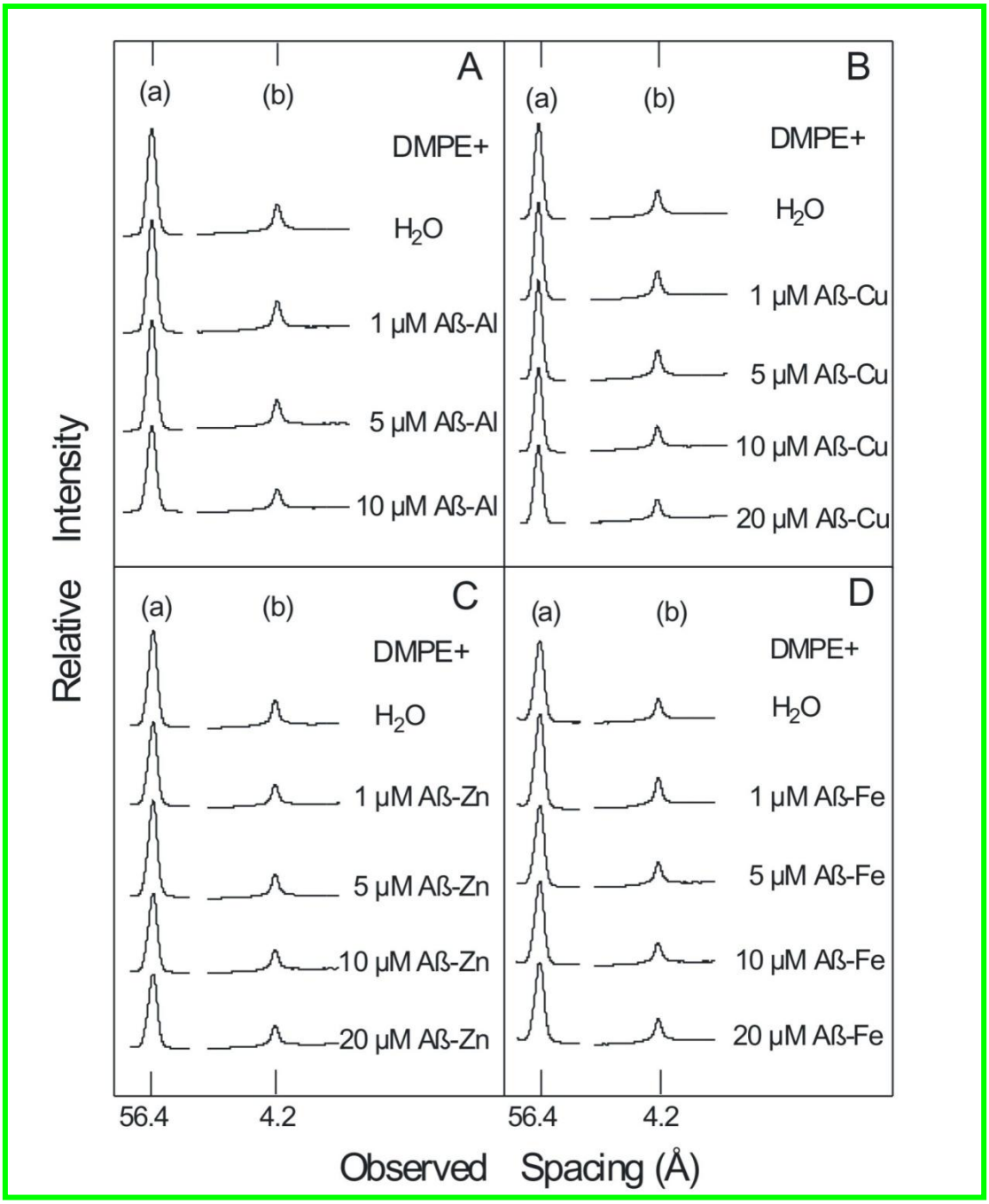

Figure 3.1.3 ***Microdensitograms from X-ray diffraction diagrams of DMPE*** *in water and aqueous solutions of Aβ-Al (A); Aβ-Cu (B); Aβ-Zn (C) and Aβ-Fe (D); (a) low-angle and (b) wide-angle reflections (N=3).*

The results presented in Fig. 3.1.1 A demonstrate that the strong interaction of the Aβ-Al complex with DMPC bilayers was not due to the metal-free peptide, as a concentration as high as 50 µM did not induce any structural perturbation to DMPC nor to DMPE.

The results presented in Fig. 3.1.4 demonstrate that, of the four free assayed metal salts, only that of Al significantly affected the DMPC bilayer structure, and only at concentrations several orders of magnitude higher than those of the Aβ–Al complex that produced similar alterations to DMPC.

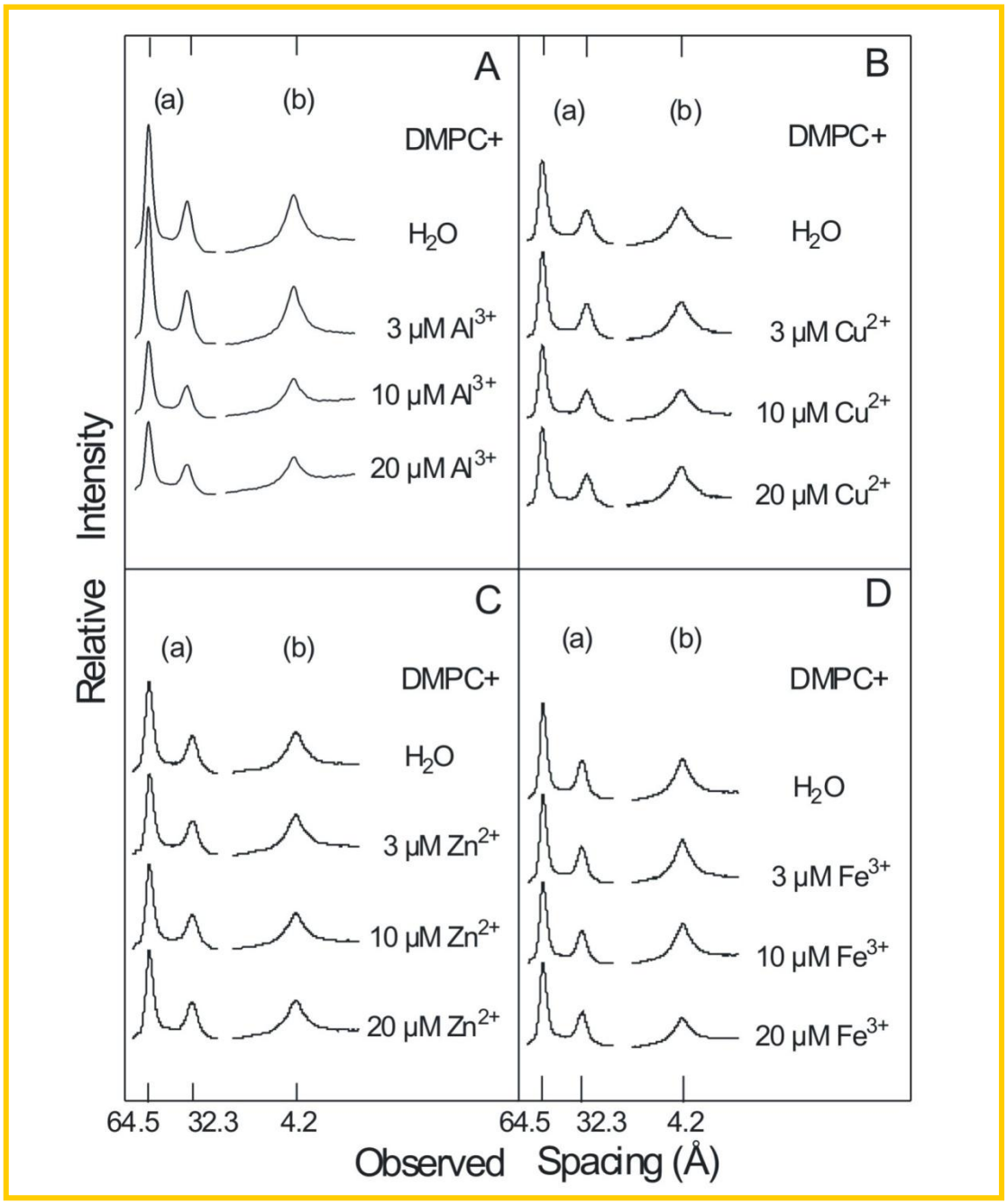

Figure 3.1.4 ***Microdensitograms from X-ray diffraction diagrams of DMPC*** *in water and aqueous solutions of of Al-lactate (A); $CuCl_2$ (B); $ZnCl_2$ (C) and $FeCl_3$ (D); (a) low-angle and (b) wide-angle reflections (N=3).*

As can be seen in Fig. 3.1.5, none of the four metal salts significantly affected DMPE, not even when it was incubated with the highest assayed concentrations.

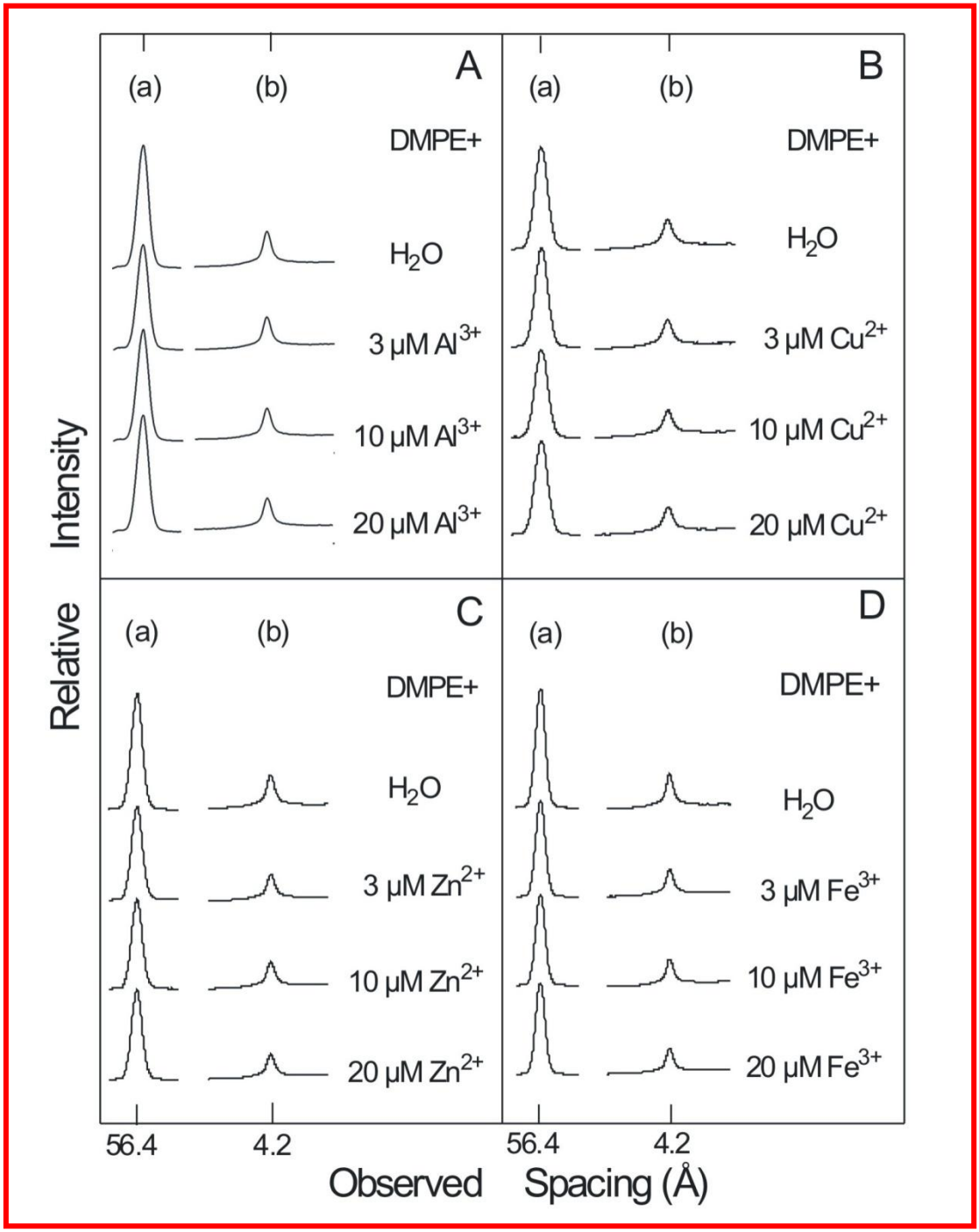

Figure 3.1.5 ***Microdensitograms from X-ray diffraction diagrams of DMPE*** *in water and aqueous solutions of of Al-lactate (A); $CuCl_2$ (B); $ZnCl_2$ (C) and $FeCl_3$ (D); (a) low-angle and (b) wide-angle reflections (N=3).*

Therefore, it can be concluded that only the association of Al with Aβ is able to interact and disturb the structure of this class of lipid, which is preferentially located in the outer monolayer of many cell membranes (Boon & Smith, 2000).

3.2. Characterization of Aβ and Aβ-metal complexes

3.2.1. Chemical and biophysical characterization

ESI-MS

Aβ and its four metal complexes (Aβ-Al, Aβ-Zn, Aβ-Cu, Aβ-Fe), were analysed comparatively through ESI-MS spectrometry. Deconvoluted ESI-MS spectra of the above samples are shown in Figure 3.2.1. In line with previously reported results, it is evident that electrospray ionization causes a significant release of bound metals. Thus, the peak of native Aβ-is of predominant intensity in all cases. However, peaks that may be straightforwardly assigned to metal adducts are also clearly observed for all metallated species with an appreciable intensity. From spectral analysis it emerges that all tested metals apparently bind to the Aβ as bare ions. Monometalated derivatives are the major metallated species; in a few cases, bis metalated derivatives are also detected. The extent of metallation is rather similar in the various cases. On the other hand, oxidation of Aβ at Met 35 appears to be rather modest.

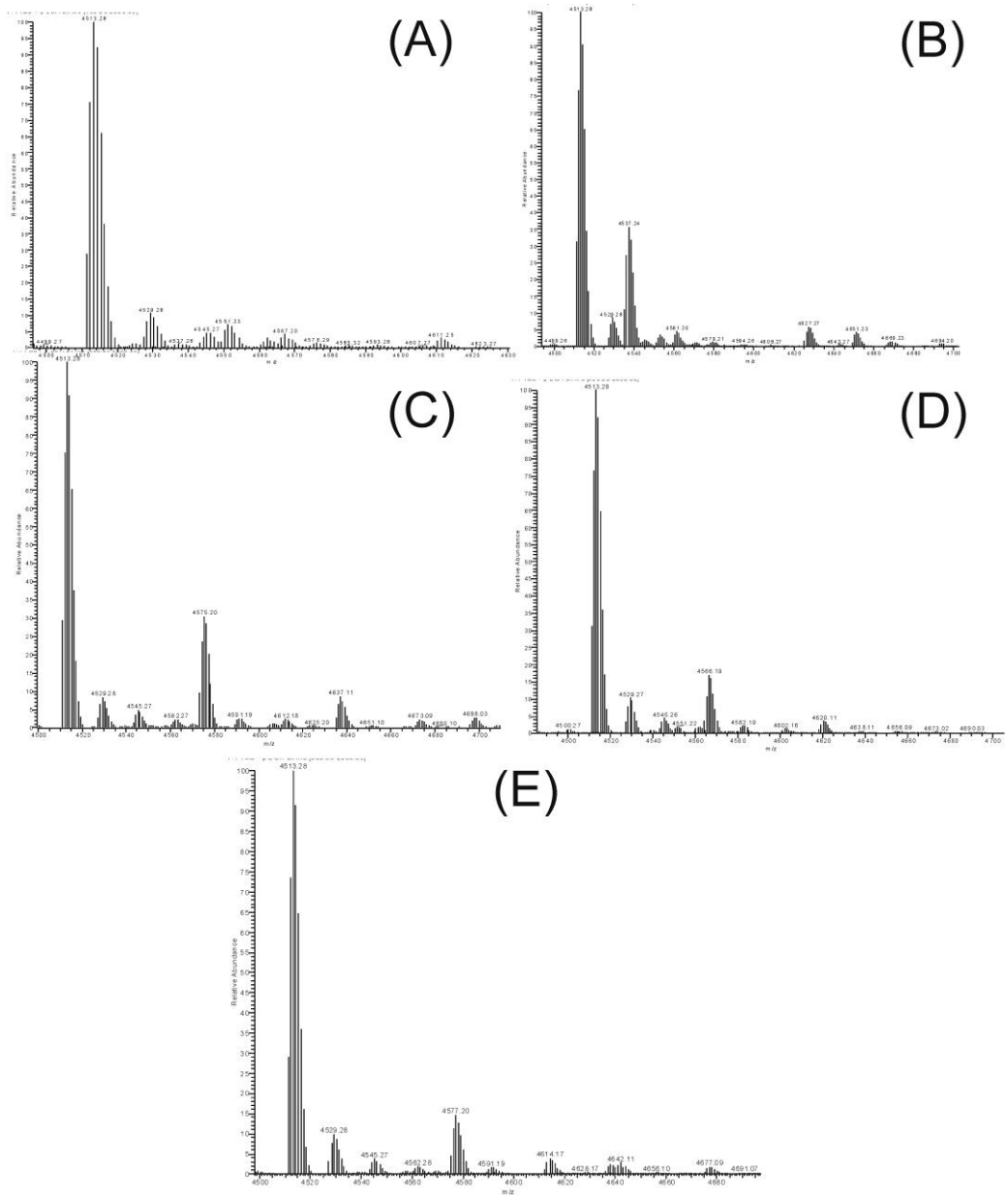

Figure 3.2.1. *Deconvoluted ESI-MS spectra of: Aβ alone (a), and with Al (b), Cu (c), Fe (d) and Zn (e).*

DOT BLOT

In the present study, Aβ and Aβ-metal complexes (Aβ-Al, Aβ-Zn, Aβ-Cu, Aβ-Fe) were also immunologically characterized by dot blot using conformation-dependent antibodies. Conformation-dependent antibodies can distinguish different types of Aβ oligomers on the basis of their underlying structure (Kayed et al., 2003; 2007; 2009). These antibodies are specific for aggregated forms of Aβ and show low or no immunoreactivity against monomeric Aβ. In particular, A11, OC and αAPF

have been reported to recognize generic epitopes that are specifically associated with prefibrillar oligomers (A11) (Kayed et al., 2003), fibrils or soluble fibrillar oligomers (OC) (Kayed et al., 2007) and annular protofibrils or pores (αAPF) (Kayed et al., 2009).

As shown in Figure 3.2.2 A, the reactivity of Aβ-Al and Aβ-Fe with OC suggested the presence of fibrillar oligomers that were absent in Aβ, Aβ-Zn and Aβ-Cu samples, due to their lack of immunoreactivity with OC. The specificity of OC for soluble fibrillar oligomers of Aβ-Al and Aβ-Fe was also in agreement with TEM microscopy which showed no mature fibrils for these preparations (Figure 3.2.6). As recently reported by Tomic et al. (2009), soluble fibrillar oligomers detected by the OC antibody may play a key role in the pathology of AD. Indeed, their levels have been found to be significantly elevated in multiple brain regions of AD patients and to correlate with cognitive decline as well as the neuropathological hallmarks of AD.

Aβ, Aβ-Al, Aβ-Fe also revealed a strong reactivity with annular protofibril antiserum (αAPF) that is still lacking in Aβ-Zn and Aβ-Cu preparations (Figure 3.2.2 B). However, none of the sample tested showed immunoreactivity with the prefibrillar oligomer-specific antibody A11 (data not shown). Prefibrillar oligomers and annular protofibrils are structurally and immunologically distinct from fibrillar oligomers, although the sizes of these oligomers broadly overlap (Kayed et al., 2003; 2007; 2009). A11 positive prefibrillar oligomers and αAPF positive annular protofibrils have been found not correlate with cognitive dysfunction in AD brain and their levels were also elevated in some age-matched non demented control brains (Tomic et al., 2009).

The presence of fibrillar oligomers in Aβ-Al and Aβ-Fe preparations, as shown by their preferential immunoreactivity with OC that was absent for Aβ, and the better correlation of these oligomers with pathology and cognitive dysfunction in AD brain compared to APFs is therefore consistent with our previous data where Aβ was less toxic than Aβ-Al under our experimental conditions (Drago et al., 2008).

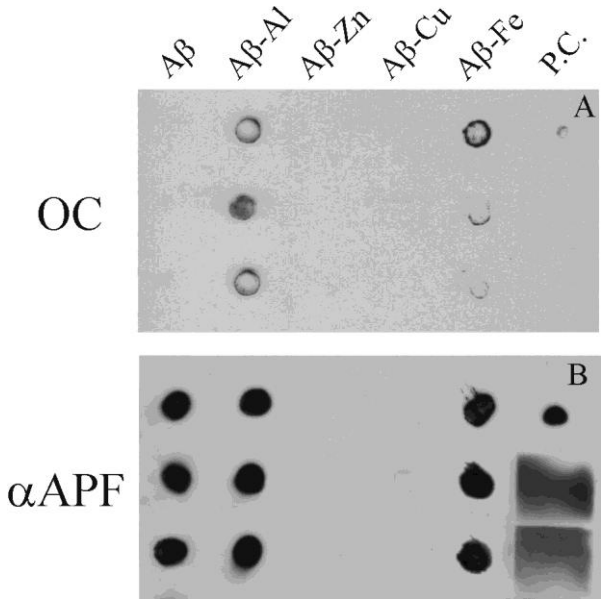

Figure 3.2.2. ***Dot blot analysis of Aβ and Aβ-metal complexes (Aβ-Al, Aβ-Zn, Aβ-Cu, Aβ-Fe) with the anti-fibril/fibrillar oligomer antibody OC (A) and the anti-annular protofibrils antibody αAPF (B).*** *Oligomers were analysed by dot blots in triplicate, using synthetic Aβ fibrillar oligomers (for OC), and annular protofibrils (for αAPF) as positive control (P.C). The signal present in this figure indicates the presence of soluble fibrillar oligomers in Aβ-Al and Aβ-Fe samples but not in Aβ (A) and the presence of annular protofibrils for Aβ, Aβ-Al and Aβ-Fe (B). No reactivity was detected for Aβ-Zn and Aβ-Cu.*

DLS

For what concern Aβ-Zn and Aβ-Cu complexes, the acquired DLS data were not sufficiently stable to produce reliable correlograms, most likely due to the presence of very large particles, fluctuating and precipitating during the data sampling. This observation is coherent with ThT (Figure 3.2.4) and TEM (3.2.6) herein reported showing that Aβ-Zn and Aβ-Cu are characterized by a highly polydisperse population giving rise, especially in the case of Aβ-Zn, to precipitation phenomena. Thus, only Aβ, Aβ-Al and Aβ-Fe are reported and discussed (Figure 3.2.3). The light scattering measurements were also repeated after 24h of incubation indicating that while Aβ-Al profile was unaltered the other 2 samples, Aβ and Aβ-Fe were quite unstable (data not shown). This finding is in accordance with the intrinsic propensity of the peptide to aggregate. While the intensity/radius diagram highlights the contribution of the biggest particles, which give the major contribution to the scattered light, the actual relative abundance of the different species strongly differ from the intensities ratios and needs to be extrapolated, as indicated in Figure 3.2.3. Aβ-Al showed

the presence of a roughly monodisperse population with 29.3 nm mean radius which cover the 48 % of the oligomers, and a more polydisperse contribution (52%) by higher size components with a 110.5 nm mean radius. Also Aβ-Fe showed two main peaks, even if both with a quite polydisperse profile centered at 45.9 nm (59% in mass) and 107.7 (41%) respectively. Finally, Aβ displayed the more polydisperse and unstable profiles, due to the coexistence of oligomeric species with a mean radius slightly lower than Aβ-Al (25.2 nm, 27 % mass) and a large predominant population ranging from 100 to more than 600 nm in radius, most likely including the protofibrillar aggregates observed by TEM (Figure 3.2.6).

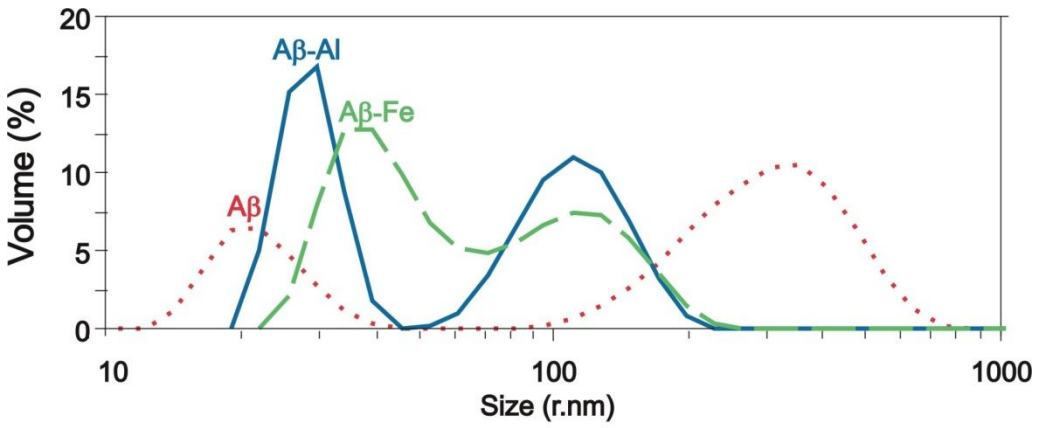

	Intensity (%)	Mass (%)	Mean radius (nm)	Standard deviation (nm)
Aβ	6	27	25.1	± 5.5
	94	73	263	± 101
Aβ-Al	11	48	29.4	± 3.2
	89	52	110.5	± 25.4
Aβ-Fe	31	59	45.6	± 9.9
	69	41	107.7	± 32.2

Figure 3.2.3. ***Size distribution by volume*** *obtained by analysis of dynamic light scattering data (T=20°C). Curves correspond to Aβ, Aβ-Al and Aβ-Fe each at a concentration of 10 μM in water.*

Fluorescence

ThT is known to rapidly bind β-sheet-rich aggregated form of peptides. We examined the dependence of ThT fluorescence on time for samples of Aβ and Aβ-metal complexes (5 μM). As shown in Figure 3.2.4 the time-course of Aβ aggregation was consistent with a nucleation-dependent model (Naiki et al., 1997) and followed a

sigmoidal curve which reached the plateau after ~22h in our experimental conditions. The aggregation was enhanced in the presence of Aβ-Al, indicating that the binding of Al effectively promoted the aggregation process. The absence of an initial lag time in the sample Aβ-Al could suggest the possibility of an immediate conversion of monomeric Aβ into more ThT-reactive species. Then, the complex appeared to be stable from ~3 to 22h and produced a small increase in ThT-fluorescence between 22 and 24h. In the case of Aβ-Zn the nucleation and elongation phase are skipped and ThT fluorescence decreased over time indicating that the equilibrium of the proteic species in solution was forced toward amorphous aggregates. The mechanism was not reversible since mixing the solution did not resuspend the aggregate. In the case of Aβ-Fe we observed a lag time before the formation of β-sheet structures which occur after ~3h even if at a lesser extent than Aβ. The plateau was reached after ~22h of incubation. Aβ-Cu showed low initial ThT fluorescence intensity which did not significantly change over a 24h period.

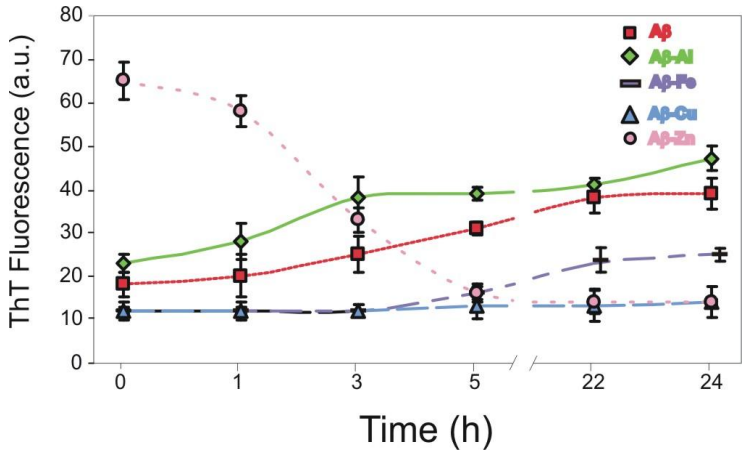

Figure 3.2.4. ***Time-dependence of the fluorescence emission intensity of ThT*** *bound to Aβ and to Aβ-metal complexes (5μM). ThT (20 μM) fluorescence at 482 nm (λ_{exc}=450 nm) was followed for 24 hours. The signals due to the free dye and buffer were subtracted. The data represented are mean ± SD of three individual experiments.*

Aβ and Aβ-metal complexes (5 μM) were also tested for the exposure of hydrophobic clusters by following the ANS fluorescence. According to Uversky et al., changes in ANS fluorescence (enhancement of intensity and blue shift of the emission maximum) are characteristic hallmarks of the interaction of this dye with the solvent-exposed hydrophobic clusters of partially folded peptides and proteins. Fig-

ure 3.2.5 showed the spectra registered after 24h of incubation. Aβ-Al induced a wide increase of ANS fluorescence intensity as well as a blue shift compared to Aβ alone. This implies that Aβ-Al complex was converted into more folded conformations with solvent-exposed hydrophobic clusters. This conversion was also observed in the presence of Aβ-Zn even if at a lesser extent. On the contrary, for Aβ-Fe and Aβ-Cu we observed a slightly decrease in ANS fluorescence compared to Aβ alone.

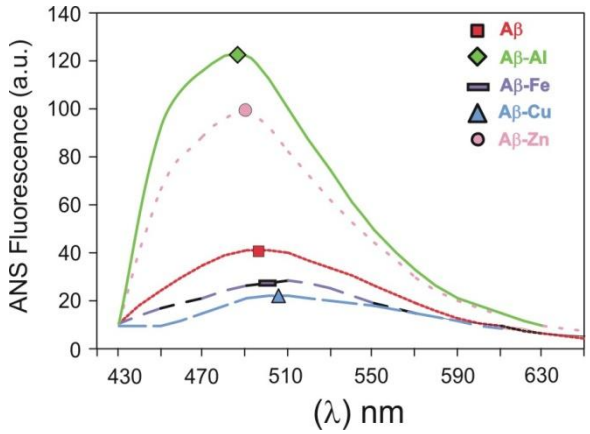

Figure 3.2.5. ***Fluorescence emission spectra of ANS*** *(25 μM) after interaction with Aβ and to Aβ-metal complexes (5μM). Emission spectra were recorded from 430 to 650 nm with excitation at 360 nm. The signals due to the free dye and buffer were subtracted. The peptide samples were left to incubate for 24 hours at room temperature, then the fluorescence was measured.*

TEM

To assess the morphology of the aggregates Aβ and Aβ-metal complexes were analyzed by TEM (Figure 3.2.6). Aliquots of each samples were removed at time zero and after 24h of incubation at round temperature. Aβ alone displayed mature unbranched fibrils along with agglomerates which after 24h evolved forming groups of randomly oriented fibers. In the presence of Aβ-Al we observed small spherical oligomers at 0h resembling those of previously reported by Drago et al., 2008. After 24h of incubation there were still small oligomers, supporting the fact that the preparation was rather stable, besides few well-formed and double-paired filaments whit irregular twist. These spherical oligomers contained extended β-sheet and hydrophobic structure as detected by ThT and ANS fluorescence (Fig.s 3.2.4 and 3.2.5). Aβ-Zn showed granular aggregates at time zero which became larger, but still without

appearance of fibrils, upon longer incubation. Aβ-Fe produced few small branched fibrils along with small oligomers as well as amorphous aggregates giving rise to a very unhomogeneous population. Then, after 24h the unstructured assemblies became the dominant specie. In the presence of Aβ-Cu the aggregation reaction was quite slow both at time zero as well as after 24h, being the majority of the peptide in a fibril-free amorphous form.

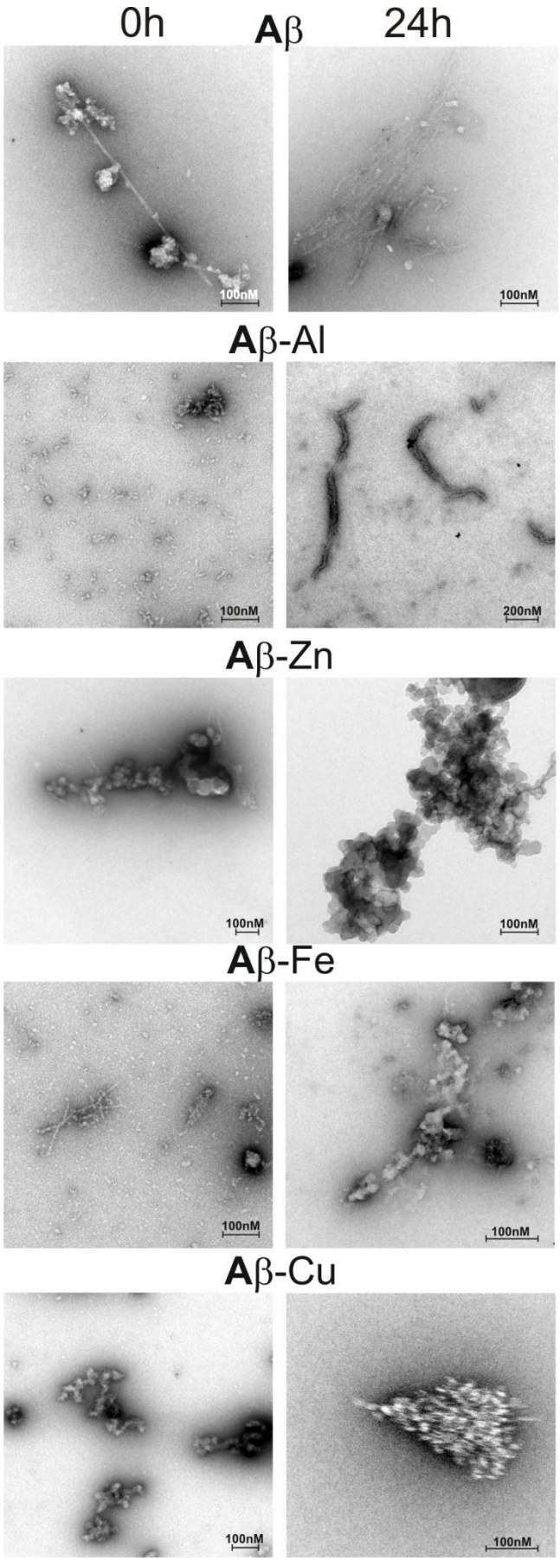
0h
Aβ
24h
100nM
100nM
Aβ-Al
100nM
200nM
Aβ-Zn
100nM
100nM
Aβ-Fe
100nM
100nM
Aβ-Cu
100nM
100nM

Figure 3.2.6. ***TEM micrographs of Aβ and Aβ-metal complexes.*** *Aliquots of each sample (10 μM) were removed at time zero and after 24h of incubation at round temperature.*

3.2.2. Biological effects of Aβ and Aβ-metal complexes on human neuroblastoma cells

MTT assay

We tested the effect of Aβ, Aβ-metal complexes (0.5 μM) and metals (5 μM) on the vitality of human neuroblastoma cells (Table 3.2.1) after 24 hours incubation. Aβ-Al was the only treatment which affected significantly the MTT reduction. It is interesting to notice that treatment with Al alone did not produce such a reduction, even at a 10 fold higher concentration. When Aβ-metal complexes were used in combination their toxicity was increased. Particularly, Aβ-Al+Aβ-Cu and Aβ-Al+Aβ-Fe determined a marked decrease of cell viability. Less pronounced was the effect of Aβ-Al+Aβ-Zn and Aβ-Cu+Aβ-Zn while Aβ-Cu+Aβ-Fe and Aβ-Zn+Aβ-Fe systems displayed negligible toxicity, its effect being comparable to the control.

Aβ and Aβ-metal complexes (0.5μM)	Cell viability (% of control)	Metals (5 μM)	Cell viability (% of control)	Combined Aβ-metal complexes (0.5μM)	Cell viability (% of control)
Aβ	84.01 ± 2.91			**Aβ-Al+Aβ-Cu**	71.12 ± 9.58 (* *)
Aβ-Al	79.66 ± 1.58 (*; °)	**Al**	100.41 ± 1.15	**Aβ-Al+Aβ-Fe**	70.53 ± 7.36 (* *)
Aβ-Cu	85.13 ± 2.86	**Cu**	88.38 ± 0.90	**Aβ-Al+Aβ-Zn**	78.68 ± 12.2 (*)
Aβ-Zn	90.08 ± 0.57	**Zn**	98.04 ± 8.10	**Aβ-Cu+Aβ-Zn**	80.16 ± 7.73 (*)
Aβ-Fe	94.99 ± 1.62	**Fe**	98.08 ± 7.98	**Aβ-Fe+Aβ-Cu**	82.6 ± 5.29
				Aβ-Fe+Aβ-Zn	82.37 ± 7.01

Table 3.2.1 ***Viability assay in SH-SY5Y cells.*** *SH-SY5Y neuroblastoma cells were incubated for 24h with human Aβ, Aβ–metal complexes and combined Aβ–metal complexes (0.5 μM) and metals alone (5 μM). Cell viability was measured by MTT assay. The data represented are mean ± SD of three individual experiments, each done in triplicate. *p <0.05, ** p<0.01 compared with control, °p <0.01 compared with Al alone.*

SEM

The toxic effect of Aβ-Al was evident also in SEM experiments (Figure 3.2.7). In the presence of this metal-complex micrographs clearly showed relevant membrane impairment: cells appeared to be smaller without the typical branches with respect to the control and the other treatments.

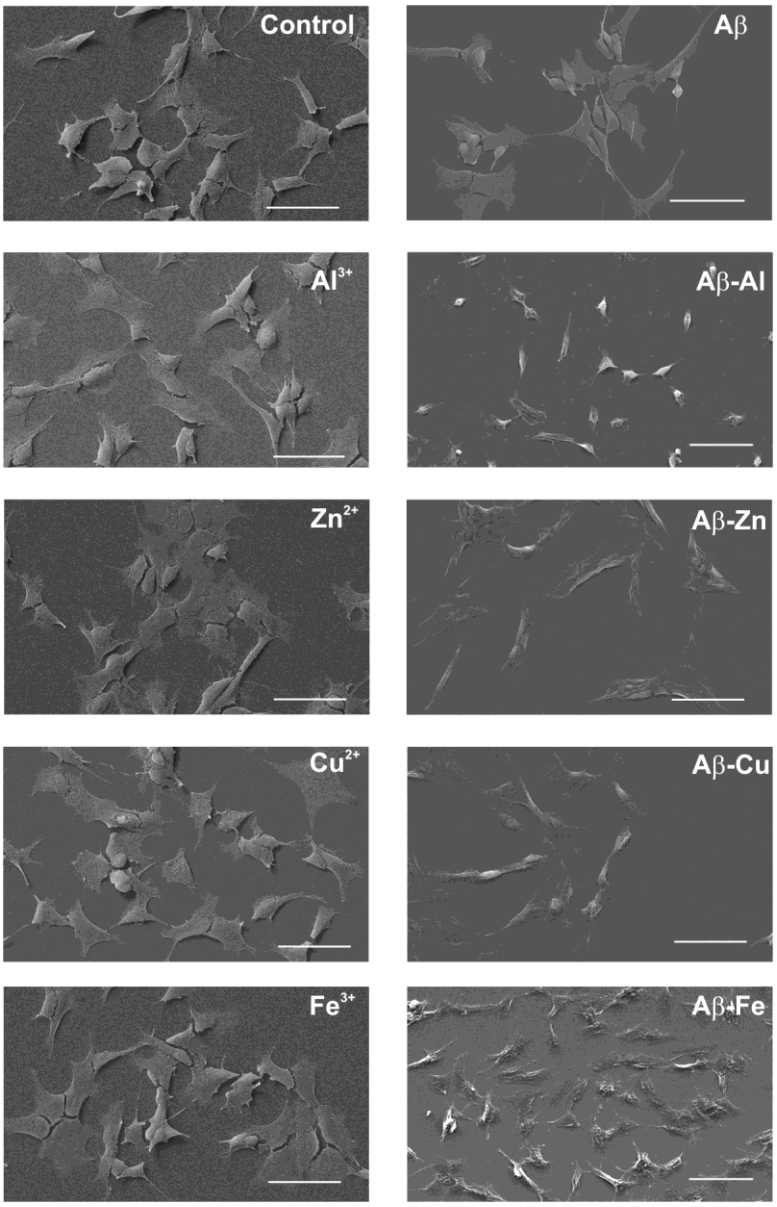

Figure 3.2.7 ***SEM micrographs of human neuroblastoma cells.*** *SH-SY5Y were treated for 24h with Aβ, Aβ-metal complexes (0.5 μM) and metals (5 μM). The scale bars correspond to 50 μm. The experiment was performed three times, in duplicate*.

Also in the presence of Aβ-Fe cells seem to be slightly damage but not as markedly as in the treatment with Aβ-Al where cells lost their typical morphology which can be yet observed after Aβ-Fe treatment.

Quantification of APP and Tau181 by ELISA in SHSY5Y

To evaluate the effect of Aβ and Aβ-metal complexes on APP metabolism we measured APP levels in SHSY5Y cell lysates after 48h treatment (Figure 3.2.8). A higly statistical significant increase in APP level was observed following treatment with Aβ-Al. All the other metal complexes exerted negligible effects being the APP level comparable to the control. It is worth of noticing that metals alone, tested at 10-fold higher concentrations compared to the respective complexes, did not produce any relevant alteration.

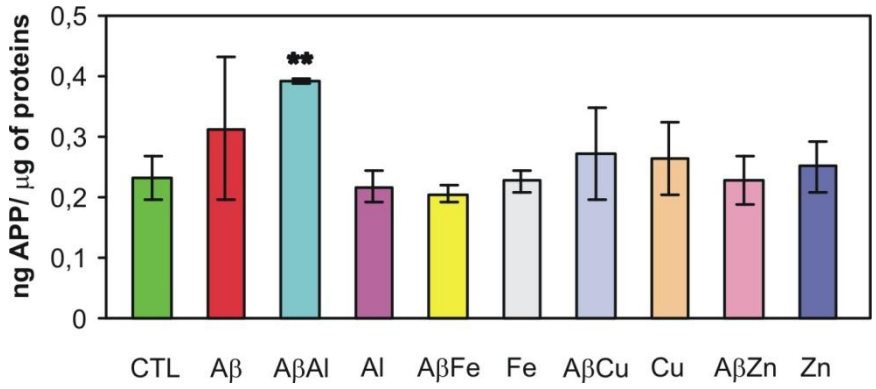

Figure 3.2.8 ***APP levels were quantified by ELISA.*** *SH-SY5Y cells were incubated for 48h with Aβ, Aβ-metal complexes (0.5 μM) and metals (5 μM). The data represented are mean ± SD of three individual experiments, each done in duplicate. ** P< 0.01 vs control.*

Concomitantly with APP data, Tau 181 levels were increased after 72h treatment with Aβ-Al while the effect of the other treatments were negligible compare to the control (Figure 3.2.9).

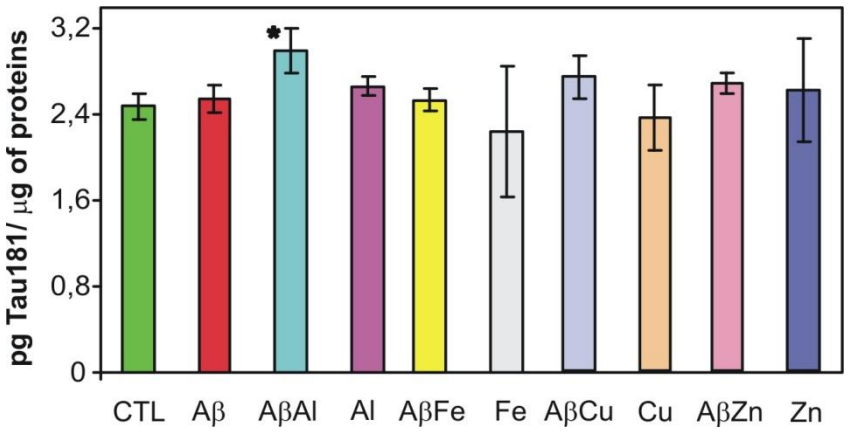

Figure 3.2.9 ***Tau181 levels were quantified by ELISA.*** *SH-SY5Y cells were incubated for 72h with Aβ, Aβ-metal complexes (0.5 μM) and metals (5 μM). The data represented are mean ± SD of three individual experiments, each done in duplicate. * P< 0.05 vs control.*

3.3. Effect of $A\beta_{17-28}$ fragment on Aβ-metal complex oligomerization and toxicity

3.3.1. Chemical and biophysical characterization

Fluorescence measurements: ANS and ThT

$A\beta_{1-42}$ and $A\beta_{17-28}$ metal complexes were tested for the formation of hydrophobic surface by following the ANS fluorescence. Figure 3.3.1 showed that $A\beta_{17-28}$+Al induced an increase of ANS fluorescence intensity and a blue shift of the emission maximum compared to the other $A\beta_{17-28}$-metal complexes. This implies that the peptide is converted into more a folded conformation with solvent-exposed hydrophobic clusters. This conversion was dramatically enhanced in the presence of $A\beta_{1-42}$-Al+$A\beta_{17-28}$.

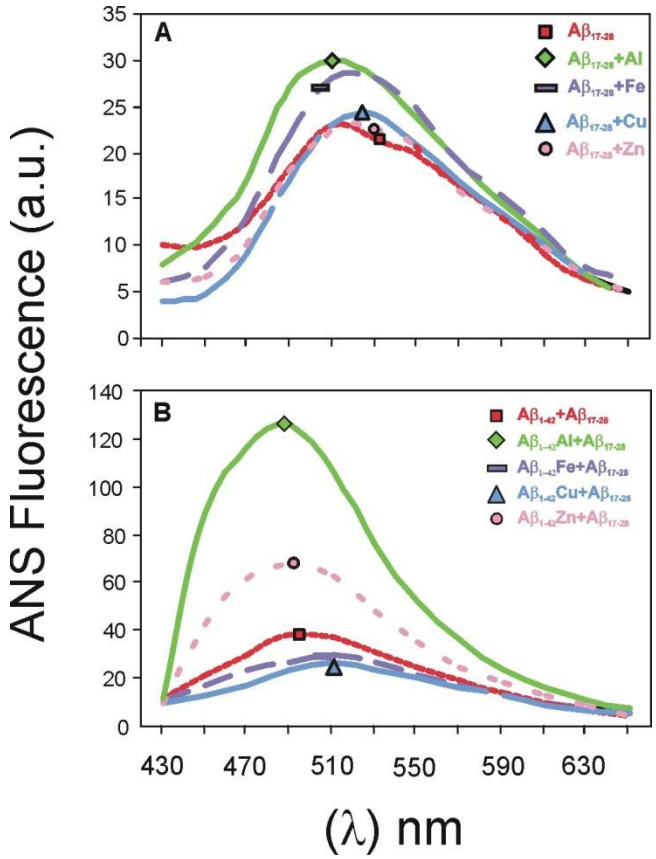

Figure 3.3.1 ***Fluorescence emission spectra of ANS (25 μM)*** *after interaction with $A\beta_{17-28}$ both in the absence and in the presence of Al, Cu, Fe and Zn at the concentration of 5μM (A), and to $A\beta_{17-28}$ in the presence of $A\beta_{1-42}$–metal complexes (B). Emission spectra were recorded from 400 to 700 nm with excitation at 360 nm. The $A\beta_{17-28}/A\beta_{1-42}$ ratio was equal to 1. The signals due to the free dye and buffer were subtracted. The peptide samples (5 μM) were left to incubate for 24 hours at room temperature, then the fluorescence was measured.*

The dependence of ThT fluorescence on time for samples of $A\beta_{1-42}$, $A\beta_{1-42}$-metal complexes and $A\beta_{17-28}$ was examined (Figure 3.3.2). $A\beta_{17-28}$ and $A\beta_{17-28}$+Fe are characterized by a lag time before the formation of β-sheet structure which occur after ~5h. The aggregation is enhanced in the presence of the other metals tested being Al the most affected in promoting the process. The absence of a lag time in the sample $A\beta_{17-28}$+Al could suggest the possibility of an immediate conversion of monomeric $A\beta_{17-28}$ into ThT-reactive species.

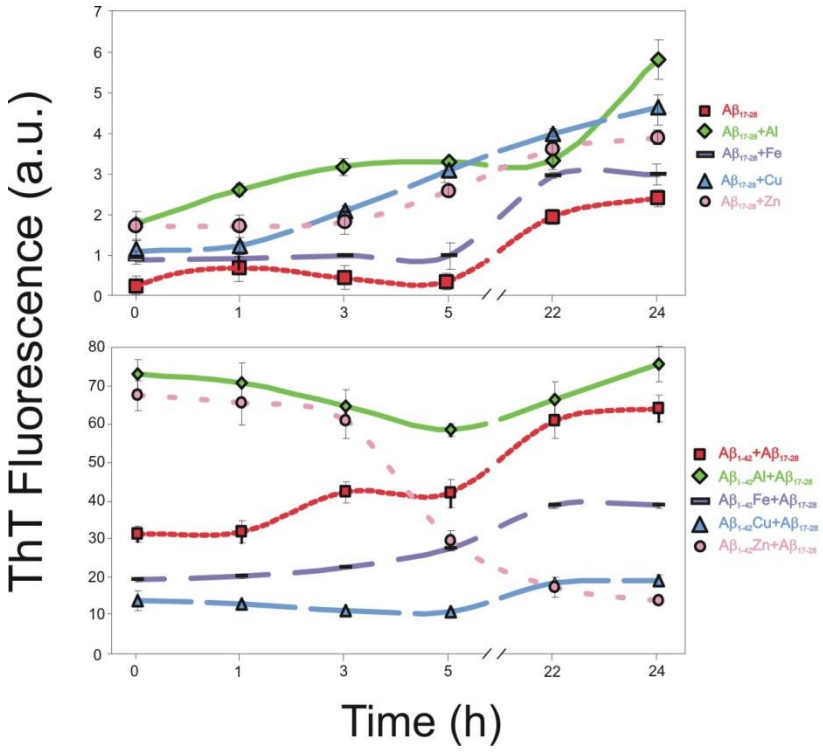

Figure 3.3.2 ***Time-dependence of the fluorescence emission intensity of ThT*** *bound to $A\beta_{17-28}$ both in the absence and in the presence of Al, Cu, Fe and Zn at the concentration of 5 μM and to $A\beta_{17-28}$ in the presence of $A\beta_{1-42}$–metal complexes. The $A\beta_{17-28}$, $A\beta_{1-42}$ and $A\beta_{1-42}$–metal complexes peptide concentrations were 5μM. ThT (20 μM) fluorescence at 482 nm (λ_{exc}=450 nm) was followed for 24 hours. The signals due to the free dye and buffer were subtracted. The data represented are mean ± SD of three individual experiments.*

ThT was employed also to check changes in β-sheet content in samples of $A\beta_{1-42}$/ $A\beta_{1-42}$-metal complexes to which were initially added $A\beta_{17-28}$. A marked increase in ThT fluorescence was observed with $A\beta_{1-42}$-Al+$A\beta_{17-28}$ compared to $A\beta_{1-42}$-Al alone, suggesting that the interaction between the oligomers of the metal complex and the peptide fragment was effectively in promoting nucleation assembly.

$A\beta_{1-42}$-Zn+$A\beta_{17-28}$ precipitated indicating that the equilibrium of the proteic species was forced toward amorphous aggregates. The mechanism was not reversible since mixing the solution did not resuspend the aggregate.

$A\beta_{1-42}$-Fe+$A\beta_{17-28}$ as well as $A\beta_{1-42}$-Cu+$A\beta_{17-28}$ showed low initial ThT fluorescence intensity, which did not significantly change over a 24h period.

Turbidity assay

To clarify the effect of $A\beta_{17-28}$ on $A\beta_{1-42}$/$A\beta_{1-42}$-metal complexes fibrillization, aggregation was also assayed by turbidity at a 405 nm wavelength. The presence of Al favoured an increase in the $A\beta_{17-28}$ aggregation which stabilized after 24h of incubation. The other metals exerted only negligible effects on the quantity of $A\beta_{17-28}$ aggregates. The presence of $A\beta_{17-28}$ stimulated the aggregate formation in the $A\beta_{1-42}$-Al and $A\beta_{1-42}$-Fe samples while the other conditions were not affected.

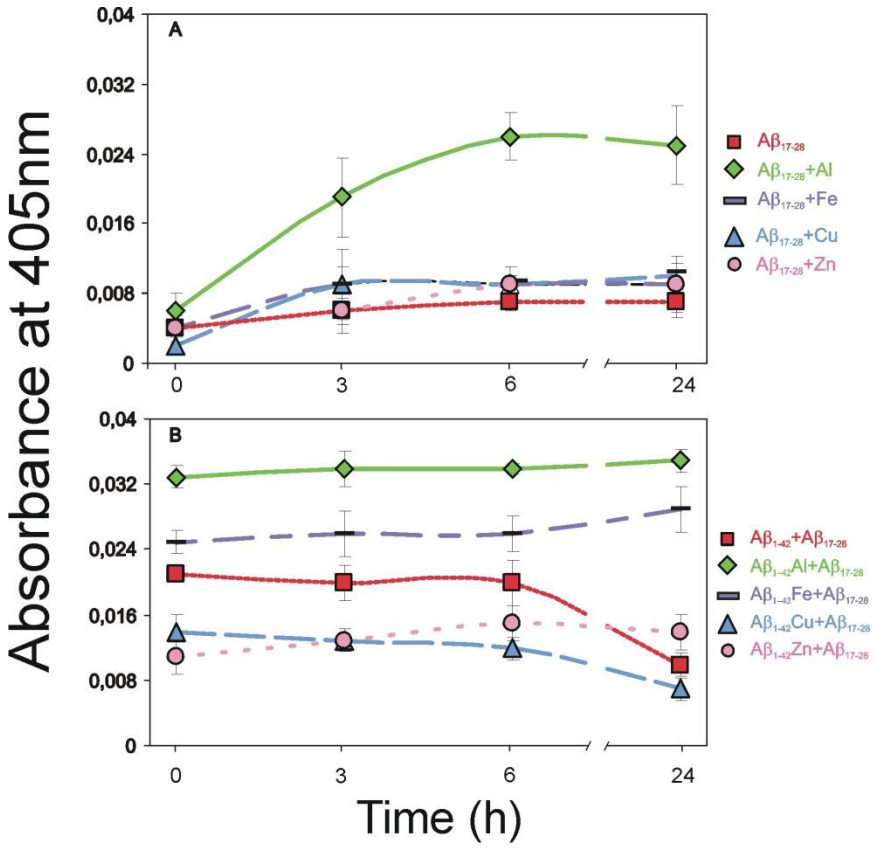

Figure 3.3.3 ***Turbidity kinetic assay*** *of $A\beta_{17-28}$ both in the absence and in the presence of Al, Cu, Fe and Zn at the concentration of 5μM (A), and of $A\beta_{17-28}$ in the presence of $A\beta_{1-42}$–metal complexes (B). The $A\beta_{17-28}$, $A\beta_{1-42}$ and $A\beta_{1-42}$–metal complexes peptide concentrations were 5μM. Turbidity was measured at 405 nm. The data represented are mean ± SD of three individual experiments. All readings were corrected for the background absorbance.*

3.3.2. **Viability assay on SHSY5Y**

We initially examined the concentration dependence of toxicity of $A\beta_{17-28}$ SHSY5Y with $A\beta_{17-28}$ in a range of concentration between 0.01 μM to 5 μM (Figure 3.3.4). The toxicity on SHSY5Y was evaluated by a standard MTT assay. We found that the fragment concentration needed to inhibit 50% (IC_{50}) of cell viability is higher than 5 mM. The other concentrations tested showed no or minimal toxicity. We choose 0.1 μM as non toxic concentration to treat cells in the presence of $A\beta_{1-42}$/$A\beta_{1-42}$-metal complexes. As shown in Figure 3.3.4 the co-treatment with $A\beta_{17-28}$+$A\beta_{1-42}$-Al determined a highly significant decrease of cell viability. Also $A\beta_{17-28}$+$A\beta_{1-42}$ treatment seemed to be deleterious even if at a lesser extent.

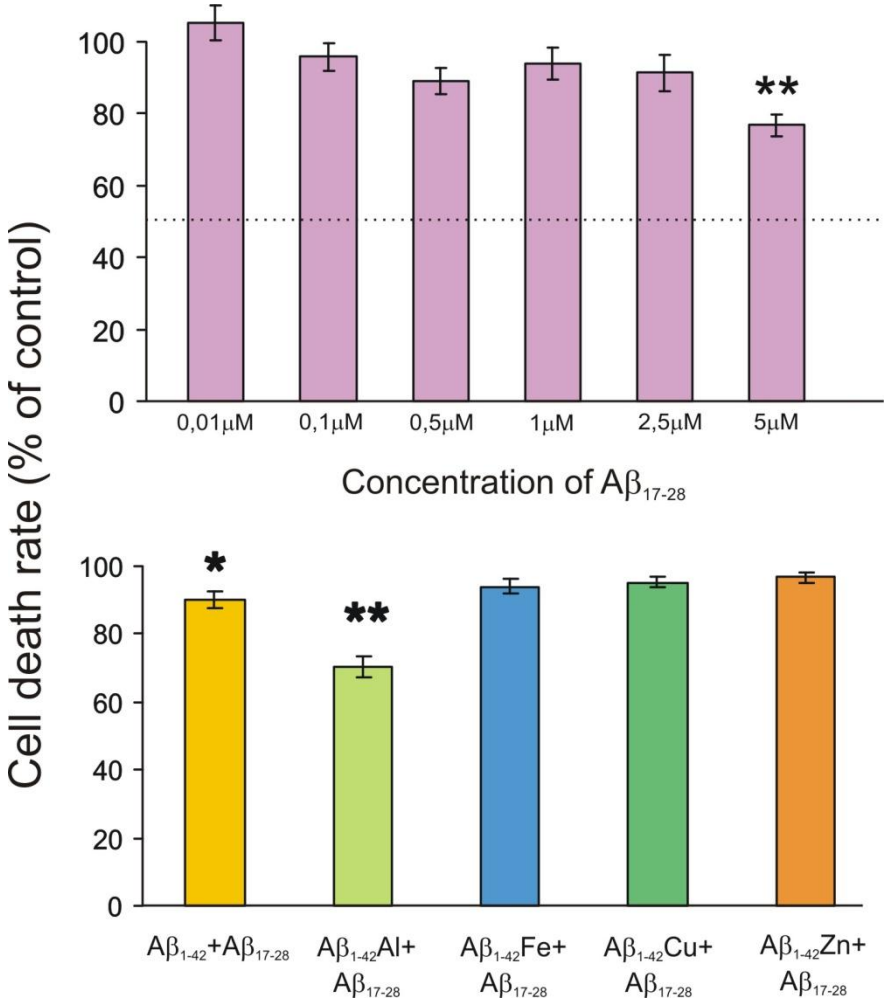

Figure 3.3.4 ***Viability of human neuroblastoma cells measured by MTT assay.*** *Shown is the dependence of neurotoxicity (% cell death as compared to control) on the concentration of $A\beta_{17-28}$. SH-SY5Y cells were also incubated for 24h with $A\beta_{17-28}$ (0.1 μM) and $A\beta_{1-42}$-metal complexes (0.5 μM). The*

*peptides mixture was kept 24h to incubate at room temperature to aloud peptides interaction before adding them to the cell medium. The data represented are mean ± SD of three individual experiments, each done in triplicate. ** P< 0.01 vs control.*

3.4. Mutual stimulation of β-amyloid fibrillogenesis by clioaquinol and divalent metals

3.4.1. Effects of CQ on the aggregation pattern of Aβ and Aβ-metal complexes

The progress of Aβ and Aβ-metal complexes ± CQ aggregation was monitored by measuring the increment of ThT fluorescence emission at 482 nm (λ_{exc}: 450 nm). Our results clearly show a time-dependent aggregation of human Aβ even in the absence of the addition of any metal ion (Figure 3.4.1), as already reported (Ricchelli et al., 2005). Under the experimental conditions herein used, Cu^{2+} and Zn^{2+} negligibly modified the peptide self-aggregation.

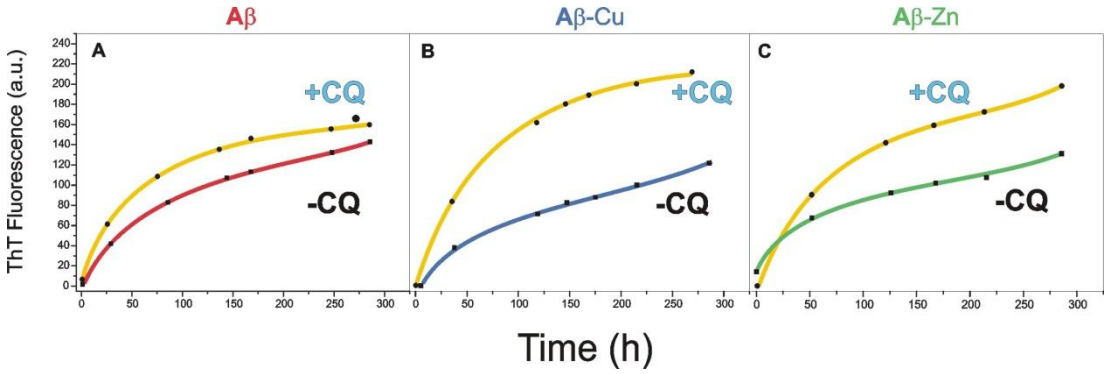

Figure 3.4.1 ***Time-dependence of the fluorescence emission intensity of ThT bound to human Aβ (A), Aβ-Cu (B) and Aβ-Zn (C)****. 5μM peptide were dissolved in the standard medium both in the absence and the presence of 25 μM CQ. ThT (12 μM) fluorescence at 482 nm (λ_{exc}=450 nm) was followed for 300 hours. The signals due to the free dye and CQ were subtracted.*

Unexpectedly, the addition of CQ increased the amplitude of the aggregational process for both Aβ alone and, more drastically, Aβ-Cu and Aβ-Zn complexes. The pro-aggregating effect of CQ could be observed also for Aβ sequences which showed *per*

se a low propensity to undergo polymerization, as is the case for rat Aβ see the negligible changes in ThT fluorescence obtained in the absence of CQ (Figure 3.4.2).

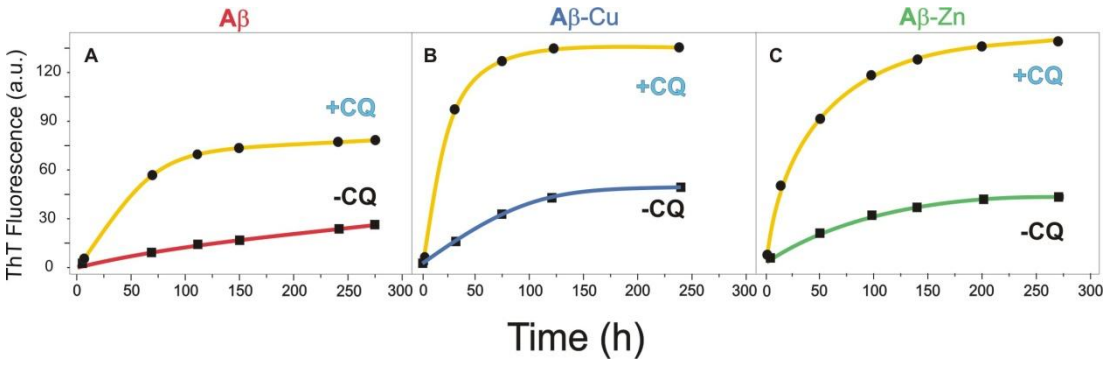

Figure 3.4.2 ***Time-dependence of the fluorescence emission intensity of ThT bound to rat Aβ (A), Aβ-Cu (B) and Aβ-Zn (C)****. 5μM peptide were dissolved in the standard medium both in the absence and the presence of 25 μM CQ. ThT (12 μM) fluorescence at 482 nm (λ_{exc}=450 nm) was followed for 300 hours. The signals due to the free dye and CQ were subtracted.*

Also in this case, the CQ-promoted increase of aggregation was more evident for Aβ-metal complexes. Similar CQ-induced effects were achieved when the metal chelator was added during the progress (Figure 3.4.3) or at the end (not shown) of the aggregational process.

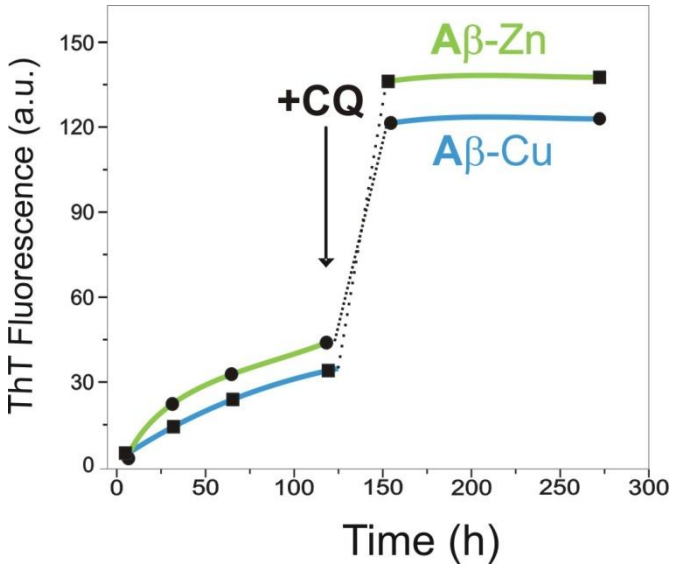

Figure 3.4.3 ***Time-dependence of the fluorescence emission intensity of ThT bound to to rat Aβ-Cu and Aβ-Zn (5μM)****. Where indicated (arrow) 25 μM CQ was added. The experimental conditions were the same as those described in the legend to figure 2.*

In close analogy with the results obtained by ThT fluorescence experiments, the turbidity assays revealed an enhanced aggregation of both human and rat peptides after

co-incubation with CQ (Fig. 4). The effect was less pronounced for Aβ alone; on the other hand , it became particularly evident for the Aβ-Zn and Aβ-Cu complexes, whose absorbance underwent a statistically significant increase when CQ was added.

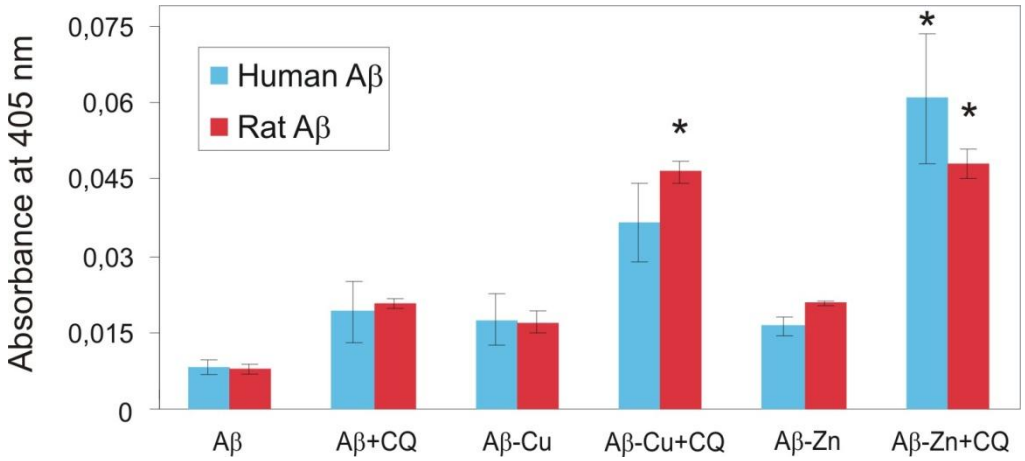

Figure 3.4.4 ***Turbidity assay of human Aβ (blue bars) and rat Aβ (red bars) alone and complexed with Cu^{2+} and Zn^{2+} in the absence and in the presence of CQ (25 μM)****. The peptide samples (5 μM) were left to incubate for 3 hours at room temperature, then the absorbance was measured at 405 nm. The data represented are mean ± SD of three individual experiments. * Significant difference (P< 0.05) as compared to the corresponding peptide without CQ.*

3.4.2. **Characterization of Aβ aggregates by TEM**

TEM studies were performed to obtain information on the possible evolution of Aβ aggregates to higher, structured polymers and their morphological characteristics. The protein concentrations chosen (10 μM) were higher than those used in the fluorescence experiments, in order to accelerate the structural organization of Aβ aggregates. Figures 3.4.5 and 3.4.6 report the electron micrographs obtained after 150 hours incubation.

Under our experimental conditions, human Aβ was able to form well-ordered, branched fibrillar filaments, as shown in Figure 3.4.5A. The presence of CQ did not destroy or prevent the aggregate organization; on the contrary, fibrillar formations similar to those obtained for Aβ alone were observed (Figure 3.4.5B). TEM studies on human Aβ complexed with Cu^{2+} showed no evidence of the formation of defined structures (Figure 3.4.5C). In the presence of CQ, however, a dense fibril network could be observed (Figure 3.4.5D). Human Aβ-Zn aggregates evolved into few,

poorly branched, short filamentous structures (Figure 3.4.5E), together with amorphous agglomerates (not shown). The fibrillogenesis was clearly stimulated in the presence of CQ, which generated mainly clumps of short protofibrils together with mature fibrils (Figure 3.4.5F).

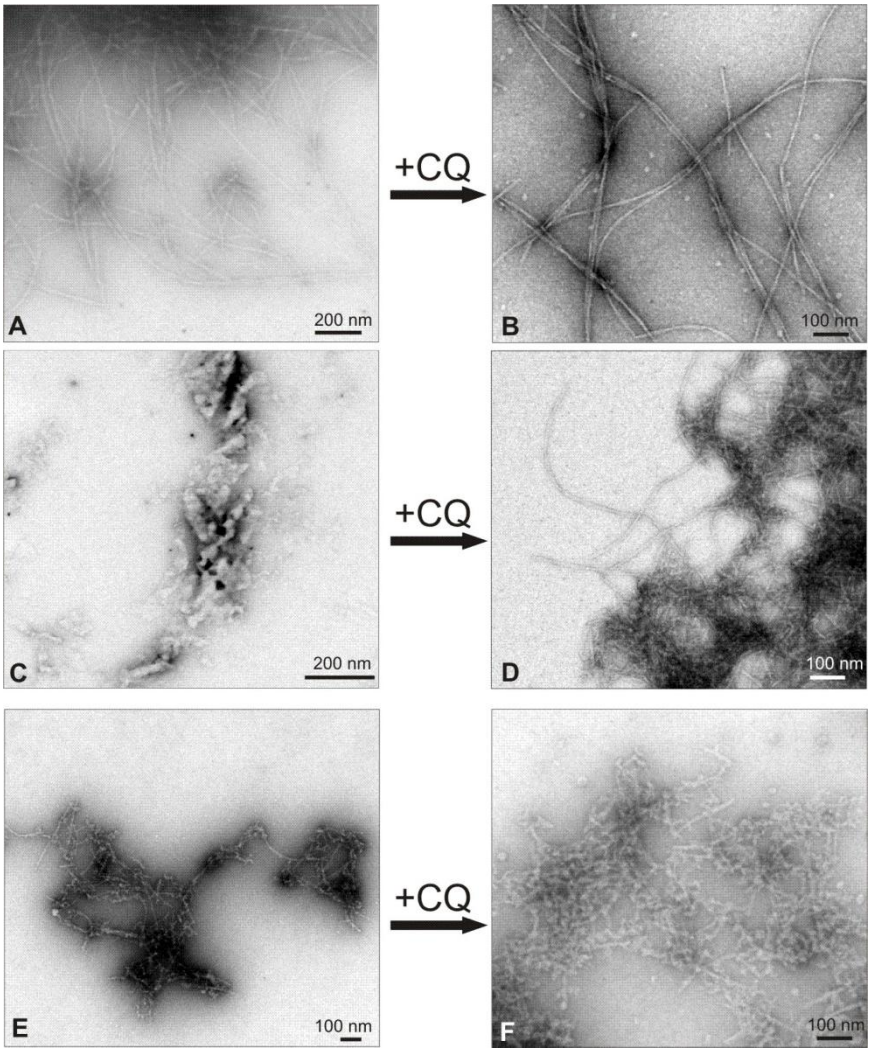

Figure 3.4.5. ***TEM micrographs of human Aβ and Aβ-metal complexes in the absence and the presence of CQ.*** *(A) Aβalone; (B) Aβ plus CQ; (C) Aβ-Cu alone; (D) Aβ-Cu plus CQ; (E) Aβ-Zn alone; (F) Aβ-Zn plus CQ. The peptide samples (10 μM) were left to incubate in the standard medium for 150 hours at T=25 ˚C, both in the absence and the presence of 50 μM CQ.*

The electron micrographs of rat Aβ in the absence of added metals revealed the presence of small spherical structures (oligomers) (Figure 3.4.6A), in agreement with a slower pattern of aggregation, compared to human Aβ (see Figs 3.4.1 and 3.4.2).The presence of CQ did not significantly influence the aggregate structural organization, even though it increased the density of spherical oligomers (Figure

3.4.6B). In the presence of Aβ-Cu and Aβ-Zn complexes no defined structures were detected (Figs. 3.4.6C, E); in contrast, the metal complexes gave rise to fibrillar filaments when incubated with CQ (Figs. 3.4.6D, F).

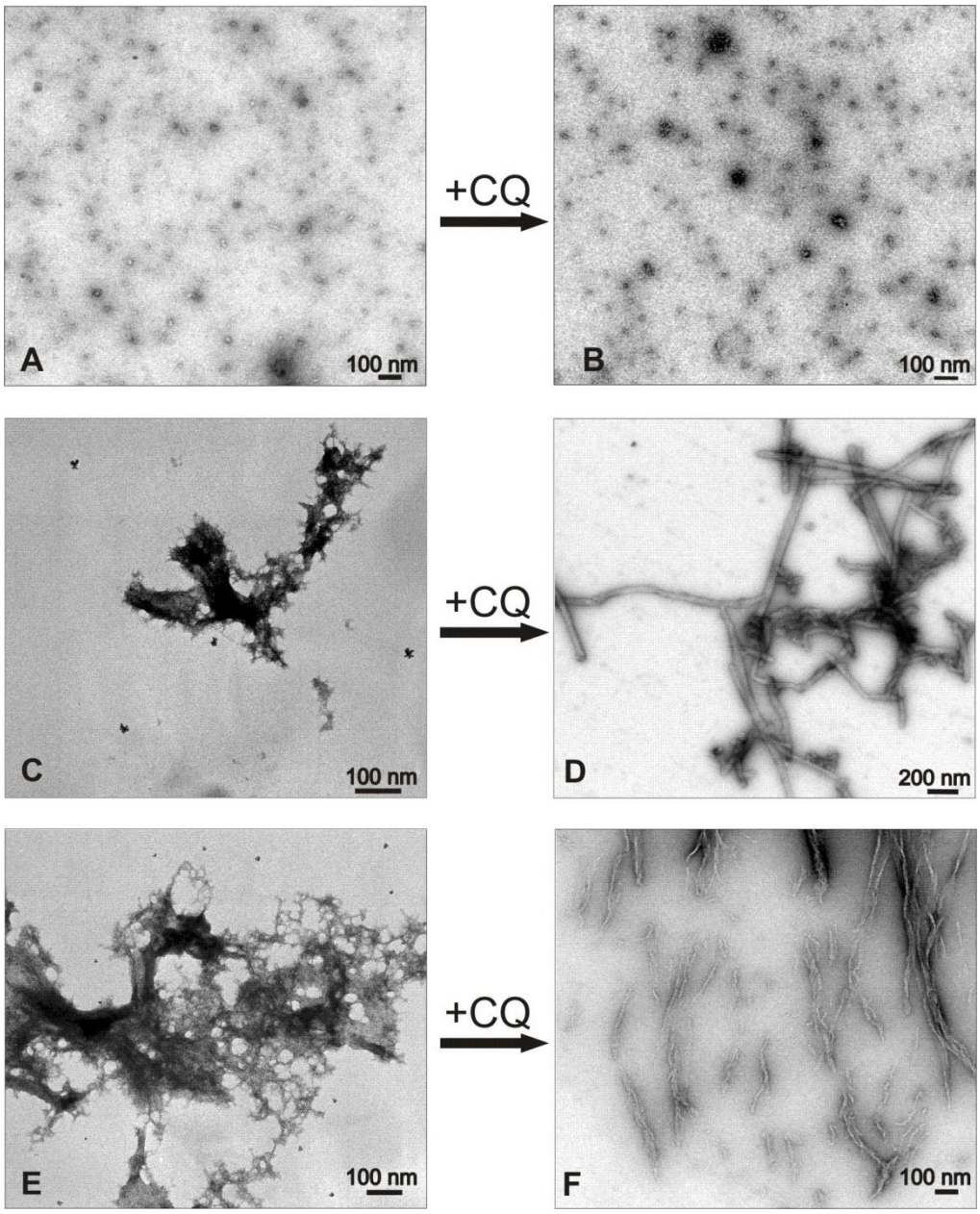

Figure 3.4.6 ***TEM micrographs of rat Aβ and Aβ-metal complexes in the absence and the presence of CQ.*** *(A) Aβalone; (B) Aβ plus CQ; (C) Aβ-Cu alone; (D) Aβ-Cu plus CQ; (E) Aβ-Zn alone; (F) Aβ-Zn plus CQ. The peptide samples (10 μM) were left to incubate in the standard medium for 150 hours at T=25 °C, both in the absence and the presence of 50 μM CQ.*

3.4.3. **Cell Viability assay**

We tested the effect of CQ (1 nM), both alone and in the presence of Aβ, Aβ-Cu, Aβ-Zn, free Cu^{2+} and Zn^{2+}, on the vitality of human neuroblastoma cells (Figure 3.4.7). After 24 hours incubation, a marked decrease of cell viability (~ 35% of the control) was observed with Aβ-Zn+CQ treatment. This effect was peculiar since CQ and Aβ-Zn alone, as well as CQ+Zn^{2+}, only negligibly affected the cell viability. A decrease of viability, even though less than that observed with Aβ-Zn+CQ, was also observed with Aβ-Cu+CQ, whereas exposure to CQ+Cu^{2+} did not produce any toxic effect. It is interesting to notice that while Zn^{2+} and Zn+CQ did not alter the viability of SH-SY5Y cells, the slight decrease observed in treatment with Cu^{2+} alone was eliminated with CQ+Cu^{2+}. This pattern of toxicity was still evident after 48h (data not shown).

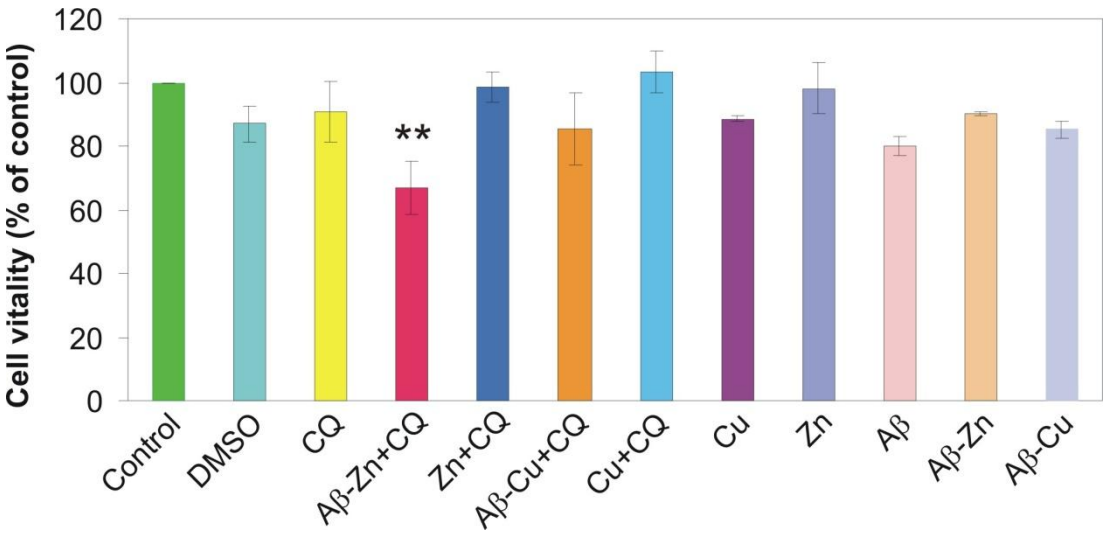

Figure 3.4.7. ***Effect of CQ, both alone and in the presence of Aβ, Aβ-Cu, Aβ-Zn, Cu^{2+} and Zn^{2+}, on the viability of human neuroblastoma cells.*** *SH-SY5Y cells were incubated for 24h with Aβ alone, Aβ-metal complexes (peptide concentration = 0.5 μM), Cu^{2+} or Zn^{2+} (5μM), with or without CQ (1 nM, from a 10 mM stock solution in DMSO). Cell viability was measured by MTT assay (see Materials and Methods). The data represented are mean ± SD of four individual experiments, each done in triplicate. ** P< 0.01 vs control, CQ, CQ+Zn^{2+}, Zn^{2+} and Aβ-Zn.*

3.4.4. **SEM of neuroblastoma cells**

To examine the morphological effects of the treatments on SH-SY5Y cells we performed SEM microscopy (Figure 3.4.8). In the presence of Aβ-Zn+CQ an evident membrane impairment was observed. Cells displayed a different shape and the membrane seemed to be largely altered with respect to the control and the other treatments. It is worth noting that this effect was not achieved by CQ alone. Co-treatment with the drug and metals alone did not produce any alterations in the morphology of neuroblastoma cells (data not shown).

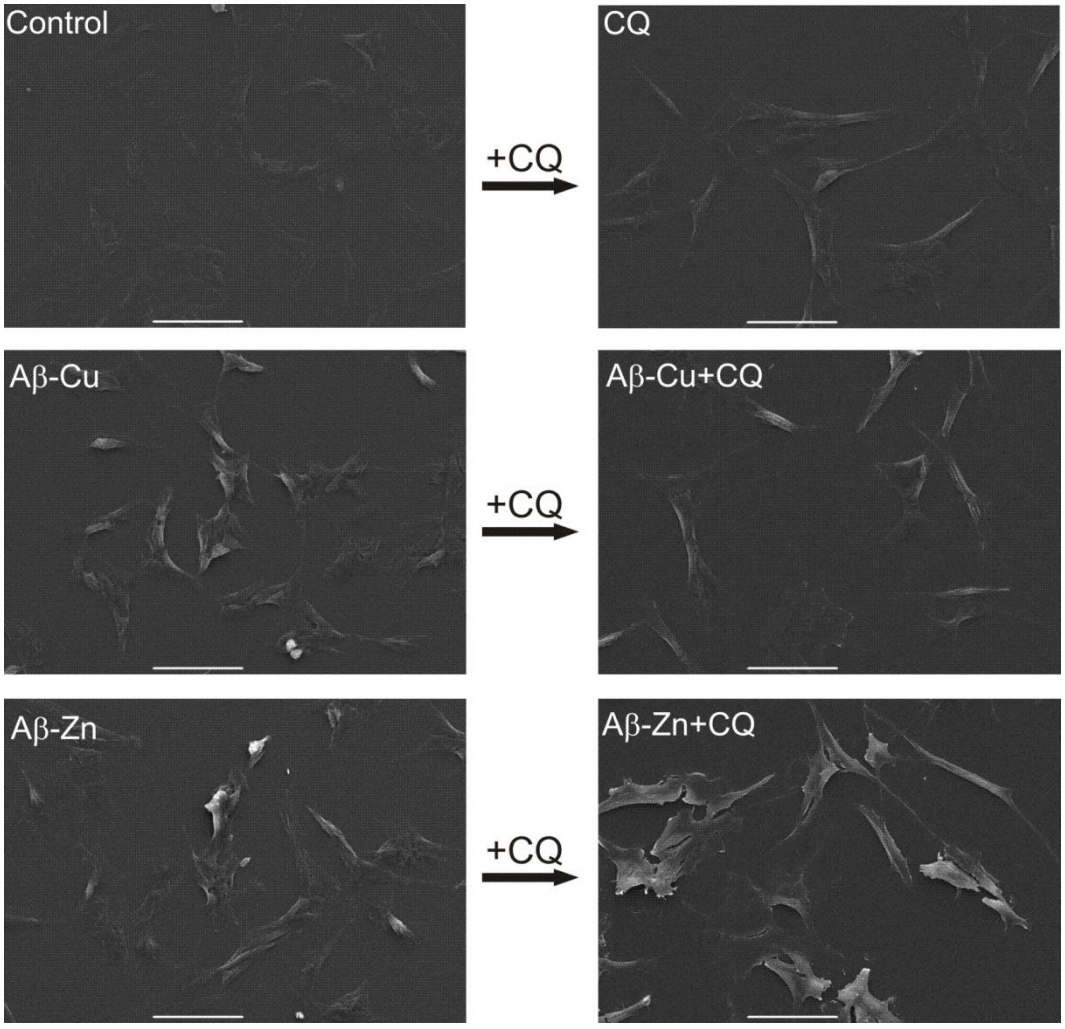

Figure 3.4.8 ***SEM micrographs of human neuroblastoma cells.*** *SH-SY5Y cells were treated for 24h with Aβand Aβ-metal complexes, with or without CQ, under the same experimental conditions described in the legend to Fig. 6. SEM microscopy was performed as described in Materials and Methods. In the figure, the scale bars correspond to 50 μm.*

3.5. Overexpression of QPCT as potential biomarker for AD: influence of Aβ-metal complexes

qRT-PCR analysis of QPCT gene was performed on SH-SY5Y human neuroblastoma cells under the same experimental condition used for viability assay. A high significant increase of mRNA levels (as shown by fold of control expression levels) was found after 24h treatment with Aβ-Al complex and at a lesser extent with Aβ-Zn (Figure 3.5.1). Negligible was the effect of the other treatments compare to the control.

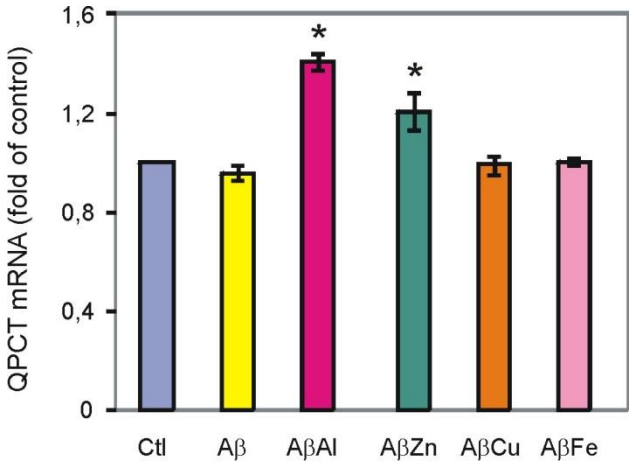

Figure 3.5.1 ***Effects of Aβ-metal complexes on the mRNA levels of QPCT in SH-SY5Y.*** *(*p<0.05)*

The expression of this gene was also tested in the pheripheral blood of AD patients compared to elderly subjects. Figure 3.5.2 showed the significant increase in QPCT expression in the affected patients.

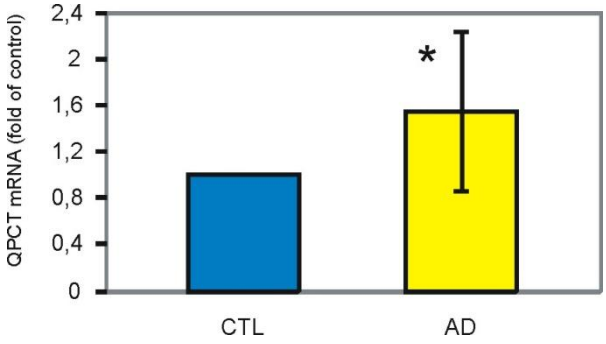

Figure 3.5.2. ***QPCT expression in pheripheral blood of AD patients compare to control subjects*** (*p<0.05).

3.6. Accumulation of Cu and other metal ions, and MT I/II expression in the bovine brain as a function of aging

3.6.1. Metal content

The levels of Cu and Zn were significantly increased in relation with age in almost all brain regions considered (Figure 3.6.1A-B). The only exception was the white matter of the cerebellum, where Cu concentrations were lower in the series of older animals. Zn displayed a pronounced age-related increase in the cerebellum and thalamus. An increment, less evident, was detected also in the *corpus callosum*, *gyrus dentatus*, *medulla oblongata*, temporal, parietal and frontal cortex.

Mn seemed to redistribute in the brain rather than change in relation to age (Figure 3.6.1C). Only the parietal cortex and *corpus callosum* of young subjects displayed higher Mn levels than the corresponding adult tissue. Meanwhile, in occipital cortex and pons a significant decrease was observed.

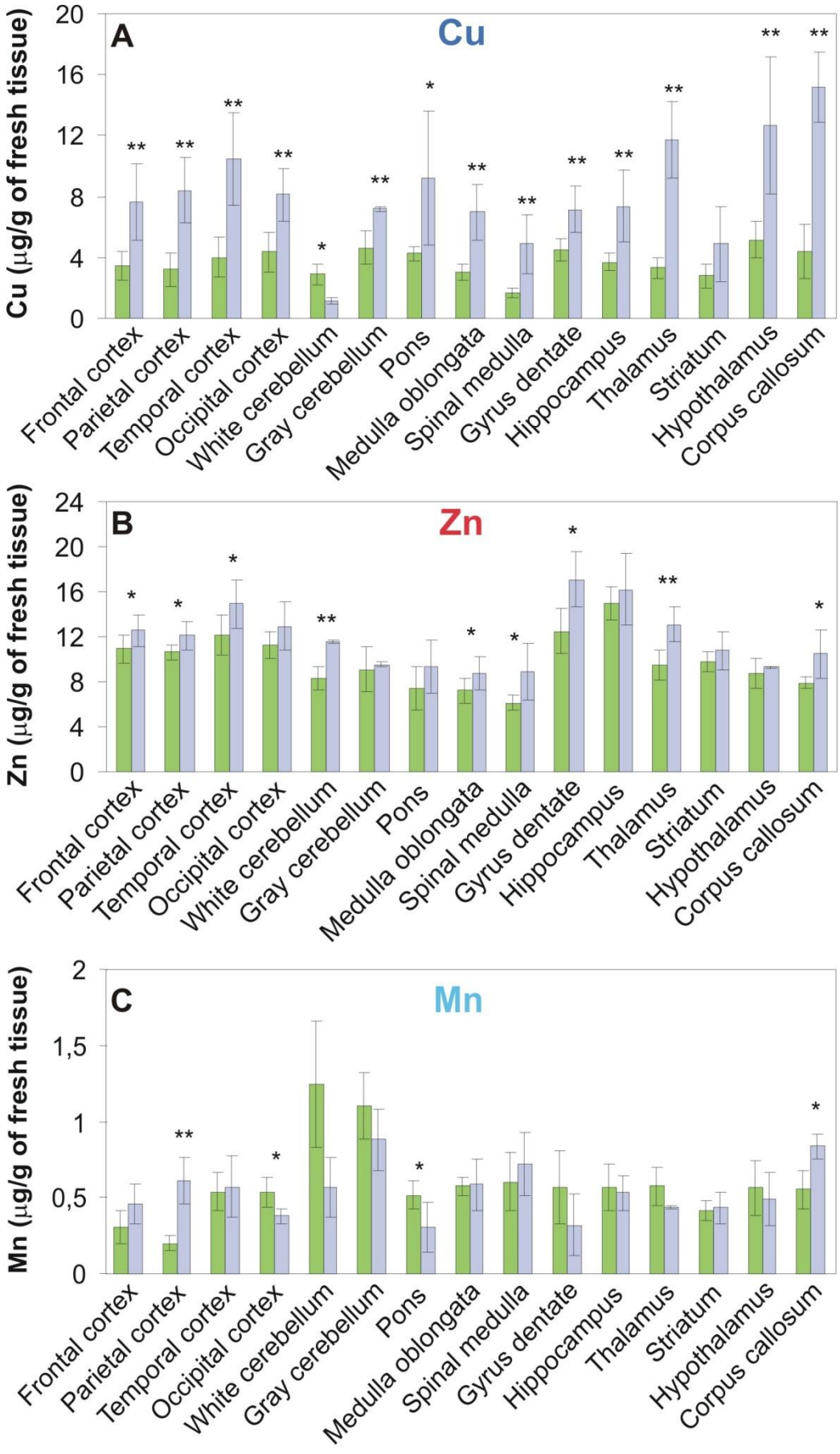
A
Cu
Cu (µg/g of fresh tissue)
20
16
12
8
4
0
B
Zn
Zn (µg/g of fresh tissue)
24
20
16
12
8
4
0
C
Mn
Mn (µg/g of fresh tissue)
2
1,5
1
0,5
0
Frontal cortex
Parietal cortex
Temporal cortex
Occipital cortex
White cerebellum
Gray cerebellum
Pons
Medulla oblongata
Spinal medulla
Gyrus dentate
Hippocampus
Thalamus
Striatum
Hypothalamus
Corpus callosum

Figure 3.6.1 ***Cu (A), Zn (B) and Mn (C) concentrations*** *in fifteen different brain regions with respect to animal age (μg/g fresh tissue): 8-12 months (n=10) white bars, 9-12 years (n=3) grey bars.*

3.6.2. **Immunohistochemistry**

The use of immunohistochemical methods to investigate the presence and distribution of MT I/II and GFAP in the brain of bovine yielded better results in the sections in which microwave unmasking of the antigens was performed.

MT I-II

MT I/II immunoreactive (-ir) neural cells were identified in the cerebellar cortex of all subjects and in the ependyma lining the lateral ventricles of young animals. The animals (young and old) showed also rare MT I/II-ir cells also in sections of the frontal and temporal cortex.

In the cerebellar cortex, presence, distribution and density of MT I/II-ir elements resulted constant independently from the age of the bovine. MT I/II-ir cells were present in the middle layer, in the same location as the larger Purkinje neurons (Figure 3.6.2).

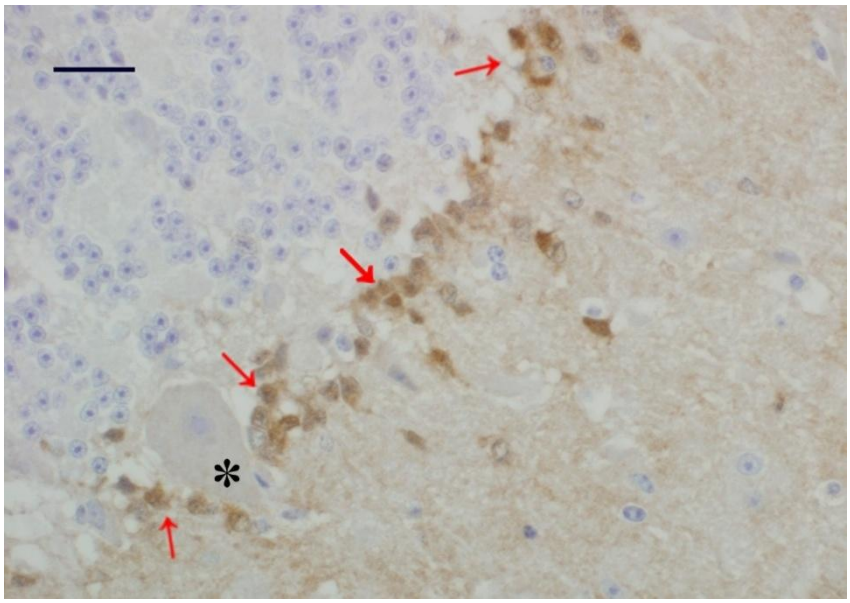

Figure 3.6.2 ***Arrows indicate MT I/II****- containing elements in the cerebellar cortex in a young animal. Scale bar = 50 μm.*

In young subjects, ependymal-ir elements were dispersed along the ventricular lining among immuno-negative elements. Fine cytoplasmatic extensions arose from the ventricular surface of metallothionein-ir ependymal cells towards the liquor. The cell surfaces facing away from the ventricle displayed slender conical extensions directed towards adjacent cell laminae (Figure 3.6.3).

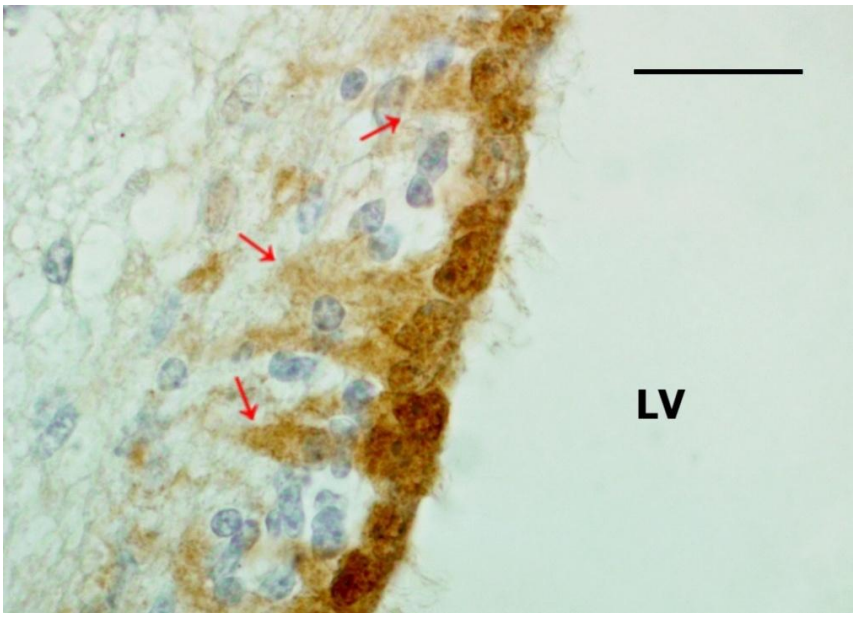

Figure 3.6.3 ***MT I/II- containing elements in the ependyma*** *of the lateral ventricle in a young animal. Arrows point to deeper portions of the cytoplasm. Scale bar = 50 µm.*

A few MT I/II-ir cells were evident also in the temporal (Figure 3.6.4) and frontal cortex, independently of age classes (see also below under colocalization).

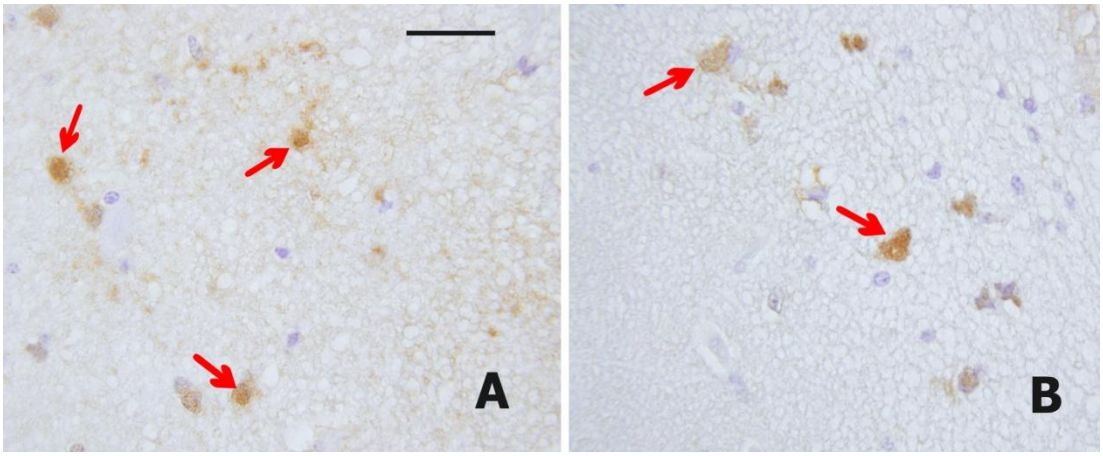

Figure 3.6.4 ***Arrows point towards MT I/II- containing elements*** *in the temporal cortex of a young (1 year old, A) and an old (12 years old, B) bovine. Scale bar = 100 µm.*

GFAP

GFAP-ir cells were present in all the sections of the two experimental series, and especially in the cortex. No significant difference in density was found in relation to age, since certain subjects showed marked individual variations in density, especially in the frontal cortex (Figure 3.6.5).

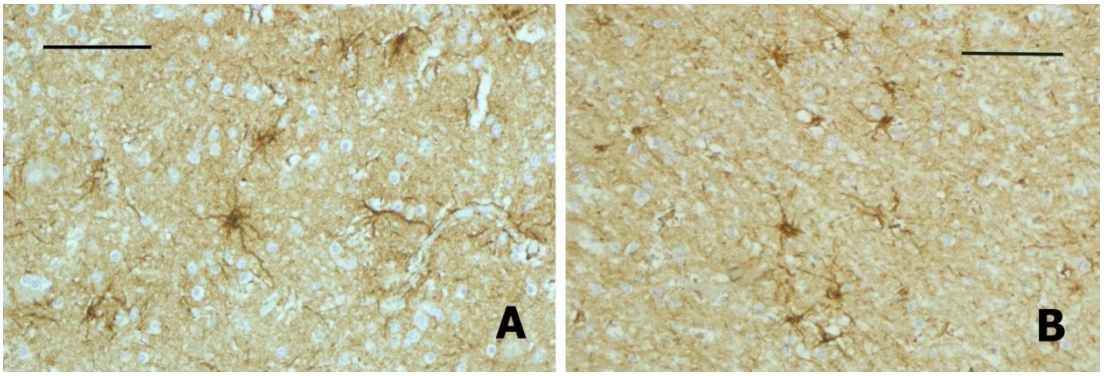

Figure 3.6.5 ***GFAP-containing elements in the frontal cortex.*** *A, 1 year old bovine; B, 9 years old bovine. Scale bars, A= 70 μm; B = 100 μm.*

CO-LOCALIZATION

Analysis at the confocal microscope, using sections of the frontal cortex of MT I/II immunopositive animals where GFAP-ir cells were also especially numerous, indicated that GFAP and MT I/II were co-localized in the same cell type (Figure 3.6.6). In fact superimposition of the two images showed that MT I/II-ir was localized within the cell body, while GFAP-ir included also cytoplasmic extensions typical of astrocytes. No immunoreactivity was detected in the nuclei.

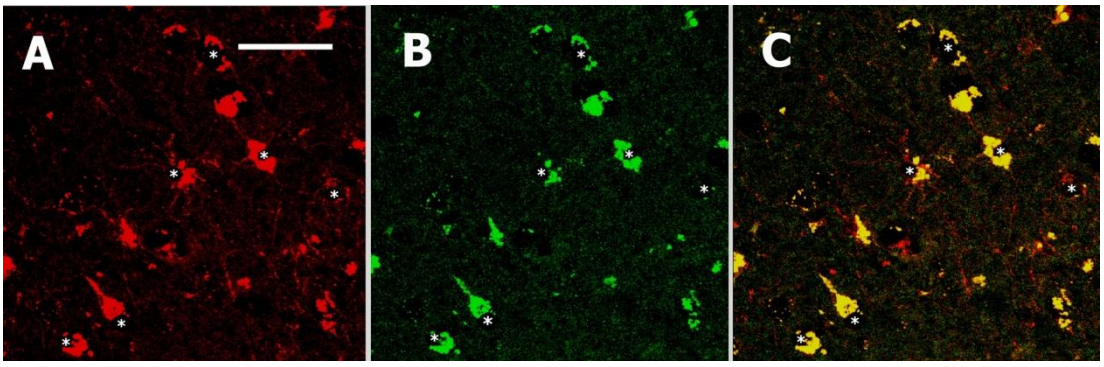

Figure 3.6.6 ***Frontal cortex of a young animal.*** *A, GFAP-ir cells (red); B, MT I/II-ir cells (green); C, merged image obtained at the confocal microscope showing colocalization in the cytoplasm; cellular nuclei (white asterisks) show no stain. Scale bar = 50 μm.*

3.7. Biochemical and behavioural effects of a Cu-deficient diet in adult mice

3.7.1. Metal content

Several metals were measured to asses the effect of the Cu-deficient diet on general metal distribution. A widespread decrease of metal content was observed in each of the four brain regions analyzed and for each metal investigated (Figure 3.7.1).

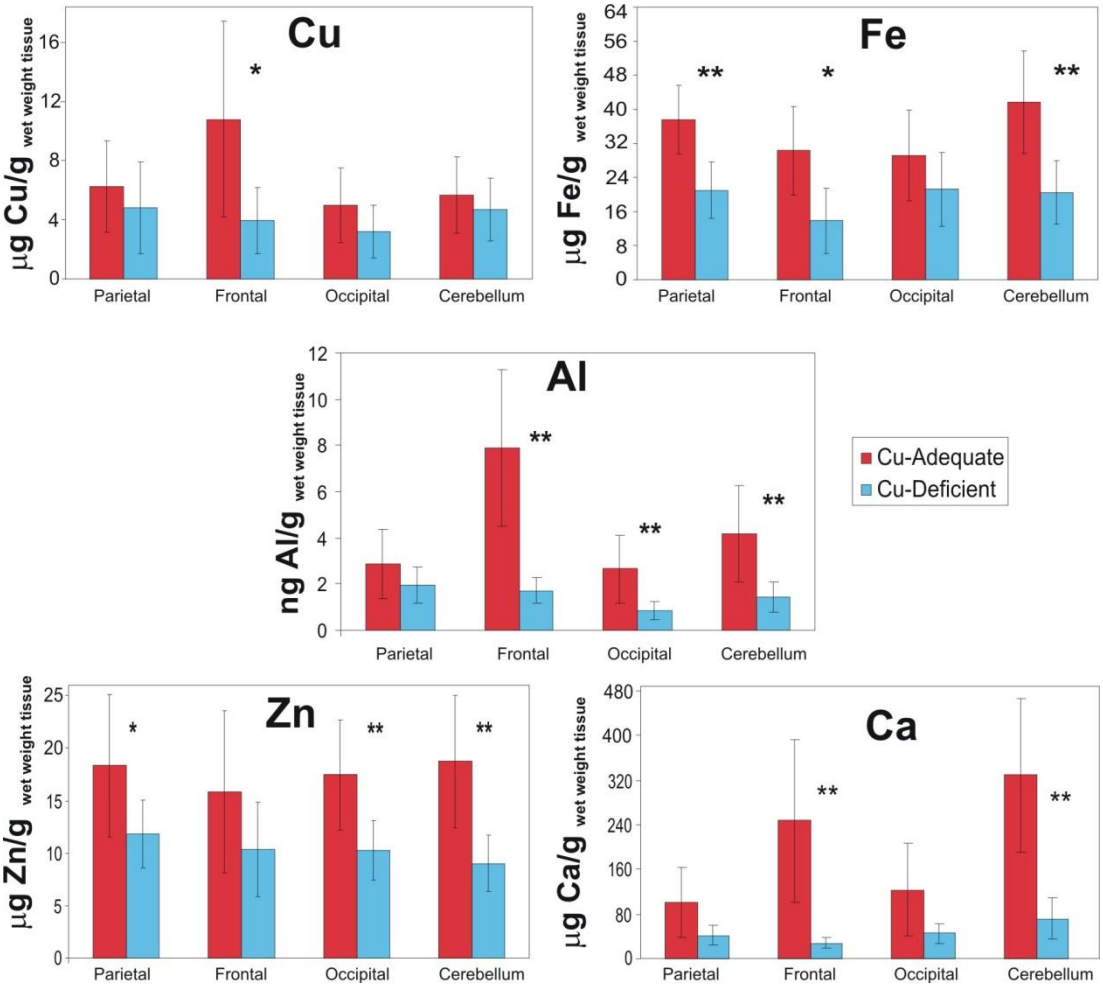

Figure 3.7.1 ***Cu, Fe, Al, Zn, Ca concentrations*** *in the homogenate of 4 brain regions of Cu-adequate (n=11) and Cu-depleted mice (n=12). The data represented are mean ± SD, **=p<0.01, *p<0.05.*

In particular, Cu-deficient mice had a statistically significant decrease of brain Cu, Fe, Al and Ca in the frontal area, concurrent with a highly statistically significant decreased of Fe, Al, Zn and Ca in the cerebellum. The non-physiological Al was markedly decreased also in the occipital area. Altogether, the frontal area and the cerebellum appeared to be the two regions most affected by the metal depletion. Figure 3.7.2 shows Cu concentration in the other main organs: only in the liver a significative Cu decrement was observed even if a general reduction was common also to the other organs. Fe was strongly decreased in lungs, small and large intestine and muscle (Figure 3.7.3), Zn in kidneys and hearth (Figure 3.7.4) and Ca in spleen, liver and kidneys (Figure 3.7.5).

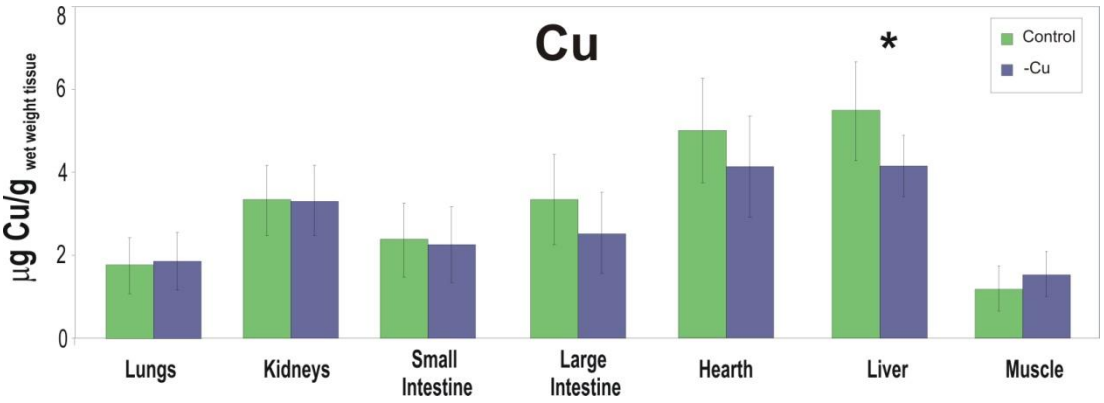

Figure 3.7.2 ***Cu concentration*** *in the homogenate of organs of Cu-adequate (n=11) and Cu-depleted mice (n=12). The data represented are mean ± SD, *p<0.05.*

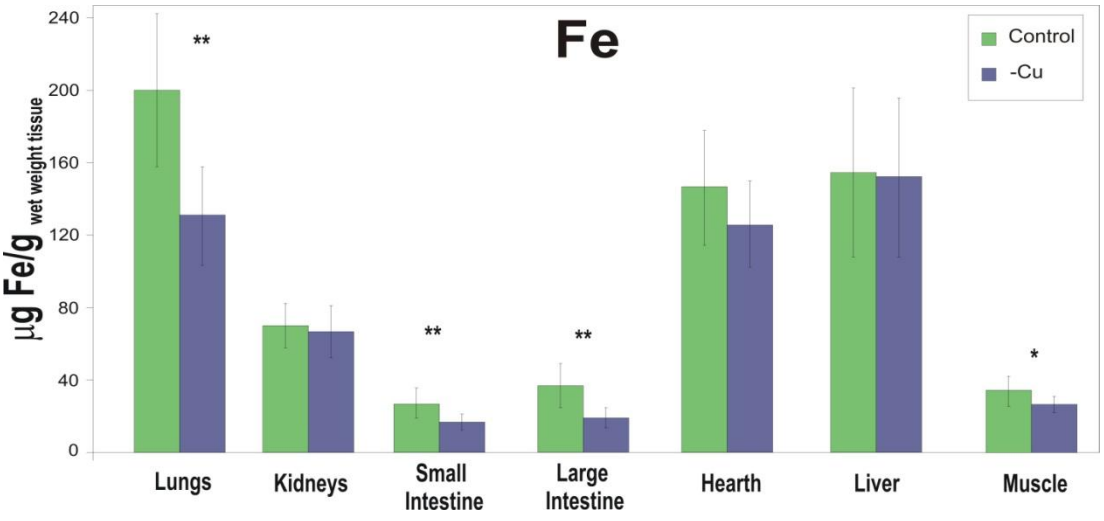

Figure 3.7.3 ***Fe concentration*** *in the homogenate of organs of Cu-adequate (n=11) and Cu-depleted mice (n=12). The data represented are mean ± SD, **=p<0.01, *p<0.05.*

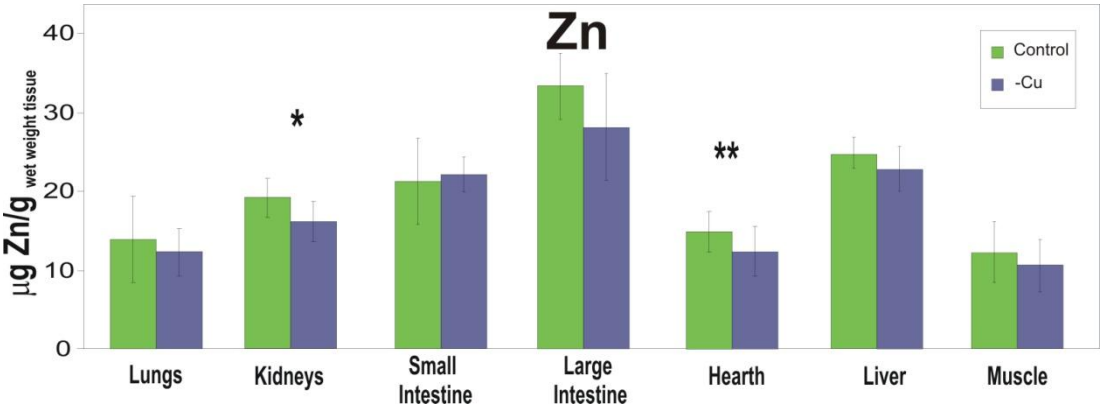

Figure 3.7.4 ***Zn concentration*** *in the homogenate of organs of Cu-adequate (n=11) and Cu-depleted mice (n=12). The data represented are mean ± SD, **=p<0.01, *p<0.05.*

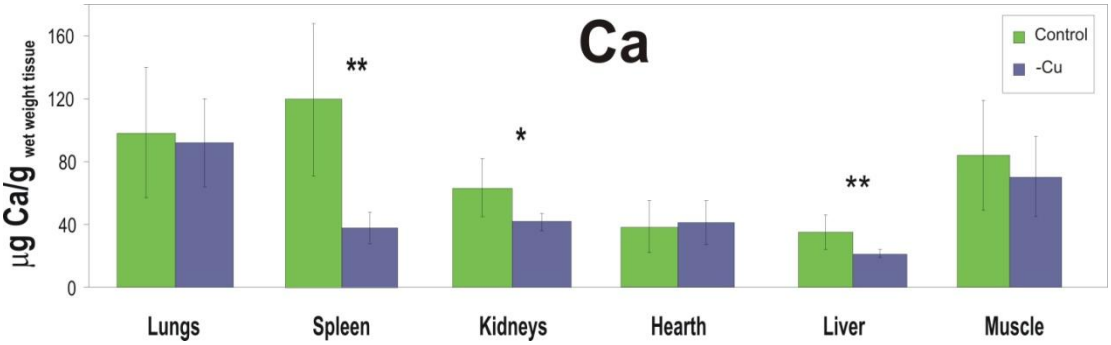

Figure 3.7.5 ***Ca concentration*** *in the homogenate of organs of Cu-adequate (n=11) and Cu-depleted mice (n=12). The data represented are mean ± SD, **=p<0.01, *p<0.05.*

3.7.2. **Metallothioneins (MTs)**

The total amount of MTs was found diminished in all the brain regions considered, with a statistically relevance only in the frontal area (Figure 3.7.6).

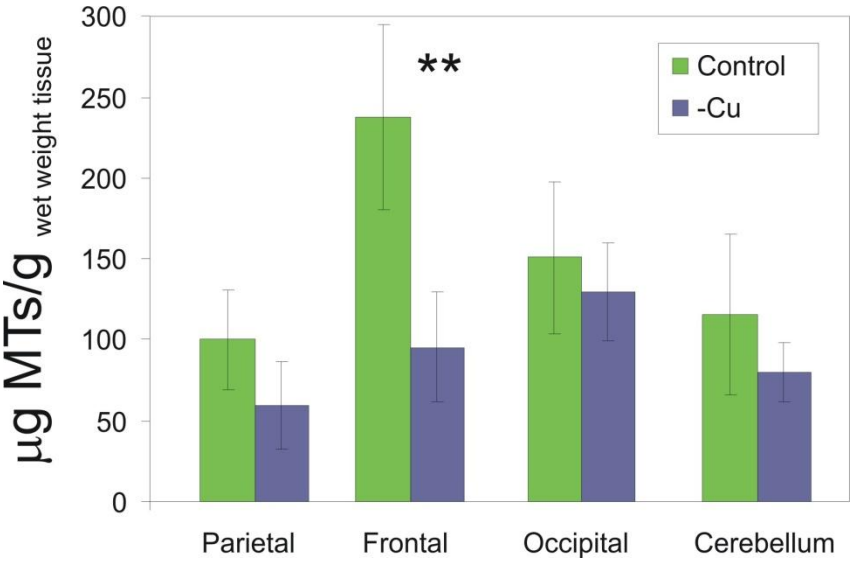

Figure 3.7.6 ***Total MT concentration*** *in the homogenate of 4 brain regions of Cu-adequate (n=11) and Cu-depleted mice (n=12). The data represented are mean ± SD, **=p<0.01, *p<0.05.*

Concerning the other organs a general increased in MTs concentrations was observed in almost all sections considered with a statistically significant increase in the large intestine and heart. The only exception was the small intestine where MTs concentration was lower in the Cu-deficient animals compared to controls. MTs quantification was not detectable in muscle tissue (Figure 3.7.7).

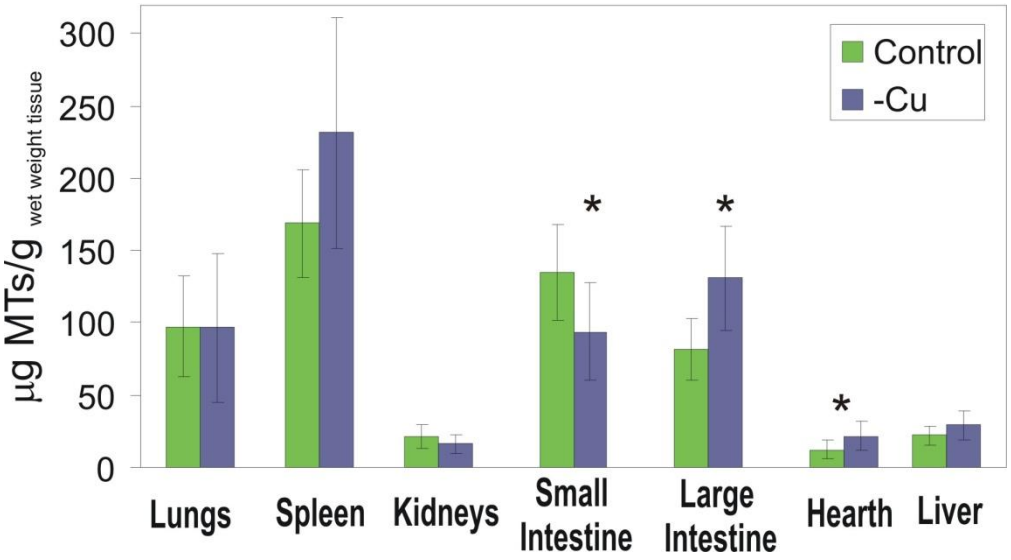

Figure 3.7.7 ***Total MT concentration*** *in the homogenate of organs of Cu-adequate (n=11) and Cu-depleted mice (n=12). The data represented are mean ± SD, *p<0.05.*

3.7.3. **Immunochemistry**

Representative images are shown in Figure 3.7.8. TH immunoreactivity in the substantia nigra-ventral tegmental area appeared more intense in the brains of mice receiving the copper-deprived diet, showing more intense cell bodies and labelled fibers (for cell bodies median grade + in controls vs. ++ in copper-deprived; for fibers, median +/- for controls and ++ for copper-deprived).

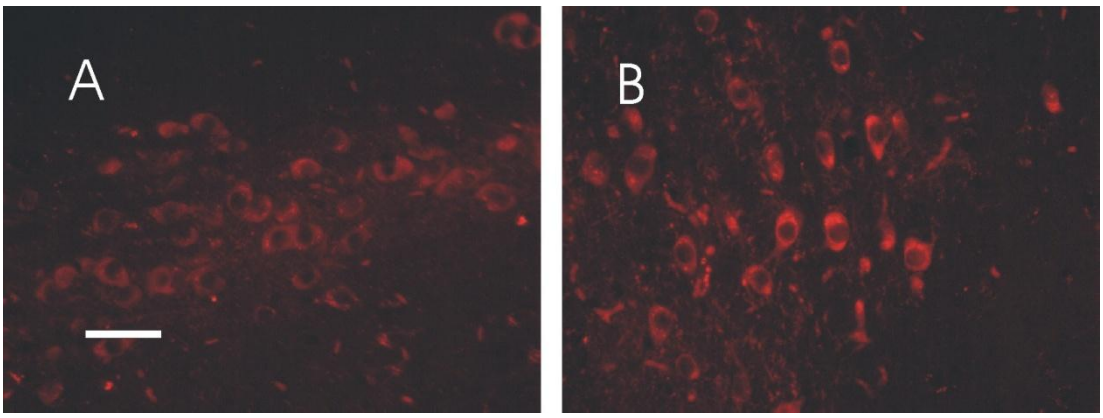

Figure 3.7.8 ***TH immunochemistry.*** *Representative sections of the sustantia nigra of a control mouse (A) and of a Cu-deficient mouse (B) are shown. Immunolabeling appears fainter in the control mouse. Scale bar = 50 μM.*

3.7.4. **Behavioural tests**

In the open field test, no difference was detected between controls or Cu-depleted mice in the distance travelled, $F(1,21)=0.071$, $p=0.792$, in the number of rearings, $F(1,21)=0.022$, $p=0.883$, in the resting time, $F(1,21)=0.0237$, $p=0.879$, in the number of urine drops, $F(1,21)=0.913$, $p=0.350$ and in the number of fecal boli, $F(1,21)=1.434$, $0=0.244$.

The open field test shows that mice had no motor impairment and did not differ in their exploratory activity, since both group recognize the open field as a new environment and behave consequently.

The pole test (Figure 3.7.9) shows that no significant difference is present between the groups, that behave in the same way ($F(1,21)=0.049$, $p=0.826$ the first day, $F(1,21)=0.406$, $p=0.531$ the second day, $F(1,21)=0.161$, $p=0.692$ the third day): the first day both groups don't know what to do and take a long time to reach the ground,

while the subsequent days both groups are equally fast in reaching the ground. This means that the mice do not have any motor deficit, but also that both can learn what to do, retain this information for one or more days (four days between the second and third repetition of the test) and use it efficiently when the test is administered again.

The predatory aggression test does not show any difference in the latency to attack the prey, $F(1,21)=1.347$, $p=0.258$, therefore no deficit in the sensory perception of the prey (that is mainly olfactory), in the emotional reactivity to the prey, nor in the motor execution of the attack sequence is present.

The habituation-dishabituation test shows no difference between the groups in either variable. Concerning the distance travelled in the target zone, the factors Odor and Repetition were significant, $F(2,42)=9.489$, $p<0.0005$ and $F(2,42)=10.679$, $p<0.0005$ respectively. These results are best explained by the interaction Odor x Repetition, $F(4,84)=2.772$, $p<0.05$, that show that when water was presented, a similar distance was travelled, when thymol was presented, the distance was shorter for the third presentation ($p<0.05$), when camphor was presented, both the second and the third presentation induced mice to move for a shorter distance ($p<0.005$ compared to the first presentation). The latency to the first entry into the target zone is similar between the groups, since only the factor Repetition is different, $F(2,42)=7.564$, $p<0.005$, with a shorter latency to enter the target zone at the first presentation, compared to the second ($p<0.005$) and third ($p<0.01$). These data show that both groups are able to discriminate the novel stimulus, which promptly elicits a fast exploratory behaviour, while the second and third presentation of the same stimulus induce a similarly slow response.

When considering the overall time spent in the target zone, that comprise the time spent moving and resting, only the factor Repetition was significant, $F(2,42)=10.033$, $p<0.0005$, with the first presentation inducing a longer permanence in the proximity of the new stimulus ($p<0.002$ and $p<0.001$ compared to the second and third presentation, respectively). A similar result is obtained for the resting time in the target zone, with the factor Repetition which is significant, $F(2,40)= 6.884$, $p<0.005$, with the first presentation inducing a longer resting in the target zone, $p<0.005$ and $p<0.01$ compared to the second and third presentation. This time is most used by mice to rest in the proximity of the new stimulus and explore it.

When considering the number of entries in the target zone, the factor Odor was significantly different, $F(2,42)=10.143$, $p<0.0005$, with the first condition (no odor) inducing a higher number of entries ($p<0.005$ and $p<0.001$ compared to thymol and camphor, respectively): these data are probably confounded by the fact that mice were not accustomed to the test, therefore their firstly exhibited a higher level of anxiety due to the novel situation, when replacing the wells. The factor Repetition was different, $F(2,42)=25.660$, $p<0.05$, with the first presentation inducing a higher number of entries, compared to the second and the third ($p<0.05$ for both).

These results show that both groups of mice have no difficulty in detecting odor substances present in the environment; both groups can recognize the new stimuli as such, and retain the information for the short period intervening between the subsequent presentations.

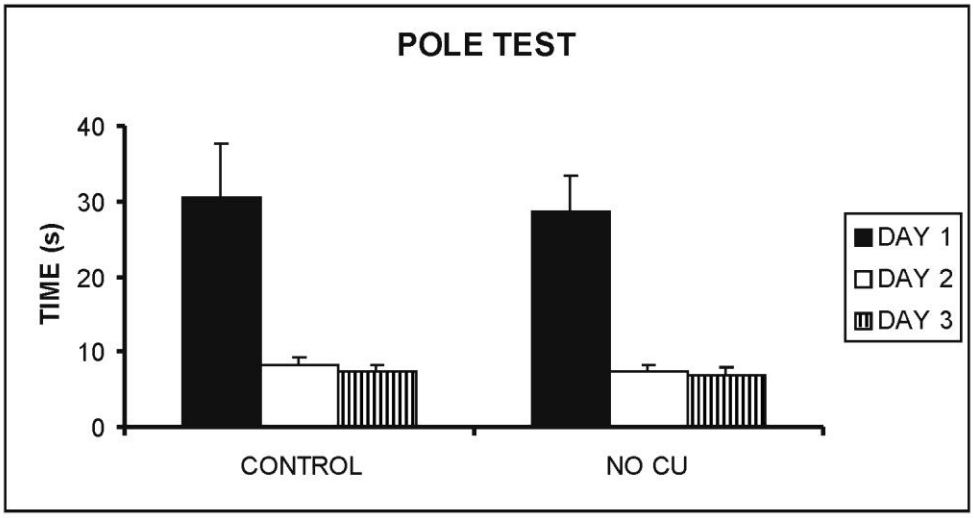

Figure 3.7.9 ***Pole test****. Means+SEM are shown. Both groups can learn efficiently to climb down from the pole.*

4 Discussion

The aggregation pathway of Aβ in AD has become a crucial issue during the last decade since it has been realized that the culprit of the wide neurodegeneration observed in AD brains cannot be solely ascribed to the deposition of SP. An increasing number of studies highlighted the active role played, in AD pathogenesis, by the early intermediates in the Aβ aggregation. This triggered a radical revision of the amyloid cascade hypothesis, stating that oligomers rather than mature fibrils are the first responsible for the severe neurodegeneration (Cole and Frautschy, 2006; Glabe, 2006; Ferreira et al., 2007). However, despite being under continuous and intensive investigation, the involvement of Aβ peptide in AD etiology is still elusive and there is not a convergent consensus on the mechanism through which it exerts its detrimental effects on neurons. In addition, the interaction of Aβ with several metals may further contribute to peptide's accumulation and toxicity (Opazo et al., 2002).

To better understand the different experimental approaches, **the discussion has been divided in six parts.**

4.1. Interaction between Aβ and Aβ-metal complexes with cell membranes: *X-ray diffraction studies of phospholipid multilayers*

Curtain et al., 2003 showed that penetration of the lipid bilayer is closely related to conditions favourable to Aβ oligomerization. This highlights the possible role played by metal ions in promoting pathological events finally leading to AD.

The aim of the first part of the study was to investigate the effect of Aβ and various Aβ-metal complexes (Aβ-Al, Aβ-Cu, Aβ-Fe, Aβ-Zn) on a lipid model of cellular membrane. DMPC and DMPE bilayers were used because they represent phospholipids located in the outer and in the inner monolayer of the membrane, respectively (Boon & Smith, 2000; Devaux & Zachowsky, 1994). Aβ-Al was the most effective complex in perturbing DMPC bilayer (Figure 3.1.2A) compared to the other metal complexes (Figure

3.1.2B-D). It is worth noticing that this effect was peculiar only to the Aβ-Al complex since neither the peptide alone (Figure 3.1.1A) nor the Al salt (Figure 3.1.4A) affected DMPC when incubated with concentrations similar to those of the Aβ-Al complex that produced relevant alterations. Considerably less pronounced was the effect of Aβ-Al complex on DMPE bilayer (Figure 3.1.3A) compared to that induced to DMPC (Figure 3.1.2A). This result can be explained on the basis of their different structures. DMPC and DMPE differ only in their terminal amino groups, these being $^{+}N(CH_3)_3$ in DMPC and $^{+}NH_3$ in DMPE. Moreover, both molecular conformations are very similar in their dry crystalline phases (Suwalsky, 1988) with the hydrocarbon chains mostly parallel and extended, and the polar head groups lying perpendicularly to them. However, the gradual hydration of DMPC results in water filling the highly polar interbilayer spaces with the resulting increase of their width. This phenomenon allows for the incorporation of the Aβ-Al complex into DMPC bilayers disrupting their arrangement and consequently the whole of the bilayer structure. DMPE molecules pack tighter than those of DMPC due to their smaller polar groups and higher effective charge, resulting in a very stable bilayer system that is not significantly affected by water (Suwalsky et al., 2005). On the other hand, the Al complexed with Aβ may induce a change in the net charge of the peptide which can promote abnormal lipid-peptide interactions, thus promoting pathological oligomerization of Aβ. Recently, our group has demonstrated that when Al was bound to Aβ, forming a stable metallorganic complex, the surface hydrophobicity of the peptide dramatically increased as a consequence of metal-induced conformational changes, favouring misfolding/aggregation phenomena (Ricchelli et al., 2005). Aβ-Al, thanks to its higher lypophilicity compared to the other Aβ-metal complexes, could intercalate with the acyl chain region altering the bilayer arrangement. In accordance, our group has previously showed that Aβ-Al was able to promote a greater increase in membrane fluidity mostly in the lipid tail/polar heads border areas of cell membrane with respect to the other Aβ-metal complexes (Drago et al., 2008a).

An interesting hypothesis would be to relate the different ability of the Aβ-metal complexes in perturbing membranes to the different toxic species produced. In this context, Al seemed to be able to "freeze" the oligomeric state of Aβ, stabilizing this assembly with respect to the conformations obtained with the other complexes (see next paragraph). In support of our hypothesis, Demuro et al., 2005 proposed that Aβs are responsible for a

generalized increase in membrane permeability induced specifically by spherical amyloid oligomers.

In our experimental conditions, negligible was the effect of the sole peptide in disturbing lipid bilayer structures. On the contrary, Ambroggio and colleagues (Ambroggio et al., 2005) demonstrated that Aβ1-42 was incorporated into the membrane and remained in the lipid environment, finally altering the cohesive forces and membrane permeability. We suggest that the dependence of the behaviour of peptide-lipid monolayers on the lipid composition could account for the discrepancy between different studies.

4.2. Effects of biologically relevant metal ions on the conformation and the aggregation properties of Aβ

The x-ray study led us to investigate in more detail and comparatively Aβ and its metal complexes; particular attention was paid to analyse the consequences of such metal binding on the Aβ aggregation profiles.

ESI-MS of the resulting samples (Figure 3.2.1) provided clear evidence of Aβ metallation, showing a clear prevalence of mono-metallated derivatives. ESI-MS measurements pointed out that the various metals are bound to Aβ as bare ions and that comparable levels of peptide metallation were achieved.

Immunological analysis of the various metal species by using conformation sensitive antibodies turned out to be very effective in discriminating the structural features of the various metal complexes (Figure 3.2.2). Remarkably, it could be established that both Al and Fe ions were capable of inducing the formation of both fibrillary oligomers and annular protofibrils while such kinds of aggregates were not observed at all in Aβ-Zn and Aβ-Cu samples. As fibrillar oligomers and annular protofibrils have been proposed to constitute neurotoxic species, our findings strongly support the view that Aβ-Al and Aβ-Fe complexes may be far more effective that Aβ-Zn and Aβ-Cu complexes in causing neuronal cell death.

Prefibrillar oligomers and annular protofibrils are structurally and immunologically distinct from fibrillar oligomers, although the sizes of these oligomers broadly overlap (Kayed et al., 2009). A11 positive prefibrillar oligomers and αAPF

positive annular protofibrils have not been found to correlate with cognitive dysfunction in AD brain and their levels were also elevated in some age-matched non demented control brains (Tomic et al., 2009). The presence of fibrillar oligomers in Aβ-Al and Aβ-Fe preparations, as shown by their preferential immunoreactivity with OC, that was absent for Aβ, and the stronger correlation of these oligomers with pathology and cognitive dysfunction in AD brain compared to APFs is therefore consistent with MTT data (Table 3.2.1) demonstrating that Aβ was less toxic than Aβ-Al under our experimental conditions. The presence of the $A\beta_{17-28}$ fragment enhanced the detrimental effects exerted by Aβ-Al in terms of reducing the cell viability (Figure 3.3.4).

Notably, the results of the immunological characterisation are in substantial agreement with DLS results (Figure 3.2.3). Nevertheless, Aβ-Al displayed a quantitative relevant presence of intermediates of 29.3 nm mean radius which were not observed for Aβ-Fe. It is likely that binding of Al to the Aβ-peptide, differently from the other tested metals, stabilizes a rather peculiar peptide conformation. Indeed, these Aβ-Al intermediates are characterized by a specific exposure of hydrophobic residues as revealed by the marked increased of ANS fluorescence (Figure 3.2.5).

In turn, Aβ-Fe which provided results very similar to Aβ-Al in the course of the immunological characterization, showed a far lower exposure of hydrophobic clusters, supporting the existence of considerable structural differences between the two species.

These differences were confirmed also in terms of the presence of β-sheet structure as revealed by the ThT study (Figure 3.2.4). The increase of ThT fluorescence with Aβ-Al complex could appear contradictory considering early studies postulating that this dye can only bind fibrils (LeVine, 1993) and that β-sheet formation directly correlated only with amyloid fibril formation. Nevertheless, recent investigations highlighted that ThT binds Aβ protofibrils (Ferreira et al., 2007) but surprisingly also oligomers (Maezawa et al., 2008). This observation suggests that ThT reactivity does not unambiguously demonstrate that misfolded aggregates are necessarily amyloidogenic (Ricchelli et al., 2005). In the light of these new findings the in-

creased ThT signal along with Aβ-Al (Figure 3.2.4) well matches with the population of oligomers observed by TEM (Figure 3.2.6).

In contrast, Zn and Cu were found to inhibit Aβ fibrillization in agreement with some recent reports (Tougu et al. 2009). It was similarly found that Zn-mediated aggregation of Aβ was rapid, giving rise to amorphous aggregates (Noy et al., 2008; Tougu et al., 2009) as confirmed in our study by TEM (Figure 3.2.6). This could be probably due to hydrophobic interactions as also confirmed by the notable increase of ANS fluorescence in the presence of Aβ-Zn (Figure 3.2.5). In addition, we found that also Cu disfavoured the formation of fibrillary species while giving rise to a prevalent population of amorphous aggregates which, differently from Aβ-Zn, did not appear hydrophobic in character (Figure 3.2.5).

It is worth noting that the oligomeric population of Aβ-Al was responsible of a statistically significant increase of the production of soluble APPα (Figure 3.2.8). Although APP protein has been extensively studied, several aspects of its biological functions and processing have to be elucidated yet (Jacobsen and Iverfeldt, 2009). The mechanism by which oligomers interact with plasma membranes and eventually produce the activation of numerous downstream biochemical effects is under study. Small oligomeric species of Aβ could indeed readily diffuse through cell membrane and affect neuronal survival. Aβ-Al was indeed responsible for the significant toxicity on neuroblastoma cells in terms of alteration of cell morphology (Figure 3.2.7), decrease in cell viability (Table 3.2.1). As Aβ-Al was also the most effective, among the tested complexes, in affecting cellular membrane architecture (Figure 3.1.2) it is likely to penetrate effectively into the membrane bilayer core, potentially interacting with transmembrane proteins such as APP.

Notably, in a set of microarray and Real time PCR experiments, in which we investigated the gene expression profile of SHSY-5Y cells (about 35.000 genes) treated with various Aβ-metal complexes, Aβ alone and the metal ions, we observed that the Aβ-Al complex was able to produce a selective up-regulation of APP gene (Drago *et al*., unpublished observations, manuscript in preparation) fitting with the up-regulated expression of the APP gene which occurs in brains of AD patients (Lukiw, 2004). Walton and Wang (2009) suggested that APP up-regulation, neuropathology, and cognitive deterioration could result from the Al accumulation in AD-

vulnerable brain regions and thus, susceptible individuals with efficient Al absorption, can accumulate in neural cells sufficient amount of the metal to up-regulate APP expression. We can add that the deleterious binding of Al to Aβ may enhance this pathological alteration, favoring the focal accumulation of the metal. In this regard, Al and Aβ peptides have been showed to colocalized in the cores of Aβ fibers of SP (Yumoto et al., 2009).

Therefore, it can be hypothesized that enhancement of APPα production might represent a protective mechanism as soluble APPα has been shown to prevent neuronal death in human cortical cell cultures exposed to excitotoxins (Mattson MP et al., 1993). Indeed, increased α-secretase activity and in turn APPα release have been shown to limit Aβ release (Jager et al., 2009).

Very significant was also the production of τ181 protein in SHSY-5Y upon Aβ-Al treatment (Figure 3.2.9). This protein turned out to be an important biomarker as, even if total τ concentration in the CSF of AD patients have been reported to be higher compared to controls (Andreasen & Blennow, 2005; Hampel et al., 2009), this increased is shared also by other neurodegenerative disorders such as mild cognitive impairment (Andreasen et al., 2003). On the contrary, targeting specific phosphorilated epitopes of τ protein could aloud differential diagnosis between AD and other kind of dementia. Ravaglia et al. (2008) proposed that higher τ181 values predicted, independently of the clinical diagnosis, a more rapid evolution of cognitive decline, underlining that phosphorylation at this site could be relevant.

The detrimental interaction between τ and Aβ-Al could be explained by the fact that Al, a highly reactive element, can easily cross-link hyperphosphorylated proteins (Perl & Moalem, 2006). Aβ-Al metal complex was found to have high permeability across the blood brain barrier, a phenomenon that was leading to its intracerebral accumulation (Banks et al., 2006), potentially contributing to both τ- and Aβ-dependent pathology. In accordance, signs of Al dyshomeostasis were also recently found in a triple transgenic AD mouse, the 3xTg-AD, which is considered to recapitulate the hallmarks of AD pathology (Drago et al., 2008b).

4.3. Mutual stimulation of Aβ fibrillogenesis by CQ and divalent metals

A huge number of pharmacological studies highlighted that cellular metal-chelation could produce a protective effect in animal models of neurological disorders by preventing the toxicity arising from intracellular accumulation of free metal ions. In particular, the membrane-permeable, Cu^{2+}- and Zn^{2+}-selective chelator CQ would reduce the size and number of Aβ plaques, spontaneously generated in a mouse model of AD (Cherny et al., 2001), presumably by chelation of Aβ-associated metal ions.

Despite the plethora of literature, the *in vivo* mechanisms of CQ effects and Aβ physiology remain unsolved. The beneficial effect of CQ was mainly correlated with blocking the adverse generation of H_2O_2 that is catalyzed by the metal-binding site on Aβ; whereas disruption of metal-induced aggregation was considered as a secondary effect, probably mediated by an alternative metal binding-site (Bush, 2002). The findings in cell culture studies suggested that CQ degraded Aβ by a metal-dependent up-regulation of a metallo-protease activity (White et al., 2006). According to Schäfer et al. (2007), the chelating effect of CQ plays a secondary role with respect to its properties as an intracellular metal (Cu^{2+}) transporter, thus counteracting its supposed therapeutic effects as an agent for pharmaceutical therapy in AD.

For a better understanding of the mechanism of CQ action, we investigated the interaction properties of CQ on isolated Aβ and Aβ-metal complexes both in monomeric and aggregated form, without interference of the complex cell regulatory systems present *in vivo*.

Under our experimental conditions, Cu^{2+} and Zn^{2+} did not promote human Aβ aggregation; in fact, the aggregational trend of Aβ-Cu and Aβ-Zn complexes, as detected by the increment of ThT fluorescence and by turbidity measurements, was very similar to that observed for the native protein (Figs.3.4.1 and 3.4.4). Most importantly, Cu^{2+} eliminated the ability of Aβ to spontaneously form fibrils (Figure 3.4.5), in agreement with previous results (House et al., 2004; Ricchelli et al., 2005).

The inhibitory effect of Cu^{2+} on Aβ fibrillogenesis at pH 7.4 was attributed to a preferential binding of metal to high-affinity protein sites, which stabilizes Aβ in a non-amyloidogenic conformation (Miura et al., 2000). The inhibitory potential of Zn^{2+} on human Aβ fibrillogenesis was less pronounced: Aβ-Zn aggregates were still capable of producing fibrils, although less branched than those generated spontaneously (Figure 3.4.5). Metal-suppression of protein fibrillogenesis capacity was even more evident in the case of rat Aβ: both Cu^{2+}- and Zn^{2+}-induced aggregates (Figure 3.4.2) did not evolve into any defined structures (Figure 3.4.6).

Surprisingly, early incubation of CQ with human and rat Aβcomplexed with both Cu^{2+} and Zn^{2+} led to a dramatically higher propensity of the protein to aggregation (Figs. 3.4.1, 3.4.2 and 3.4.4) and fibrillization (Figs. 3.4.5 and 3.4.6).

The simplest explanation of these findings relates to the metal-chelating properties of CQ; namely, incubation with CQ prevents metal binding to Aβ, thus counteracting the obstacle to the protein structural conversions, which was observed in our experimental conditions. In agreement, CQ alone exhibited a negligible effect on the fibrillogenesis of human and rat Aβ in the absence of added metal ions (Figs. 3.4.5A-B and 3.4.6A-B). Similarly, Raman et al. (2005) showed that CQ induced resumption of the Cu^{2+}-suppressed fibril growth of Aβ(1-40).

Other data, however, conflict with a pure metal-chelation mechanism: i) metal removal by CQ from Aβ-Cu and Aβ-Zn complexes should restore the conformation and aggregational properties of the native peptide; on the contrary, a fibril population dramatically higher than that observed for Aβ alone was observed, especially in rat Aβ–metal complexes added with CQ (compare Figs. 3.4.6D,F with 3.4.6A), ii) while the stability constant of CQ-Zn^{2+} is in the same range of values as that of β-amyloid-Zn^{2+} (Ferrada et al., 2007), the affinity of Cu^{2+} for CQ is extremely lower than that for β-amyloid, which lies in the attomolar range (Bush, 2003). Therefore, it is unlikely that Cu^{2+} competes between Aβ and CQ.

In our interpretation, the initial step of the process could imply a modulating effect of the hydrophobic CQ on the Aβ structural organization: interaction of the drug with hydrophobic domains of Aβ could stimulate protein conversion to misfolded conformations. Consistently, in the presence of CQ, Aβ exhibited an increase

in the aggregational process (Figs. 1, 2 and 4), indicative of a growth of misfolded structures. These abnormal structures did not evolve *per se* to organized fibrillar forms (see Figs. 5 and 6). However, CQ-promoted conformational alterations could allow for the unmasking of previously inaccessible, abnormal metal binding sites with highly fibrillogenic properties, as already reported to occur for β-amyloids (Bocharova et al., 2005) and other neurotoxic proteins (Ricchelli et al., 2006) following the action of different stimuli.

Alternative mechanisms for the CQ effect, however, cannot be excluded. Thus, sequestration by the drug of loosely bound Cu^{2+} from low-affinity binding sites of Aβ was proposed by Butterfield & Boyd-Kimball (2005). A possible low-affinity Cu^{2+}-binding site may be found on Met-35, a critical residue in Aβ mediated neurotoxicity (Yatin et al., 1999).

Literature data indicate that CQ alone can induce toxicity in murine cortical cultures (Benvenisti-Zarom et al., 2005), BE(2)-M17 human neuroblastoma and murine N2a neuroblastoma cell lines (Filiz et al., 2007) at concentrations that may occur *in vivo*. However, Filiz et al. (2008) have found that CQ toxicity *in vitro* is dependent on the CQ concentration, metal levels and how CQ is prepared before administration to cultures. Our studies with SH-SY5Y human neuroblastoma cells suggest that neither CQ alone nor CQ combined with free metals significantly altered the cell integrity (Figs. 3.4.7 and 3.4.8). Under our experimental conditions, CQ was toxic only in the presence of the Aβ-Zn complex, as demonstrated by both the decrease of cell viability and the morphological cell alterations. Cell dysfunction due to CQ plus Aβ-Zn confirms the suggestion arising from in solution studies that a synergic action of CQ and metal on Aβ peptide is necessary to stimulate toxicity. These results appear to be particularly important considering the low concentration (1 nM) of CQ used, as compared to those of previous publications (from 10 to 25 μM) (White et al., 2006; Filiz et al., 2007). Also the concentrations of Aβ and Aβ-Cu/Zn used in cell culture were very low (0.5 μM) compared with other works where a higher amyloid concentration (20 or 100 μM) was utilized (Boyd-Kimball et al., 2004; Awasthi et al., 2005). In our cell model, Aβ-Cu+CQ system displayed a negligible toxicity. An attractive hypothesis would be to relate the different behaviours of the two complexes to the different neurotoxic species produced in the presence of CQ. Actually, while

both Aβ alone and Aβ-Cu+CQ induced a time-dependent aggregation into amyloid-like fibrillar forms, short protofibrillar species were mainly detected for CQ+human Aβ-Zn (see Figure 3.4.5).

Our findings suggest that the literature data on CQ effects should be re-interpreted and, furthermore, they should induce some cautions in the CQ employment in AD clinical treatment. The interaction of Aβ-metal ions and CQ needs to be investigated in more detail even more in the light of the conflicting data recently published.

4.4. Overexpression of QPCT as potential biomarker for AD: influence of Aβ-metal complexes

QPCT is the gene encoding for glutaminyl cyclase (QC), an enzyme highly expressed in the brain (Hartlage-Rübsamen et al., 2009) but also in peripheral tissues (Sykes et al., 1999). It has been localized in the Golgi complex, ER and in secretory granules implying a potential role in protein maturation (Cynis et al., 2008; Hartlage-Rübsamen et al., 2009). Thus, QC is thought to stabilize neuropeptides in that it can convert the N-terminal glutamine to pyroglutamate (Schilling et al., 2004) and it has been uncovered few years ago that also Aβ could be a substrate of this enzyme (Schilling et al., 2004) as pyroglutamate-modified Aβ (pGlu-Aβ) have been shown to preferentially deposit in SP (Tomidokoro et al., 2005). As a matter of fact, QC-inhibitors suppress the pGlu-Aβ formation in cell culture (Cynis et al., 2006) and it has been hypothesized that uneffective clearance of these pyroglutamate peptides could contribute to SP formation (Russo et al., 2002). Animal models accumulating high amount of pGlu-Aβ showed hippocampal neuron loss and neurological deficits (Casas et al., 2004; Wirths et al., 2009) as the peptide becomes more hydrophobic (Schilling et al., 2006) and may form mixed aggregates with $A\beta_{1-42}$, as shown in rat cortex (Schilling et al., 2008). pGlu-Aβ peptides exhibited an up to 250fold increase of the initial rate of aggregation compared to the unmodified peptide suggesting that it can act as seed for neurotoxic aggregate formation (Schilling et al., 2006). More-

over, QC is expressed in brain regions typically affected by AD as cortex and hippocampus (Schilling et al., 2008).

High effort in finding biomarkers to facilitate the AD diagnosis are currently under investigation and among recent possible targets QC has emerged as one of the most interesting option. One of the most accepted AD biomarker consist in the combination of three parameters, namely $A\beta_{1-42}$ phosphorylated and total τ levels in the CSF even if there is not an agreement on the significance of their quantification in terms of discrimination between AD and healthy subjects or others kinds of ND (Le Bastard et al., 2009; Stefani et al., 2009). Nevertheless, the identification of more readily accessible and less invasive biomarker would be preferable. For this reason we tested QPCT gene in the peripheral blood of AD patients. Although the role of N-terminal truncated Aβ and its relevance to the etiology of AD are still obscure, efforts should be address to clarify weather this overexpression could be useful to differentiate between AD and controls but also among different types of dementia. At this regard, few clues has substantiated pGlu-Aβ as potential promising target as it was highly present in sporadic AD brain compared to age-match controls who displayed amyloid deposits (Piccini et al., 2005).

Despite the relatively small number of patients used in this study, the increase in QPCT expression in AD patients appeared to be relevant. Schilling et al., (2006) reported that QC expression was upregulated in the cortices of AD patients. Clearly, the maintenance of this upregulation in peripheral mononuclear cells (PBMC), which was here reported for the first time, may contribute to an early diagnosis of the pathology.

Furthert efforts are clearly necessary to increase the number of subjects and to investigate if this overexpression could be peculiar of AD compared to other types of dementia. Clarification of the role played by QC and truncated peptide may offer a new insight for the understanding of the neurodegenerative process, thus verifying if CQ-inhibitors could indeed be a valuable, selective therapeutic options.

4.5. Accumulation of Cu and other metal ions, and MT I/II expression in the bovine brain as a function of aging

Data reported in the literature on the level of metal ions in the bovine brain are scant and generally not discussed in relation to aging. Our data indicate that Cu content increases in aging animals, a fact most evident in basal and central regions of the brain, including hypothalamus, thalamus and corpus callosum. High levels of Cu in humans are associated with a series of ailment impairing brain functions, including also AD (Zatta and Frank, 2007). Age-related accumulation of Cu in the brain may induce oxidative stress and thus lead to adverse effects (Perry et al., 2003; Barnham et al., 2004). However, although some neurodegenerative conditions may be associated with aging, accumulation could be due also to several other factors (Zatta and Frank, 2007). The relationship between Cu accumulation and aging is therefore hard to define precisely in the bovines as well as in humans and the discussion on this issue is widely open.

Cu deficiency in animals may induce relevant neurological consequences, including loss of appetite, gait disturbances, blindness and other (Zatta and Frank, 2007). In ruminants Cu deficiency may occur mainly because of forestomach pathology and differences exist in Cu metabolism among ruminants; between sheep and cattle, and between sheep and deer.

The level of Mn in our bovine brain samples was not affected by ageing and a balanced distribution in the fifteen regions considered has been observed (see also Zatta et al., 2003). Mn is essential to the brain but its neurotoxicity in human is well known (Verity, 1999) since last century as manganism, that has been described and characterized by extrapyramidal dysfunction and neuropsychiatric symptoms. Therefore, brain Mn is thought to play an important role in some neurodegenerative diseases and to lead to a neurological disorder resembling PD (Ponzoni et al., 2002). The basis of Mn neurotoxicity lies on the ability of bivalent form Mn^{2+} to oxidize to the trivalent form Mn^{3+}, a powerful oxidizing species.

Zinc is an essential element that participates in carbohydrate and protein metabolism, nucleic acid synthesis and other vital functions. In contrast to other metals, the mechanisms regulating Zn homeostasis are so efficient that no disorders are

known to be associated with its excessive accumulation (Vallee and Falchuk, 1993). However, some evidences suggested that Zn may be involved in several neurological dysfunctions. The mechanisms by which Zn exerts its toxicity could involve signalling pathways such as mitochondrial superoxide production (Weiss et al., 2000), activation of apoptotic process (Sensi and Jeng, 2004) and also extra-mitochondrial generation of free radicals. The higher level of Zn found in aged animals compared with young bovines showed the same trend as found in a previous work in bovine pineal gland (from 13.25 to 22.78 μg/g fresh tissue) (Zatta et al., 2006). Despite many studies, the relation between Zn and aging has not already been well clarified.

In the brain, aging is considered as one of the most relevant risk factors for neurodegenerative disorders and a state in which pathological alterations may exist without a clinical expression (Hidalgo et al., 2001). In the presence of transition metals like Cu, Mn and others, radicals as superoxide and hydroxyl radical can be produced. Also neuroinflammation is an important factor which increases the formation of reactive oxygen species (ROS) that could be a major risk in neurodegenerative process. Astrocytes play a central role in the inflammatory phenomena and are also a relevant marker for neurodegeneration. It has been recently reported that MTs tend to be highly expressed in both astrocytes and hippocampal neurons in the aging human brain (Mocchegiani et al., 2005). This increased expression might represent a physiological defence against stress factors in order to protect neurons. However, our immunohistochemical data in bovine brain did not show any significant difference in the distribution of MT I/II in relation to age. In addition, in Zatta et al. (2006) was shown that positivity to MT I/II in young bovine pineal gland was wider compared to old animals. This result may be related to specific difference related to specie.

Moreover, our findings indicate that MTs, as classical copper-binding proteins, were co-localized with GFAP in astrocytes in our tissue sections, and constantly identified both in young and old animals only in the cerebellar cortex, showing immunoreactive elements in the middle layer. MT I/II cells were present also in the ependyma of the lateral ventricles of young animals, while scarce immunoreactive neural cells were present in the cortex of young and adult bovine. The location and nature of the ependymal elements containing MT I/II-ir materials suggest a pos-

sible exchange with the liquor compartments. Similar findings were recently reported in the bovine pineal recess of the third ventricle (Zatta et al., 2006).

4.6. Biochemical and behavioural effects of a Cu-deficient diet on adult mice.

We examined the effect of Cu-deficiency, obtained feeding mice with a no Cu-containing diet, on general metal ion distribution and markers of oxidative stress. A large number of publications gain insight the effect of Cu-deprivation during development, extensively demonstrating that Cu is essential for brain development. On the other hand, to our knowledge rather scarce are investigations related to the effects of experimental Cu-deficient diet on adult mice. Certainly, an essential metal as Cu acts critical roles in many physiological functions (Lalioti et al., 2009). It follows that a deficiency, as well as an excess, of Cu but also of other essential metals, besides causing direct deleterious effects in the pathway in which the metal is involved, can also influence the up-take of other metals (Smith et al., 1997). Our results confirm this cross-interaction and, interestingly, demonstrated that also the concentration of Al, which is not a physiological element, was markedly changed in the brain of Cu-D compare to Cu-A animals. We stress the importance of this observation in the light of the potential use of metal chelation therapy as a clinical option for ND and particularly AD. Notably, in our experimental model, the brain appeared to be the organ most susceptible to the metal dyshomeostasis. More specifically, independently of metals being a primary cause or consequence of AD, the fact that a change in the concentration of a single metal ion will upset the whole elemental homeostatic pool, resulting in a significant imbalance in the elemental levels in the body has to be considered when designing therapeutically useful approach. The reason for the close interconnection between different metals has not been completely understood, but could lie in the sharing of same transporters: for example Al, which shares with Fe a number of physiochemical features such as a similar ionic radius and charge density, is believed to enter the brain through the Fe transporter transferrin receptor (Tf) (Yokel, 2006). Moreover, there is also evidence for Al transporter-

mediated efflux from the brain (Yokel, 2006). On turn, Fe is closely linked with Cu metabolism (Kosman et al., 2002). It is well established that severe Cu deficiency impaires the correct absorption of dietary Fe (Reeves & DeMars, 2005). The mechanism is not completely clear but it may be related to the decrease activity of Cu-enzymes such as ceruloplasmin and hephaestin, which are required for Fe transport (Vulpe et al., 1999). Accordingly, we found decreased level of Fe in the large and small intestine (Figure 3.7.3), as previously found by Chen et al. (2006), and in the brain (Figure 3.7.1), in particular in the occipital area and cerebellum. According to several investigations, symptoms of Fe deficiency (anaemia and low plasma Fe level) were recorded in weanling rats within days after treatment with Cu-D (Reeves et al., 2005) or in mice treated soon after the parturition (Chen et al., 2006). This is probable due to an impaired activity of multicopper ferroxidases resulting in defects of Fe metabolism with a consequent accumulation in the liver (Miyajima et al., 2003). Nevertheless, in our study we did not observed neither a liver Fe accumulation nor anaemia. A recent work by Pyatskowit & Prohaska (2008) reported that plasma Fe did not change in mice treated with a Cu-D diet while in rat, upon comparative experimental conditions, was significantly decreased. The different species and age of the animals used could account for these discrepancies. Alternatively, can not be excluded that also the different duration of the diet could constitute a source of variability. On the other hand, it has been also reported that humans with Cu deficiency and anaemia can have normal plasma Fe (Miyoshi et al., 2004).

Prohaska's laboratory has widely demonstrated the effect of Cu-deficiency in mice and rats when this nutritional restriction is imposed throughout gestation as well as lactation: as a result, brain Cu concentration resulted dramatically affected by the diet (Pyatskowit & Prohaska 2008). Notably, if the diet begun shortly after birth the effect in terms of Cu-brain alteration was strongly limited (Prohaska & Bailey, 1993). This could explained the fact that, in our experimental model, Cu seems to be the metal less affected by the diet.

In this study there was no significant effect of the diet on animal body weight and both groups were healthy as found by Welch et al. (2007) in rats upon 60 days of Cu-deficient diet. On the contrary, rat and mice offspring both when the deficiency

occurred during lactation or gestation/lactation had decrease body weight compared to controls (Pyatskowit & Prohaska, 2008).

Not surprisingly, the content of MTs, one of the most studied family of metalloproteins and a classical Cu-binding proteins, was affected by the diet. These ubiquitous low molecular weight cysteine-rich proteins are present in mammals with four isoforms. The role played by MTs in the detoxification of heavy metals and the distribution of essential metals is clearly established, but in recent years there has grown a wider appreciation of MTs functions (Zatta, 2008). The extensive presence of MTs within the CNS and the identification of a specific brain isoform, MT-III, are reasonable clues which support the hypothesis of this family of protein having important neurological functions. We speculate that the decrease of MTs content in the frontal area could be due to the related decrease of Cu and Zn in that area. MTs are indeed regulator of bivalent metal ions. Concerning trivalent metals, alteration in their content is not likely solely to be due to alteration of these proteins and other transporter proteins must be involved. The biochemical decrease of total MTs content, especially in the brain, could be detrimental in the light of its function as free radical scavenger. The mechanism by which MTs exerts a protective function is not clear. However, a reaction between the MT thiolate cluster and hydroxyl radicals has to be envisaged (Maret, 2008).

Although the array of alteration produced by Cu-deficient diet in adult mice appeared to be relevant we did not observed any signs of neurological impairment. This suggested that Cu deficiency, at least in our model, was not sufficient to trigger the activation of pathways determining signs of cognitive disability. This issue is indeed higly controversial as few studies reported that cellular Cu deficiency in AD could promote an environment for potentially adverse interaction between Aβ, the metal itself and other cellular components (Hung et al., 2009). Nevertheless, the existence of a Cu deficiency in AD patients have never been demonstrated. Increased understanding of Cu homeostasis may help in unravelling its potential involvement in neurological disorders.

Concluding remarks

The results presented in this thesis provide significant insights into the biophysical and biological behaviour of Aβ and Aβ-metal complexes. We found that the binding of the four tested metals (Al, Cu, Fe, Zn) differentially altered the aggregational properties of the peptide. Aβ-Cu and Aβ-Zn showed a similar profile as they kept the peptide in an amorphous state, while Aβ-Al and Aβ-Fe promoted the formation of oligomers which were recognized by OC as well as by αAPF. Nevertheless, these two complexes differed for the exposure of hydrophobic clusters, being the Al the most effective in increasing the peptide superficial hydrophobicity. This aspect and the relevant presence of smaller oligomeric species compared to the other complexes were responsible of a significant decrease of cell viability and of a peculiar increase in the production of APP and τ181 upon Aβ-Al treatment in neuroblastoma cell culture. Therefore, this study suggests that, besides the well-established neurotoxic activity of the Al, new evidence can somehow highlight the importance of this metal when reacting with Aβ as co-factor in AD. Although Al itself cannot be a sufficient trigger of AD (see Bolognin et al., 2009; Perl & Moalem, 2006), the direct binding of Al to Aβ can give rise to stable neurotoxic species. However, we do not know yet whether this specie interacts with specific receptor or whether there is a non-specific interaction, driven from hydrophobical properties, to different receptors/channels which activate a set of signalling pathways or if the interaction is far more aspecific forming pore- assemblies. Future investigations will address this issue in the attempt of better clarifying the correlation between amyloid-metal complex structure and the potential interaction with biological structures.

Clearly the fundamental biochemical mechanisms linking brain biometal metabolism, environmental metal exposure, and AD pathophysiology warrant further investigation as demonstrated by the relevant array of alterations determined by the deprivation of a single metal, Cu, in the diet of adult mice.

References

Adlard PA, Cherny RA, Finkelstein DI, Gautier E, Robb E, Cortes M, Volitakis I, Liu X, Smith JP, Perez K, Laughton K, Li QX, Charman SA, Nicolazzo JA, Wilkins S, Deleva K, Lynch T, Kok G, Ritchie CW,Tanzi RE, Cappai R, Masters CL, Barnham KJ, Bush AI (2008) Rapid restoration of cognition in Alzheimer's transgenic mice with 8-hydroxy quinoline analogs is associated with decreased interstitial Abeta. *Neuron* **59**, 43-55.

Age-Related Eye Disease Study Research Group, 2001 Age-Related Eye Disease Study Research Group, A randomized, placebo-controlled, clinical trial of high-dose supplementation with vitamins C and E, beta carotene, and zinc for age-related macular degeneration and vision loss: AREDS report no. 8, *Arch Ophthalmol* **119**, 1417–1436.

Alfrey AC (1986) Aluminum metabolism. *Kidney Int Suppl* **18**, S8-S11.

Alfrey AC, LeGrendre GR, Kaehny WD (1976) The dialysis encephalophaty syndrome. Possible aluminum intoxication. *N Engl J Med* **294**, 184-188.

Altamura S, Muckenthaler MU (2009) Iron toxicity in diseases of aging: Alzheimer's disease, Parkinson's disease and atherosclerosis. *J Alzheimers Dis* **16**, 879-895.

Ambroggio EE, Kim DH, Separovic F, Barrow CJ, Barnham KJ, Bagatolli LA, Fidelio GD (2005) Surface behavior and lipid interaction of Alzheimer beta-amyloid peptide 1-42: a membrane-disrupting peptide. *Biophys J* **88**, 2706-2713.

Awasthi A, Matsunaga Y, Yamada T (2005) Amyloid-beta causes apoptosis of neuronal cells via caspase cascade, which can be prevented by amyloid-beta-derived short peptides. *Experimental Neurol* **196**, 282-289.

Bala Gupta V, Anitha S, Hedge ML, Zecca L, Garruto MR, Ravid R, Shankar SK, Stein R, Shanmugavelu P, Jagannatha Rao KS (2005) Aluminium in Alzheimer's disease: are we still at a crossroad? *Cell Mol Life Sci* **62**, 143-158.

Banks WA, Niehoff ML, Drago D, Zatta P (2006) Aluminum complexing enhances amyloid beta protein penetration of blood-brain barrier. *Brain Res* **1116**, 215-221.

Barnham KJ, Masters CL, Bush AI (2004) Neurodegenerative diseases and oxidative stress. *Nat Rev Drug Discov* **3**, 205-214.

Bayer TA, Schäfer S, Breyhan H, Wirths O, Treiber C, Multhaup G (2006) A vicious circle: role of oxidative stress, intreneuronal Abeta and Cu in Alzheimer's disease. *Clin Neuropathol* **25**, 163-171.

Bayer TA, Schäfer S, Simons A, Kemmling A, Kamer T, Tepest R, Eckert A, Schüssel K, Eikenberg O, Sturchler-Pierrat C, Abramowski D, Staufenbiel M, Multhaup G (2003) Dietary Cu stabilizes brain superoxide dismutase 1 activity

and reduces amyloid Abeta production in APP23 transgenic mice. *Proc Natl Acad Sci U S A* **100**, 14187-14192.

Benvenisti-Zarom L, Chen J, Regan R (2005) The oxidative neurotoxicity of clioquinol. *Neuropharmacol* **49**, 687-694.

Bertoni-Freddari C, Fattoretti P, Paoloni R, Caselli U, Galeazzi L, Meier-Ruge W (1996) Synaptic structural dynamics and aging. *Gerontology* **42** 170–180.

Bertoni-Freddari C, Fattoretti P, Casoli T, Di Stefano G, Giorgetti B, Balietti M (2008) Brain aging: The zinc connection. *Exp Gerontol* **43**, 389-393.

Bhak G, Choe YJ, Paik SR (2009) Mechanism of amyloidogenesis: nucleation-dependent fibrillation versus double-concerted fibrillation. *BMB* **42**, 541-551.

Bhatia R, Lin H, Lal R (2000) Fresh and globular amyloid beta protein (1-42) induces rapid cellular degeneration: evidence for AbetaP channel-mediated cellular toxicity. *FASEB J* **14**, 1233-1243.

Bocharova OV, Breydo L, Salnikov VV, Baskakov I (2005) Copper (II) inhibits in vitro conversion of prion protein into amyloid fibrils. *Biochem* **44**, 6776-6787.

Bolognin S, Messori L, Zatta P (2009) Metal ion physiopathology in neurodegenerative disorders. *Neuromol Med* **11**, 223-238.

Boon JM, Smith BD (2000) Chemical control of phospholipid distribution across bilayer membranes. *Med Res Rev* **22,** 251-281.

Borchardt T, Camakaris J, Cappai R, Master CL, Beyreuther K, Multhaup G (1999) Copper inhibits beta-amyloid production and stimulates the non-amyloidogenic pathway of amyloid-precursor protein secretion. *Biochem J* **344**, 461-467.

Boyd-Kimball D, Sultana R, Mohmmad-Abdul H, Butterfield A (2004) Rodent Abeta(1-42) exhibits oxidative stress properties similar to those of human Abeta(1-42): Implications for proposed mechanisms of toxicity. *J Alzheimers Dis* **6**, 515-525.

Bush AI (2002) Metal complexing agents as therapies for Alzheimer's disease. Neurobiol. *Aging* **23**, 1031-1038.

Bush AI (2003) The metallobiology of Alzheimer's disease. *Trends Neurosci* **26**, 207-214.

Bush AI, Masters CL (2001) Clioquinol's return. Science **292**, 2251-2252.

Butterfield DA, Boyd-Kimball D (2005) The critical role of methionine 35 in Alzheimer's amyloid β-peptide(1-42)-induced oxidative stress and neurotoxicity. *Biochim Biophys Acta* **1073**, 149-156.

Butterfield DA, Reed T, Newman SF, Sultan R (2007) Roles of amyloid beta-peptide-associated oxidative stress and brain protein modifications in the patho-

genesis of Alzheimer's disease and mild cognitive impairment. *Free Radic Biol Med* **43**, 658-677.

Cahill CM, Lahiri DK, Huang X, Rogers JT (2009) Amyloid precursor protein and alpha synuclein translation, implications for iron and inflammation in neurodegenerative diseases. *Biochim Biophys Acta* **1790**, 615-628.

Campbell A (2006) The role of aluminum and copper on neuroinflammation and Alzheimer's disease. *J Alzheimers Dis* **10**, 165-172.

Caughey B, Lansbury PT (2003) Protofibrils, pores, fibrils, and neurodegeneration: separating the responsible protein aggregates from the innocent bystanders, *Ann Rev Neurosci* **26**, 267–298.

Chen H, Huang G, Su T, Gao H, Attieh ZK, McKie AT, Anderson GJ, Vulpe CD (2006) Decreased hephaestin activity in the intestine of copper-deficient mice causes systemic iron deficiency. *J Nutr* **136**, 1236-1241.

Cheng IH, Scearce-Levie K, Legleiter J, Palop JJ, Gerstein H, Bien-Ly N *et al.*, (2007) Accelerating amyloid-beta fibrillization reduces oligomer levels and functional deficits in Alzheimer disease mouse models. *J Biol Chem* **282**, 23818–23828.

Cherny RA, Atwood CS, Xilinas ME, Gray DN, Jones WD, Mclean CA, Barnham KJ, Volitakis I, Fraser FW, Kim Y, Huang X, Goldstein LE, Moir RD, Lim JT, Beyreuther K, Zheng H, Tanzi RE, Masters CL, Bush AI (2001) Treatment with a copper-zinc chelator markedly and rapidly inhibits beta-amyloid accumulation in Alzheimer's disease transgenic mice. *Neuron* **30**, 665-676.

Cole GM, Frautschy SA (2006) Alzheimer's amyloid story finds its start. *Trens in Molec Med* **12**, 395-396.

Crichton RR, Dexter DT, Roberta JW (2008) Metal based neurodegenerative diseases—from molecular mechanisms to therapeutic strategies. *Coord Chem Rev* **251**, 1189-1199.

Cross DJ, Flexman JA, Anzai Y, Morrow TJ, Maravilla KR, Minoshima S (2006) In vivo imaging of functional disruption, recovery and alteration in rat olfactory circuitry after lesion. *Neuroimage* **32**, 1265-1272.

Crouch PJ, Barnham KJ, Bush AI, White AR (2006) Therapeutic treatments for Alzheimer's disease based on metal bioavailability. *Drug News Perspect* **19**, 469-474.

Crouch PJ, Hung LW, Adlard PA, Cortes M, Lal V, Filiz G, Perez KA, Nurjono M, Caragounis A, Du T, Laughton K, Volitakis I, Bush A I, Li QX, Masters CL, Cappai R, Cherny RA, Donnelly PS, White A R, Barnham KJ (2009) Increasing Cu bioavailability inhibits Abeta oligomers and tau phosphorylation. *Proc Natl Acad Sci* **106**, 381-386.

Cuajungco MP, Faget KY (2003) Zinc takes the center stage: its paradoxical role in Alzheimer's disease. *Brain Res Rev* **41**, 44-56.

Cuajungco MP, Faget KY (2003) Zinc takes the center stage: its paradoxical role in Alzheimer's disease. *Brain Res Rev* **41**, 44-56.

Curtain CC, Ali FE, Smith DG, Bush AI, Masters CL, Barnham KJ (2003) Metal ions, pH, and cholesterol regulate the interactions of Alzheimer's disease amyloid-beta peptide with membrane lipid. *J Biol Chem* **278**, 2977–2982

Cynis H, Schilling S, Bodnár M, Hoffmann T, Heiser U, Saido TC, Demuth HU (2006) Inhibition of glutaminyl cyclase alters pyroglutamate formation in mammalian cells. *Biochim Biophys Acta* **1764**, 1618-1625.

Dahlgren KN, Manelli AM, Stine WB, Baker LK, Krafft GA, LaDu MJ (2002) Oligomeric and fibrillar species of amyloid-beta peptides differentially affect neuronal viability. *J of Biolog Chem* **277**, 32046-53.

Deibel MA, Ehmann WD, Markesbery WR (1996) Copper, iron, and zinc imbalances in severely degenerated brain regions in Alzheimer's disease: possible relation to oxidative stress. *J Neurol Sci* **143**, 137-142.

Del Corso L, Pastine F, Protti MA, Romanelli AM, Moruzzo D, Rocco L, Pentimene F (2000) Blood zinc, copper and magnesium in ageing. A study in healthy home-living elderly. *Panminerva Med* **42**, 273-277.

Demeester N, Baier G, Enzinger C, Goethals M, Vandekerckhove J, Rosseneu M, Labeur C (2000) Apoptosis induced in neuronal cells by C-terminal amyloid β-fragments is correlated with their aggregation properties in phospholipids membranes. *Mol Membr Biol* **17**, 219–228.

Demuro A, Mina E, Kayed R, Milton SC, Parker I, Glabe CG (2005) Calcium dysregulation and membrane disruption as a ubiquitous neurotoxic mechanism of soluble amyloid oligomers. *J Biol Chem* **280**, 17294-17300.

Deshpande A, Kawai H, Metherate R, Glabe CG, Busciglio J (2009) A role for synaptic zinc in activity-dependent Abeta oligomer formation and accumulation at excitatory synapses. *J Neurosci* **29**, 4004-4015.

Devaux PF, ZAchowsky A (1994) Maintenance and consequences of membrane phospholipids asymmetry. *Chem Phy Lipids* **73**, 107-120.

Di Varia M, Bazzicalupi C, Oriolo P, Messori L, Bruni B, Zatta P (2004) Clioquinol, a drug for Alzheimer's disease specifically interfering with brain metal metabolism: structural characterization of its Zn(II) and copper(II) complexes. *Inorg Chem* **43**, 3795-3797.

Dong J, Robertson JD, Merkesbery WR, Lovell MA (2008) Serum zinc in the progression of Alzheimer's Disease. *J Alzheimers Dis* **15**, 443-450.

Drago D, Bettella M, Bolognin S, Cendron L, Scancar J, Milacic R, Ricchelli F, Casini A, Messori L, Tognon G, Zatta P (2008) Potential pathogenic role of β-amyloid$_{1-42}$-aluminum complex in Alzheimer's disease. *Int J Biochem Cell Biol* **40**, 731-746,a.

Drago D, Sensi S, Ricchelli F, Cavaliere A, Zatta P (2008) Alterations of neuronal calcium homeostasis and mitochondria function by β-amyloid$_{1-42}$-aluminum complex. *Rejuvination Res* **11**, 861-871,b.

Durrel SR, Guy RH, Arispe N, Rojas E, Pollard HB (1994) Theoretical models of the ion channel structure of amyloid β-protein. *Biophysical J* **67**, 2137-2145.

Fassbender K, Simons M, Bergmann C, Stroick M, Lutjohann D, Keller P, Runz H, Kuhl S, Bertsch T, von Bergmann K, Hennerici M, Beyreuther K, Hartmann T (2001) Simvastatin strongly reduces levels of Alzheimer's disease beta -amyloid peptides Abeta 42 and Abeta 40 in vitro and in vivo. *Proc Natl Acad Sci U S A* **98,** 5856-5861.

Ferrada E, Aranciba V, Loeb B, Norambuena E, Olea-azar E, Huidobro-toto J P (2007) Stechiometry and conditional stability constants of Cu (II) or Zn (II) clioquinol complexes; implications for Alzheimer's and Hungtington's disease therapy. *Neurotoxicol* **28**, 445-449.

Ferreira ST, Vieira MNN, De Felice FG (2007) Soluble protein oligomers as emerging toxins in Alzheimer's and other amyloid diseases. *IUBMB Life* **59**, 332-345.

Ferrer M, Golyshina OV, Beloqui A, Golyshin PN, Timmis KN (2007) The cellular machinery of Ferroplasma acidiphilum is iron-protein-dominated. *Nature* **445**, 91-94.

Filiz G, Caragounis A, Bica L, Du T, Masters CL, Crouch PJ, White AR (2008) Clioquinol inhibits peroxide-mediated toxicity through up-regulation of phosphoinositol-3-kinase and inhibition of p53 activity. *Int J Biochem Cell Biol* 40, 1030-1042.

Frederickson CJ, Koh JY, Bush AI (2005) The neurobiology of zinc in health and disease. *Nat Rev Neurosci* **6**, 449-462.

Gaeta A, Hider CR (2005) The crucial role of metal ions in neurodegeneration: the basis for a promising therapeutic strategy. *Br J Pharmacol* **146**, 1041-1059.

Garrick MD, Garrick LM (2009) Cellular iron transport. *Biochim Biophys Acta* **1790**, 309-325.

Gerhardsson L, Lundh T, Minthon L, Londos E (2008) Metal concentrations in plasma and cerebrospinal fluid in patients with Alzheimer's disease. *Dement Geriatr Cogn Disord* **25**, 508-515.

Glabe CC (2005) Amyloid accumulation and pathogensis of Alzheimer's disease: significance of monomeric, oligomeric and fibrillar Abeta. *Subcell Biochem* **38**, 167-177.

Glabe CC (2006) Common mechanism of amyloid oligomer pathogenesis in degenerative disease. *Neurobiol Ageing* **4**, 570-575.

Good PF, Perl DP (1993) Aluminium in Alzheimer's? *Nature* **362**, 418.

Gotz ME, Double K, Gerlach M, Youdim MB, Riederer P (2004) The relevance of iron in the pathogenesis of Parkinson's disease. *Ann N Y Acad Sci* **1012**, 193-208.

Haass C, Selkoe DJ (2007) Soluble protein oligomers in neurodegeneration: lessons from the Alzheimer's amyloid beta-peptide. *Nat Rev Mol Cell Biol* **8**, 101-112.

Hardy J (2009) The amyloid hypothesis for Alzheimer's disease: a critical reappraisal. *J Neurochem* **110**, 1129-1134.

Hardy J, Higgins GA (1992) Alzheimer's disease: the amyloid cascade hypothesis. *Science (New York, NY)* **256**, 184–185.

Hartlage-Rübsamen M, Staffa K, Waniek A, Wermann M, Hoffmann T, Cynis H, Schilling S, Demuth HU, Rossner S (2009) Developmental expression and subcellular localization of glutaminyl cyclase in mouse brain. *Int J Dev Neurosci* **27**, 825-35.

Hidalgo J, Aschner M, Zatta P, Vasak M (2001) Roles of the metallothionein family of proteins in the central nervous system. *Brain Res Bull* **55**, 133-145.

House E, Collingwod J, Khan A, Korchazkina O, Berthon G, Exley C (2004) Aluminium, iron, zinc and copper influence the in vitro formation of $A\beta_{42}$ in a manner which may have consequences for metal chelation therapy in Alzheimer disease. *J Alzheimers Dis* **6**, 291-301.

Hu WP, Chang GL, Chen S, Kuo YM (2006) Kinetic analysis of beta-amyloid peptide aggregation induced by metal ions based on surface plasmon resonance biosensing. *J Neurosci Methods* **154**, 190–197.

Hung YH, Robb EL, Volitakis I, Ho M, Evin G, Li QX, Culvenor JG, Masters CL, Cherny RA, Bush AI (2009) Paradoxical condensation of copper with elevated beta-Amyloid in lipid rafts under cellular copper deficiency conditions implications for Alzheimer Disease. *J Biol Chem* **33**, 21899-21907.

Hwang EM, Kim SK, Sohn J, Lee JY, Kim Y, Kim YS, Mook-Jung I (2006) Furin is an endogenous regulator of alpha-secretase associated APP processing. *Biochem Biophys Res Commun* **349**, 654-659.

Innocenti A, Hilvo M, Scozzafava A, Parkkila S, Supuran CT. (2008) Carbonic anhydrase inhibitors: Inhibition of the new membrane-associated isoform XV with phenols. *Bioorg Med Chem Lett* **18**, 3593-3596.

Iqbal K, Liu F, Gong CX, Alonso Adel C, Grundke-Iqbal I (2009) Mechanisms of tau-induced neurodegeneration. *Acta Neuropathol* **118**, 53-69.

Jacobsen KT, Iverfeldt K (2009) Amyloid precursor protein and its homologues: a family of proteolysis-dependent receptors. *Cell Mol Life Sci* **66**, 2299-2318.

Jenagaratnam L, McShane R (2006) Clioquinol for the treatment of Alzheimer's disease. *Cochrane Database Syst Rev* Issue 1 Art N:CD00538.

Ji SR, Wu Y, Sui SF (2002) Cholesterol is an important factor affecting the membrane insertion of beta-amyloid peptide (A beta 1-40), which may potentially inhibit the fibril formation. *J Biol Chem* **277**, 6273-6279.

Kakio A, Nishimoto S, Yanagisawa K, Kozutsumi Y, Matsuzaki K (2002) Interactions of amyloid beta-protein with various gangliosides in raft-like membranes: importance of GM1 ganglioside-bound form as an endogenous seed for Alzheimer amyloid. *Biochem* 41, 7385-7390.

Kamenetz F, Tomita T, Hsieh H, Seabrook G, Borchelt D, Iwatsubo T, Sisodia S, Malinow R (2003) APP processing and synaptic function. *Neuron* 37, 925–937.

Katsaras J (1998) Adsorbed to a rigid substrate, dimyristoylphosphatidylcholine multibilayers attain full hydratation in all mesophases. *Biophys J* **75**, 2157-2162.

Kayed R, Pensalfini A, Margol L, Sokolov Y, Sarsoza F, Head E, Hall J, Glabe C (2009) Annular protofibrils are a structurally and functionally distinct type of amyloid oligomer. *JBC* **284**, 4230-4237.

Kayed R, Sokolov Y, Edmonds B, McIntire TM, Milton SC, Hall JE, Glabe CG (2004) Permeabilization of lipid bilayers is a common conformation-dependent activity of soluble amyloid oligomers in protein misfolding diseases. *J Biol Chem* **279**, 46363-46366.

Kessler H, Bayer TA, Bach D, Schneider-Axmann T, Supprian T, Herrmann W, Haber M, Multhaup G, Falkai P, Pajonk FG (2008) Intake of copper has no effect on cognition in patients with mild Alzheimer's disease: a pilot phase 2 clinical trial. *J Neural Transm* **115**, 1181-1187.

Kivipelto M, Helkala EL, Hänninen T, Laakso MP, Hallikainen M, Alhainen K, Soininen H, Tuomilehto J, Nissinen A (2001) Midlife vascular risk factors and Alzheimer's disease in later life: longitudinal, population based study. *BMJ* **322**, 1447–1451.

Koppaka V, Axelsen PH (2000) Accelerated accumulation of amyloid beta proteins on oxidatively damaged lipid membranes. *Biochemistry* **39**, 10011-10016.

Kosman DJ (2002) FET3P, ceruloplasmin, and the role of copper in iron metabolism. *Adv Protein Chem* **60**, 221-269.

Kramer DR, Llanos RM, Mercer JFB (2003) Molecular basis of Copper transport: cellular and physiological functions of Menkes and Wilson disease proteins. In: Metal ions and neurodegenerative disorders. Singapore, London, World Scientific. pp. 183-206.

Krewski D, Yokel RA, Nieboer E, Borchelt D, Cohen J, Harry J, Kacew S, Lindsay J, Mahfouz AM, Rondeau V (2007) Human health risk assessment for aluminium, aluminium oxide, and aluminium hydroxide. *J Toxicol Environ Health B Crit Rev.* **10**, 1-269.

LaFerla FM, Green KN, Oddo S (2007) Intracellular amyloid-beta in Alzheimer's disease. *Nat Rev Neurosci* **8**, 499-509.

Lalioti V, Muruais G, Tsuchiya Y, Pulido D, Sandoval IV (2009) Molecular mechanisms of copper homeostasis. *Front Biosci* **14**, 4878-903

Le Bastard N, Aerts L, Leurs J, Blomme W, De Deyn PP, Engelborghs S (2009) No correlation between time-linked plasma and CSF Abeta levels. *Neurochem Int* **55**, 820-825.

Lee JY, Cole TB, Palmiter RD, Sush SW, Koh JY (2002) Contribution by synaptic zinc to the gender-disparate plaque formation in human Swedish mutant APP transgenic mice. *Proc Nat Acad Sci USA* **99**, 7705-7710.

Lee JY, Friedman JE, Angel I, Kozak A, Koh JY (2004) The lipophilic metal chelator DP-109 reduces amyloid pathology in brains of human beta-amyloid precursor protein transgenic mice. *Neurobiol Aging* **25**, 1315-1321.

Lesne S, Koh MT, Kotilinek L, Kayed R, Glabe CG, Yang A, *et al.*, (2006) A specific amyloid-beta protein assembly in the brain impairs memory. *Nature* **440**, 352–357.

Lesne S, Kotilinek L, Ashe KH (2008) Plaque-bearing mice with reduced levels of oligomeric amyloid-beta assemblies have intact memory function. *Neurosci* **151**, 745–749.

Lewczuk P, Esselmann H, Otto M, Maler JM, Henkel AW, Henkel MK, Eikenberg O, Antz C, Krause WR, Reulbach U, Kornhuber J, Wiltfang J (2004) Neurochemical diagnosis of Alzheimer's dementia by CSF Abeta42, Abeta42/Abeta40 ratio and total tau. *Neurobiol Aging* **25**, 273-281.

Lin H, Bhatia R, Lal R (2001) Amyloid beta protein forms ion channels: implications for Alzheimer's Disease pathophysiology. *FASEB J* **15**, 2433-2444.

Linkous DH, Adlard PA, Wanschura PB, Conko KM, Flinn JM (2009) The effects of enhanced Zinc on spatial memory and plaque formation in transgenic mice. *J Alzheimers Dis*, in press.

Livak KJ, Schmittegen TD (2001) Analysis of relative gene expression data using real-time quantitative PCR and the 2(-Delta Delta C(T)). *Method* **25**, 402-408.

Loeffler DA, LeWitt PA, Juneau PL, Sima AA, Nguyen HU, DeMaggio AJ, Brickman CM, Brewer G J, Dick RD, Troyer MD, Kanaley L (1996) Increased regional brain concentrations of ceruloplasmin in neurodegenerative disorders. *Brain Res* **738**, 265-274.

Lovell MA, Robertson JD, Teesdale WJ, Campbell JL, Markesbery WR. (1998) Copper, iron and zinc in Alzheimer's disease senile plaques. *J Neurol Sci* **158**, 47-52.

Luna-Munoz J, Garcia-Sierra F, Falcon V, Menendez I, Chavez-Macias L, Mena R (2005) Regional conformational changes involving phosphorylation of tau protein at the Thr231, precedes the structural change detected by Alz-50 antibody in Alzheimer's disease. *J Alzheimers Dis* **8**, 29-41.

Martins IC, Kuperstein I, Wilkinson H, Maes E, Vanbrabant M, Jonckheere W, Van Gelder P, Hartmann D, D'Hooge R, De Strooper B, Schymkowitz J, Rousseau F (2008) Lipids revert inert Ab amyloid fibrils to neurotoxic protofibrils that affect learning in mice. *EMBO J* **24**, 224-233.

Miller LM, Wang Q, Telivala TP, Smith RJ, Lanzirotti A, Miklossy J (2006) Synchrotron-based infrared and X-ray imaging shows focalized accumulation of Cu and Zn co-localized with beta-amyloid deposits in Alzheimer's disease. *J Struct Biol* **155**, 30-37.

Miura T, Suzuki K, Kohata N, Takeuchi H (2000) Metal binding modes of Alzheimer's amyloid beta-peptide in insoluble aggregates and soluble complexes. *Biochem* **39**, 7024-7031.

Miyajima H, Takahashi Y, Kono S (2003) Aceruloplasminemia, an inherited disorder of iron metabolism. *Biometals* **16**, 205-213.

Mocchegiani E, Bertoni-Freddari C, Marcellini F, Malavolta M (2005) Brain, aging, and neurodegeneration: role of zinc availability. *Prog Neurobiol* **75**, 367-390.

Molina JA, Jiménez-Jiménez FJ, Aguilar MV, Meseguer I, Mateos-Vega CJ, González-Muñoz M.J, de Bustos F, Porta J, Ortí-Pareja M, Zurdo M, Barrios E, Martínez-Para MC (1998) Cerebrospinal fluid levels of transition metals in patients with Alzheimer's disease. *J Neural Transm* **105**, 479-488.

Morita A, Kimura M, Itokawa Y (1994) The effect of aging on the mineral status of female mice. *Biol Trace Elem Res* **42**, 165-177.

Naiki H, Hashimoto N, Suzuki S, Kimura H, Nakakuki K, Gejyo F (1997) Establishment of a kinetic model of dialysis-related amyloid fibril extension in vitro. *Amyloid Int J of Exp and Clin Invest* **4**, 223-232.

Nakashima AS, Dyck RH (2009) Zinc and cortical plasticity. *Brain Res Rev* **59**, 347-373.

Nakayama K, Ohkawara T, Hiratochi M, Koh CS, Nagase H (2008) The intracellular domain of amyloid precursor protein induces neuron-specific apoptosis. *Neurosci Lett* **44**, 127-131.

Näslund J, Haroutunian V, Mohs R, Davis KL, Davies P, Greengard P, Buxbaum JD (2000) Correlation between elevated levels of amyloid beta-peptide in the brain and cognitive decline. *JAMA* **283**, 1571-1577.

Nordberg A (2008) Amyloid plaque imaging in vivo: current achievement and future prospects. *Eur J Nucl Med Mol Imag* **35**, S46–S50.

Noy D, Solomonov I., Sinkevich O, Arad T, Kjaer K, Sagi I (2008) Zinc-amyloid-beta interactions on a millisecond time-scale stabilize non-fibrillar Alzheimer-related species. *J Amer Chem Society* **130**, 1376-1383.

Opazo C, Huang X, Cherny RA, Moir RD, Roher AE, White AR, Cappai R, Masters CL, Tanzi RE, Inestrosa NC, Bush AI (2002) Metalloenzyme-like activity of

Alzheimer's disease beta-amyloid. Cu-dependent catalytic conversion of dopamine, cholesterol, and biological reducing agents to neurotoxic H(2)O(2). *J Biol Chem* **277**, 40302–40308.

Pantopoulos K, Hentze MW (1998) Activation of iron regulatory protein-1 by oxidative stress in vitro. *Proc Natl Acad Sci U S A* **95**, 10559-10563.

Perl DP, Moalem S (2006) Aluminum Alzheimer's disease and the geospatial occurence of similar disorders. Med *Miner and Geochemistry* **64**, 115-134.

Perry G, Taddeo MA, Petersen RB, Castellani RJ, Harris PL, Siedlak SL, Cash AD, Liu Q, Nunomura A, Atwood CS, Smith MA (2003) Adventiously-bound redox active iron and copper are at the center of oxidative damage in Alzheimer disease. *Biometals* **16**, 77-81.

Pettegrew JW, Panchalingam K, Hamilton RL, McClure RJ (2001) Brain membrane phospholipid alterations in Alzheimer's disease. *Neurochem Res* **26**, 771-782.

Phinney AL, Drisaldi B, Schmidt SD, Lugowski S, Coronado V, Liang Y, Horne P, Yang J, Sekoulidis J, Coomaraswamy J, Chishti MA, Cox DW, Mathews PM, Nixon RA, Carlson GA, St George-Hyslop P, Westaway D (2003) In vivo reduction of amyloid-beta by a mutant copper transporter. *Proc Natl Acad Sci USA* **100**, 14193-14198.

Piccini A, Russo C, Gliozzi A, Relini A, Vitali A, Borghi R, Giliberto L, Armirotti A, D'Arrigo C, Bachi A, Cattaneo A, Canale C, Torrassa S, Saido TC, Markesbery W, Gambetti P, Tabaton M (2005) beta-amyloid is different in normal aging and in Alzheimer disease. *J Biol Chem* **280**, 34186-34192.

Plant LD, Boyle JP, Smith IF, Peers C, Pearson HA (2003) The production of amyloid beta peptide is a critical requirement for the viability of central neurons. *J of Neurosc* **23**, 5531–5535.

Ponzoni S, Gaziri LC, Britto LR, Barretto WJ, Blum D (2002) Clearance of manganese from the rat substantia nigra following intra-nigral microinjections. *Neurosci Lett* **328**, 170-174.

Prohaska JR, Bailey WR (1993) Persistent regional changes in brain copper, cuproenzymes and catecholamines following perinatal copper deficiency in mice. *J Nutr* **123**, 1226-12234.

Pyatskowit JW, Prohaska JR (2008) Iron injection restores brain iron and hemoglobin deficits in perinatal copper-deficient rats. *J Nutr* **138**, 1888-1886.

Quinn JF, Crane S, Harris C, Wadsworth TL (2009) Copper in Alzheimer's disease: too much or too little? *Expert Rev Neurother* **9**, 631-637.

Rajan MT, Jagannatha Rao KS, Mamatha BM, Rao RV, Shanmugavelu P, Menon RB, Pavithran MV (1997) Quantification of trace elements in normal human-brain by inductively coupled plasma atomic emission spectrometry. *J Neurol Sci* **146**, 153-166.

Rajendran R, Minqin R, Ynsa MD, Casadesus G, Smith MA, Perry G, Halliwell B, Watt F (2009) A novel approach to the identification and quantitative elemental analysis of amyloid deposits insights into the pathology of Alzheimer's disease. *Biochem Biophys Res Commun* **382**, 91-95.

Raman B, Ban T, Yamaguchi K, Sakai M, Kawai T, Naiki H, Goto Y (2005) Metal ion-dependent effect of clioquinol on the fibril growth of an amyloid beta-peptide. *J Biol Chem* **280**, 16157-16162.

Reeves PG, DeMars LC (2005) Copper deficiency reduces iron absorption and biological half-life in male rats. *J Nutr* **134**, 1953-1957.

Reeves PG, Demars LC, Johnson WT, Lukaski HC (2005) Dietary copper deficiency reduces iron absorption and duodenal enterocyte hephaestin protein in male and female rats. *J Nutr* **135**, 92-98.

Reid PC, Urano Y, Kodama T, Hamakubo T (2007) Alzheimer's disease: cholesterol, membrane rafts, isoprenoids and statins. *J Cell Mol Med* **11**, 383-392.

Reusche E (2003) Aluminium and central nervous system morphology in hemodialysis, in: Metal ions and neurodegenerative disorders. Singapore, London, World Scientific pp. 117-138.

Ricchelli F, Drago D, Filippi B, Tognon G, Zatta P (2005) Aluminum-triggered structural modifications and aggregation of beta-amyloids. *Cell Mol Life Sci* **62**, 1724-1733.

Ritchie CW, Bush AI, Mackinnon A, Macfarlane S, Mastwyk M, MacGregor L, Kiers L, Cherny R, Li QX, Tammer A, Carrington D, Mavros C, Volitakis I, Xilinas M, Ames D, Davis S, Beyreuther K, Tanzi RE, Masters CL (2003) Metal-protein attenuation with clioquinol targeting Abeta amyloid deposition and toxicity in Alzheimer disease: a pilot phase 2 clinical trial. *Arch Neurol* **60**, 1685-1691.

Rogers JT, Randall JD, Eder PS, Huang X, Bush AI, Tanzi RE, Venti A, Payton SM, Giordano T, Nagano S, Cahill CM, Moir R, Lahiri DK, Greig N, Sarang SS, Gullans SR (2002) Alzheimer's disease drug discovery targeted to the APP mRNA 5'untranslated region. *J Mol Neurosci* **19**, 77-82.

Roider G, Drasch G (1999) Concentration of Al in human tissues. Investigations on an occupationally non-exposed population in Southern Bavaria (Germany). *Trace Elem Electrolytes* **16**, 77-86.

Roychaudhuri R, Yang M, Hoshi MM, Teplow DB (2009) Amyloid beta-protein assembly and Alzheimer disease. *J Biol Chem* **284**, 4749-4753.

Rulon LL, Robertson JD, Lovell MA, Deibel MA, Ehmann WD, Markesber WR (2000) Serum zinc levels and Alzheimer's disease. *Biol Trace Elem Res* **75**, 79-85.

Russo C, Violani E, Salis S, Venezia V, Dolcini V, Damonte G, Benatti U, D'Arrigo C, Patrone E, Carlo P, Schettini G (2002) Pyroglutamate-modified amyloid beta-peptides-AbetaN3(pE)-strongly affect cultured neuron and astrocyte survival. *J Neurochem* **82**, 1480-1489.

Salzman MB, Smith EM, Koo C (2002) Excessive oral zinc supplementation. *J Pediatr Hematol Oncol* **24**, 582-584.

Schäfer S, Pajonk FG, Multhaup G, Bayer TA (2007) Copper and clioquinol treatment in young APP transgenic and wild-type transgenic mice: effects on the life expectancy, body weight, and metal-ion levels. *J Mol Med* **85**, 405-413.

Schilling S, Appl T, Hoffmann T, Cynis H, Schulz K, Jagla W, Friedrich D, Wermann M, Buchholz M, Heiser U, von Hörsten S, Demuth HU (2008) Inhibition of glutaminyl cyclase prevents pGlu-Abeta formation after intracortical/hippocampal microinjection in vivo/in situ. *J Neurochem* **106**, 1225-1236.

Schilling S, Hoffmann T, Manhart S, Hoffmann M, Demuth HU (2004) Glutaminyl cyclases unfold glutamyl cyclase activity under mild acid conditions. *FEBS Lett* **563**, 191-196.

Schilling S, Zeitschel U, Hoffman T, Heiser U, Francke M, Kehlen A, Holzer M, Hutter-Paier B, Prokesch M, Windisch M, Jagla W, Schlenzig D, Lindner C, Rudolph T, Reuter G, Cynis H, Montag D, Demuth HU, Rossner S (2008) Glutaminyl cyclase inhibition attenuates pyroglutamate Abeta and Alzheimer's disease-like pathology. *Nat Med* **14**, 1106-1111.

Schipper HM (2004) Heme oxygenase expression in human central nervous system disorders. *Free Radic Biol Med* **37**, 1995–2011.

Sensi SL, Jeng JM (2004) Rethinking the excitotoxic ionic milieu: the emerging role of Zn(2+) in ischemic neuronal injury. *Curr Mol Med* **4**, 87-111.

Shankar GM, Li S, Mehta TH, Garcia-Munoz A, Shepardson NE, Smith I *et al.*, Amyloid-beta protein dimers isolated directly from Alzheimer's brains impair synaptic plasticity and memory. *Nat Med* **14** (2008), 837–842.

Silvestri L, Camaschella C (2008) A potential pathogenetic role of iron in Alzheimer's disease. *J Cell Mol Med* **12**, 1548-1550.

Smith DG, Cappai R, Barnham KJ (2007) The redox chemistry of the Alzheimer's disease amyloid beta peptide. *Biochim Biophys Acta* **1768,** 1976-1990.

Smith Q, Rabin O, Chikhale E (1997) Delivery of metal to brain and the role of the blood-brain barrier. In Metals and Oxidative Damage in Neurological Disorders (J. Connor, Ed.);113-30.

Soto C, Estrada LD (2008) Protein misfolding and neurodegeneration. *Arch Neurol* **65**, 184-189.

Speziali M, Orvini E (2003) Metals distribution and regionalization in the brain, in: Metal ions and neurodegenerative disorders. Singapore, London, World Scientific. pp.15-65.

Stankiewicz JM, Brass SD (2009) Role of iron in neurotoxicity: a cause for concern in the elderly? *Curr Opin Clin Nutr Metab Care* **12**, 22-29.

Stoltenberg M, Bruhn M, Sondergaard C, Doering P, West MJ, Larsen A, Troncoso JC, Danscher G (2005) Immersion autometallographic tracing of zinc ions in Alzheimer beta-amyloid plaques. *Histochem Cell Biol* **123**, 605–611.

Storr T, Merkel M, Song-Zhao GX, Scott LE, Green DE, Bowen ML, Thompson KH, Patrick BO, Schugar HJ, Orvig C. (2007) Synthesis, characterization, and metal coordinating ability of multifunctional carbohydrate-containing compounds for Alzheimer's therapy. *J Am Chem Soc* **129**, 7453-7463.

Suwalsky M (1988) in: *Physical properties of biological membranes and their functional implications (chapter 5)* Hidalgo C. (Ed.), Elsevier, New York.

Suwalsky M (1996) Phospholipid Bilayers, in: *Polymeric Materials Encyclopedia*. CRC, Boca Raton FL, Salamone JC (Ed.), 5073-5078.

Suwalsky M, Martínez F, Cárdenas H, Grzyb J, Strzalka K (2005) Iron affects the structure of cell membrane molecular models. *Chem Phys Lipids* **134**, 69-77.

Sykes PA, Watson SJ, Temple JS, Bateman RC Jr (1999) Evidence for tissue-specific forms of glutaminyl cyclase. *FEBS Lett* **455**, 159-161.

Takeda A, Hirate M, Tamano H, Oku N (2003) Release of glutamate and GABA in the hippocampus under zinc deficiency. *J Neurosci Res* **72**, 537-542.

Tarohda T, Yamamoto M, Amamo R (2004) Regional distribution of manganese, iron, copper, and zinc in the rat brain during development. *Anal Bioanal Chem* **380**, 240-246.

Tomic JL, Pensalfini A, Head E, Glabe CG (2009) Soluble fibrillar oligomer levels are elevated on Alzheimer's disease brain and correlate with cognitive dysfunction. *Neurobiol Dis* **35**, 352-358.

Tomidokoro Y, Lashley T, Rostagno A, Neubert TA, Bojsen-Møller M, Braendgaard H, Plant G, Holton J, Frangione B, Révész T, Ghiso J (2005) Familial Danish dementia: co-existence of Danish and Alzheimer amyloid subunits (ADan AND A{beta}) in the absence of compact plaques. *J Biol Chem* **280**, 36883-36894.

Tsai J, Grutzendler J, Duff K, Gan WB (2004) Fibrillar amyloid deposition leads to local synaptic abnormalities and breakage of neuronal branches. *Nat Neurosci* **7**, 1181-1183.

Vallee BL, Falchuk KH (1993) The biochemical basis of zinc physiology. *Physiol Rev* **73**, 79-118.

Verity A (1999) Manganese neurotoxicity: a mechanistic hypothesis. *Neurotoxicol* **20**, 489-498.

Vulpe CD, Kuo YM, Murphy TL, Cowley L, Askwith C, Libina N, Gitschier J, Anderson GJ (1999) Hephaestin, a ceruloplasmin homologue implicated in intestinal iron transport, is defective in the sla mouse. *Nat Gen* **21**, 195-199.

Weiss JH, Sensi SL, Koh JY (2000) Zn(2+): a novel ionic mediator of neural injury in brain disease. *Trends Pharmacol Sci* **21**, 395-401.

Welch KD, Hall JO, Davis TZ, Aust SD (2007) The effect of copper deficiency on the formation of hemosiderin in sprague-dawley rats. *Biometals* **20**, 829-39.

White AR, Du T, Laughton KM, Volitakis I, Sharples RA, Xilinas ME, Hoke DE, Holsinger RM, Evin G, Cherny RA, Hill AF, Barnham KJ, Li QX, Bush AI, Masters CL (2006) Degradation of the Alzheimer disease amyloid beta-peptide by metal-dependent up-regulation of metalloprotease activity. *J Biol Chem* **281**, 17670-17680.

Yassin MS, Ekblom J, Xilinias M, Gottfries CG, Orleand L (2000) Changes in uptake of vitamin B12 and trace metals in brains of mice treated with clioquinol. *J Neurolog Sci* **173**, 40-44.

Yatin SM, Varadarajan S, Link CD, Butterfield DA (1999) In vitro and in vivo oxidative stress associated with Alzheimer's amyloid β-peptide (1-42). *Neurobiol Aging* **20**, 325-330.

Yokel RA (1994) Aluminum chelation: chemistry, clinical, and experimental studies and the search for alternatives to desferrioxamine. *J Toxicol Environ Health* **41**, 131-174.

Yokel RA (2006) Blood-brain barrier flux of aluminium, manganese, iron and other metals suspected to contribute to metal-induced neurodegeneration. *J Alzheimers Dis* **10**, 223-253.

Yumoto S, Kakimi S, Ohsaki A, Ishikawa A (2009) Demonstration of aluminum in amyloid fibers in the cores of senile plaques in the brains of patients with Alzheimer's disease. *J Inorg Biochem*, in press.

Zambenedetti P, Giordano R, Zatta P (1998) Metallothioneins are highly expressed in astrocytes and microcapillaries in Alzheimer's disease. *J Chem Neuroanat* **15**, 21-26.

Zatta P (Ed.) (2002) Recent topics in aluminium chemistry. *Coord Chem Rev* **228**, 91-396.

Zatta P (ed.) (2003) Metal ions and Neurodegenerative disorders, World Scientific, Singapore, London (pp. 1-508).

Zatta P, Drago D, Bolognin S, Sensi SL (2009) Alzheimer's disease, metal ions and metabolic homeostatic therapy. *Trends Pharmacol Sci* **30**, 346-355.

Zatta P, Drago D, Zambenedetti P, Bolognin S, Nogara E, Peruffo A, Cozzi B (2008) Accumulation of copper and other metal ions, and metallothionein I/II expression in the bovine brain as a function of aging. *J Chem Neuroanat* **36**, 1-5.

Zatta P, Frank A (2007) Copper deficiency and neurological disorders in man and animals. *Brain Res Rev* **54**, 19-33.

Zatta P, Lucchini R, van Rensburg SJ, Taylor A (2003) The role of metals in neurodegenerative processes: aluminum, manganese, and zinc. *Brain Res Bull* **62**, 15-28.

Zatta P, Raso M, Zambenedetti P, Rocco P, Petretto A, Mauri P, Cozzi B (2006) Metallothionein-I-II expression in young and adult bovine pineal gland. *J Chem Neuroanat* **31**, 124-129.

Zatta P, Zambenedetti P, Reusche E, Stellmacher F, Cester A, Albanese P, Meneghel G, Nordio M (2004) A fatal case of aluminium encephalopathy in a patient with severe chronic renal failure not on dialysis. *Nephrol Dial Transplant* **19**, 2929-2931.

Zatta P, Zambenedetti P, Reusche E, Stellmacher F, Cester A, Albanese P, Meneghel G, Nordio M (2004) A fatal case of aluminium encephalopathy in a patient with severe chronic renal failure not on dialysis. *Nephrol Dial Transplant* **19**, 2929-2931.

Pubblications

1. Bolognin S., Messori L., Drago D., Gabbiani C., Cendron L., Zatta P. Effects of biologically relevant metal ions on the conformation and the aggregation properties of Aβ 1-42. *Submitted*
2. Cozzi B., Giacomello M., Zambenedetti P., Bolognin S., Rossipal E., Peruffo A., Zatta P. (2010) Ontogenesis and migration of metallothionein I/II-containing glial cells in the human telencephalon during the second trimester. *Brain Research*, accepted.
3. Bolognin S., Messori L., Zatta P. (2009) Metal ion physiopathology in neurodegenerative disorders. *Neuromolecular Medicine*, 11:223-238.
4. Zatta P., Drago D., Bolognin S., Sensi S.L. (2009) Chelation Therapy: a resurrected role in Alzheimer's disease? *Trends in Pharmacological Sciences*, 30:346-355
5. Bolognin S., Drago D., Messori L., Zatta P. (2009) Chelation Therapy for neurodegenerative diseases. *Medicinal Research Reviews*, 29:547-570.
6. Suwalsky M., Gonzales R., Villena F., Aguilar L.F., Sotomayor C.P., Bolognin S., Zatta P. (2009) Structural effects of tetrachloroauric acid on cell membranes as molecular models. *Coordination Chemistry Reviews*, 253: 1599-1606.
7. Suwalsky M., Bolognin S., Zatta P. (2009) Interaction between Alzheimer β-amyloid and β-amyloid-metal complexes with cell membranes. *Journal of Alzheimer Disease*, 17:81-90.
8. Bolognin S., Zatta P., Drago D., Tognon G., Parnigotto P.P., Ricchelli F. (2008) Mutual stimulation of beta-amyloid fibrillogenesis by clioquinol and divalent metals. *Neuromolecular Medicine*, 10:322-332.
9. Drago D., Bolognin S., Zatta P. (2008) Role of metal ions in the abeta oligomerization in Alzheimer's disease and in other neurological disorders. *Current Alzheimer Research*, 5:500-507.

10. Bolognin S., Zatta P. (2008) "Metallothioneins and neurodegenerative diseases", in Metallothioneins in biochemistry and pathology. Singapore, London: World Scientific pp 47-70.

11. Zatta P., Drago D., Zambenedetti P., Bolognin S., Nogara E., Peruffo A., Cozzi B. (2008) Accumulation of copper and other metal ions, and metallothionein I/II expression in the bovine brain as a function of aging. *Journal of Chemical Neuroanatomy,* 36:1-5.

12. Suwalsky M., Villana F., Sotomayor C.P., Bolognin S., Zatta P. (2008) Human cells and membrane molecular models are affected in vitro by chlorpromazine. *Biophysical Chemistry,* 135:7-13.

13. Drago D., Bettella M., Bolognin S., Cendron L., Scancar J., Milacic R., Ricchelli F., Casini A., Messori L., Tognon G., Zatta P. (2007) Potential pathogenic role of beta-amyloid-aluminum complex in Alzheimer's disease. *International Journal of Biochemistry & Cell Biology,* 40:731-46.

14. Ricchelli F., Fusi P., Tortora P., Valtorta M., Riva M., Tognon G., Chieregato K., Bolognin S., Zatta P. (2007) Destabilization of non-pathological variants of ataxin-3 by metal ions results in aggregation/fibrillogenesis. *International Journal of Biochemistry & Cell Biology,* 39:966-77.

Acknowldgements

Tirare le somme di un’esperienza non è mai facile: le persone da ricordare sono sempre molte e si rischia di dimenticarne qualcuna.

Vorrei ringraziare prima di tutto il professor Zatta, non solo per le 1000 occasioni in cui mi ha appoggiata, dimostrato stima e fiducia, dato delle occasioni per mettermi alla prova, ma sopratutto per aver stimolato la mia curiosità e avermi dimostrato che cultura e conoscenza si possono esprimere davvero sotto tante forme. Grazie anche perché questi anni sono stati una scuola non solo professionale ma soprattutto personale. Spero la mi vita futura sia vivace come questo periodo: ricco di persone, situazioni e interessi.

Grazie ai miei genitori che hanno sempre saputo accettare le mie scelte e mi incoraggiano in ogni occasione ad avere fiducia nelle mia capacità. Ora che sono adulta riconosco che nel difficile ruolo di genitori sono stati perfetti e li ringrazio per tutti i valori che mi hanno trasmesso.

Grazie a Nicola perché c’è sempre, anche adesso che sono qui a New York cerca di darmi il massimo sostegno e nonostante la lontananza non renda le cose facili gioisce dei miei successi ed è partecipe delle mie difficoltà..grazie davvero!

Grazie a Marco a cui voglio un bene immenso e che vedo ogni giorno diventare sempre più forte e maturo e che, anche se con poche parole, sa trasmettermi il suo affetto.

Grazie allo zio Franco che ha sempre gioito dei miei successi e che immagino sarebbe orgoglioso di vedermi concludere questo percorso.

Grazie ai tanti veri amici che ho la fortuna di avere.

Grazie a Denise che porterò sempre nel cuore come la mia compagna di lab, la persona con cui ho condiviso tutte le difficoltà/gioie di questo percorso e dell’esperienza americana.

Grazie a Pamela, una persona come ce ne sono poche, e a tutte le persone con cui ho lavorato soprattutto Maria Teresa e il LURM, il Prof. Cozzi e le sue collaboratrici, i Prof. Messori e Suwalsky.

Grazie soprattutto alle mie compagne e vicine di lab Federica, Lara, Mikol, Alessandra con le quali è nata una preziosa amicizia.

Grazie al mio laureando Alberto che ha portato un pizzico di pazzia/allegria nel lab e a cui faccio il mio più grande in bocca al lupo per le esperienze che verranno.